



UNIVERSITÀ DELLA CALABRIA



UNIVERSITA' DELLA CALABRIA

Dipartimento di Ingegneria per l'ambiente e il territorio e Ingegneria chimica

Dottorato di Ricerca in

Ingegneria chimica e dei Materiali

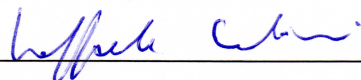
Con il contributo del Fondo Sociale Europeo (FSE)

CICLO XXVIII

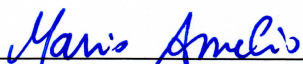
CHEMICAL LOOPING DESULPHURIZATION: MODEL AND APPLICATIONS TO POWER SYSTEMS

Settore Scientifico Disciplinare ING-IND/08

Coordinatore: Ch.mo Prof. Raffaele Molinari

Firma 

Supervisore/Tutor: Ch.mo Prof. Mario Amelio

Firma 

Dottorando: Dott.ssa Jessica Settimo

Firma 

La presente tesi è cofinanziata con il sostegno della Commissione Europea, Fondo Sociale Europeo e della Regione Calabria. L'autore è il solo responsabile di questa tesi e la Commissione Europea e la Regione Calabria declinano ogni responsabilità sull'uso che potrà essere fatto delle informazioni in essa contenute.

*‘eine Arbeit wird eigentlich nie fertig,
man muß sie für fertig erklären,
wenn man nach Zeit und Umständen
das mögliche getan hat.’*

— Johann Wolfgang von Goethe

UNIVERSITÀ DELLA CALABRIA

Sommario

Ingegneria Chimica e dei Materiali
Scuola di dottorato "Pitagora"

Dottorato di ricerca

Chemical looping per la desolfurazione: Modellazione e Applicazioni a sistemi di potenza

di Jessica Settino

I processi di assorbimento, sia fisici che chimici a base di ammine, sono attualmente utilizzati per rimuovere efficacemente i composti dello zolfo. Nonostante l'eccellente desolfurazione, questa strategia è termicamente inefficiente, in quanto richiede gas a bassa temperatura. Scopo di questo lavoro è quello di analizzare soluzioni alternative che operino a temperature più elevate. A tale scopo, è stato analizzato il processo del chemical looping. Si tratta di una nuova tecnologia, in cui un materiale sorbente, in contatto con il gas combustibile grezzo, viene convertito nel suo solfuro e poi rigenerato così da ricominciare il ciclo. Il sistema è costituito da due reattori: uno per la rigenerazione e l'altro per la desolfurazione. Un modello matematico di tale sistema è stato sviluppato con il software Athena Visual Studio ed i suoi risultati confrontati con quelli ottenuti dal modello proposto dal National Energy Technology Laboratory, validati sulla base di dati sperimentali.

Nella fase successiva, il sistema modellato è stato applicato a tre casi studio di interesse industriale: per la produzione di energia elettrica negli impianti a ciclo combinato con gassificazione integrata, nei processi di metanazione, nei processi per la sintesi del metanolo.

Mediante simulazioni, condotte con i software commerciali Thermoflex e UniSim Design, sono stati studiati gli effetti della desolfurazione a caldo sulle prestazioni dei diversi sistemi.

UNIVERSITY OF CALABRIA

Abstract

Chemical Engineering and Materials
Doctoral school "Pitagora"

Doctor of Philosophy

Chemical looping desulphurization: Model and Applications to Power Systems

by Jessica SETTINO

Absorption processes are currently used to efficiently remove sulfur compounds. In spite of the excellent desulphurization, this strategy is thermally inefficient, since it requires gas at low temperature. Aim of this work is to analyze alternative solutions operating at higher temperature. To this purpose, the chemical looping process has been investigated. It is a novel technology, where a sorbent, in contact with the raw fuel gas, is converted into its sulfide and then regenerated so as to restart the cycle. The system consists of two reactors: the regeneration and desulphurization reactor.

A mathematical model has been developed with the software Athena Visual Studio and the results compared with the model proposed by the National energy technology laboratory, validated through experimental data.

Afterward, the modeled system has been applied to three case study of industrial interest: for electricity production in the Integrated Gasification Combined Cycle, in methanation processes, in processes for methanol synthesis.

By means of simulation analysis, with the commercial software Thermoflex and UniSim Design, the effects of hot gas desulphurization on the performance of the different systems have been investigated.

Acknowledgements

I would like to thank my research advisor Prof. Mario Amelio, from University of Calabria, and Dr. Tilman Schildhauer, from Paul Scherrer Institut, for their precious guidance and support.

I am also grateful to Professors F. Di Maio and A. Di Renzo, for their valuable comments and suggestions.

A special thanks to Dr. Peter Jansohn who gave me the opportunity to be part of his research group and work in a so active and friendly environment.

Thanks to all the colleagues, always available for support from a professional and human point of view.

Thanks to all the people I met during this great experience, with its up and down.

Contents

Sommario	iv
Abstract	v
Acknowledgements	vi
Contents	vii
List of Figures	x
List of Tables	xiii
Acronyms	xiv
Nomenclature	xv
1 Introduction	1
1.1 Thesis aims and objectives	4
1.1.1 Methods and instruments	4
1.2 Overview	6
2 Syngas desulphurization and sulfur recovery	9
2.1 Cold gas desulphurization technologies	10
Physical Absorption	12
Chemical Absorption	12
2.2 Hot gas desulphurization technologies	13
2.2.1 <i>In situ</i> desulphurization	13
2.2.2 External desulphurization	14
2.3 Sulfur recovery	16
2.3.1 Claus Process	16
2.3.2 Wet Flue Gas Desulphurization	17
3 Chemical looping desulphurization process	19
3.1 Chemical looping desulphurization	20
3.2 Sorbent Screening	21
3.3 System Configuration	25

4	Chemical Looping Model	31
4.1	Reaction Kinetics	32
4.1.1	Uniform-Conversion Model	32
4.1.2	Shrinking core Model	33
4.1.3	Grain Model	37
4.2	Hydrodynamics	39
4.3	Heat transfer	41
4.4	Model assumptions	42
4.5	Model validation	43
4.6	Sensitivity Analysis & Results discussion	44
4.7	Combination of <i>In situ</i> & external desulphurization	47
4.8	Reactor Model Scale-up	48
5	Application to Integrated Gasification Combined Cycle	50
5.1	IGCC with cold gas desulphurization	50
5.2	IGCC with hot gas desulphurization	55
5.3	Energy efficiency indicators	58
5.4	Cold gas clean-up vs. Hot gas clean-up	59
5.5	Effect of the desulphurization temperature	63
5.6	Outlooks & perspective	65
6	Application to Coal-to-SNG Process	67
6.1	Syngas Cleaning & conditioning	68
6.2	Methanation reactor	71
6.2.1	Adiabatic fixed bed reactor model	71
6.3	Methanation Process	75
6.4	Gas upgrading	78
6.5	Results discussion & comparison	80
6.6	Outlooks & perspective	81
7	Application to Methanol Production	82
7.1	Methanol synthesis reactor	84
7.1.1	Boiling water reactor model for Methanol synthesis	85
7.1.2	Boiling water reactor model results	91
7.2	Process Design with cold gas desulphurization	93
7.3	Optimization & analysis	96
7.3.1	Effect of reactor size	96
7.3.2	Effect of reactor length	97
7.3.3	Effect of the reactor pressure	98
7.4	Process design with hot gas desulphurization	100
7.5	Conclusions	101
8	Conclusions and outlooks	103
A	Flowsheet of the Methanation Process with CGD	106
B	Flowsheet of the Methanation Process with HGD	117

C Flowsheet of the Methanol Synthesis Process with CGD	125
D Flowsheet of the Methanol Synthesis Process with HGD	133
Bibliography	141
Activities	149

List of Figures

1.1	Grubb curve of the development of a new technology	3
2.1	Equilibrium in chemical and physical absorption processes	11
2.2	Schematic representation of the absorption process.	11
2.3	H ₂ S equilibrium concentration	14
2.4	Sulphur Removal Technologies	15
2.5	Wet FGD	18
3.1	Scheme of Chemical looping desulphurization	20
3.2	Reactor types and possible configurations	29
3.3	Chemical looping desulphurization by transport reactors	30
4.1	Chemical reactor model: influencing aspects	31
4.2	Uniform Conversion Model: schematic representation.	33
4.3	Schematic representation of the Shrinking Core Model.	34
4.4	Schematic representation of the grain model.	37
4.5	Voidage profile	41
4.6	NETL model: H ₂ S concentration along the reactor for different solid mass flows	43
4.7	H ₂ S concentration along the reactor for different solid mass flows	44
4.8	H ₂ S concentration and ZnO conversion along the reactor for different solid mass flows	45
4.9	H ₂ S concentration for different initial sulfur concentration	46
4.10	H ₂ S concentration along the reactor for different operating temperatures	46
4.11	H ₂ S concentration along the reactor for different water concentrations	47
4.12	Solid mass flux required for <i>in situ</i> and external desulphurization for the same H ₂ S exit concentration	48
4.13	Effect of the estimated particle velocity on the H ₂ S concentration and sorbent conversion	49
5.1	Scheme of an Integrated Gasification Combined Cycle with cold gas desulphurization	53
5.2	Scheme of a Heat Recovery Steam Generator. From: Lozza 2006	55
5.3	Scheme of an Integrated Gasification Combined Cycle with hot gas desulphurization	56
5.4	Hot gas desulphurization and regeneration unit.	57
5.5	Heat recovery from the hot exhaust of the gas turbine for cold gas desulphurization	61

5.6	Heat recovery from the hot exhaust of the gas turbine for hot gas desulphurization	62
6.1	Alternative process unit technologies for each step of the Coal-to-SNG process with illustration of the energy integration system.	68
6.2	Flowsheet of the Rectisol Process in UniSim Design	70
6.3	Concentration of the main reactant under adiabatic conditions for a Pressure of 1 atm, temperature of 550 K and H_2/CO equal 3.	72
6.4	Temperature profile under adiabatic conditions	73
6.5	Methane conversion under adiabatic conditions at 1-10-30 bar	73
6.6	Temperature profile under adiabatic conditions at 1-10-30 bar	74
6.7	Equilibrium Curve for methanation process	75
6.8	Flowsheet of the methanation plant in UniSim Design	76
6.9	Flowsheet of methanation process with hot gas desulphurization in UniSim Design	77
6.10	Flowsheet of the Amine Process in UniSim Design	79
7.1	Alternative process unit technologies for each step of the Methanol Production	82
7.2	Scheme of a Quench Reactor.	85
7.3	Boiling Water Reactor	86
7.4	Temperature profile at different pressures	88
7.5	Methanol concentration at different pressures	89
7.6	Temperature profiles in the adiabatic reactor for different inlet temperature	89
7.7	Methanol conversion profiles in the adiabatic reactor for different inlet temperature	90
7.8	geometric reactor information to calculate the heat transfer coefficient	90
7.9	Effect of the inlet temperature variation (180-230-280°C) on methanol conversion.	91
7.10	Effect of the shell temperature variation on methanol conversion	92
7.11	Effect of the shell temperature variation on the temperature profile	92
7.12	Effect of the inlet flow variation on methanol fraction	93
7.13	Flowsheet of the methanol production plant in UniSim Design	95
7.14	Effect of reactor size variation on recirculated gas and methanol production	96
7.15	Effect of reactor size variation on the methanol fraction converted	97
7.16	Effect of reactor size variation on compressor power	97
7.17	Effect of reactor length variation on recirculated gas and methanol production	98
7.18	Effect of reactor size variation on the methanol fraction converted	98
7.19	Effect of reactor length variation on compressor power	99
7.20	Effect of operating pressure variation on gas recycle and methanol production	99
7.21	Effect of operating pressure variation on methanol conversion	100
7.22	Effect of operating pressure variation on the power consumption of compressor K100, K101 and K102	100
7.23	Effect of operating pressure variation on overall power consumption	101
A.1	Flowsheet of the methanation plant in UniSim Design	107

B.1 Flowsheet of methanation process with hot gas desulphurization in UniSim Design	118
C.1 Flowsheet of the methanol production plant in UniSim Design	126
D.1 Flowsheet of the methanol production plant with HGD in UniSim Design	134

List of Tables

1.1	Technology Readiness Levels	7
2.1	Cold desulphurization technologies	10
3.1	Main characteristic of reactors used for hot gas desulphurization.	26
4.1	Chemical and Physical properties of Zinc Titanate and model Parameters	39
4.2	Commercial riser characteristic.	48
5.1	Gasifier specifics	52
5.2	Coal Properties	52
5.3	Acid Gas Removal specifics	54
5.4	Power Section specifics	54
5.5	Gas Turbine specifics	59
5.6	Performance of IGCC with Cold Gas Desulphurization	60
5.7	IGCC desulphurization temperature variation	64
5.8	Contaminants and emission limits	65
5.9	Clean-up systems for hot gas desulfurization	65
6.1	Clean syngas to the methanation reactor	71
6.2	Gas composition before and after upgrading	78
6.3	Efficiency indicators & produced SNG	81
7.1	Gasification & Conditioning process	83
7.2	Parameter Values	88
7.3	Clean Syngas after Rectisol Process	93
7.4	Clean Syngas after HGD	101

Acronyms

AGR	A cid G as R emoval
ASU	A ir S eparation U nit
CCT	C lean C oal T echnologies
CFD	C omputational F luid D ynamics
CGD	C old G as D esulphurization
CGE	C old G as E fficiency
CL	C hemical L ooping
FGD	F lue G as D esulphurization
GM	G rain M odel
GT	G as T urbine
HGD	H ot G as D esulphurization
HGE	H ot G as E fficiency
HHV	H igh H eating V alue
IEA	I nternational E nergy A gency
IGCC	I ntegrated G asification C ombined C ycle
LHV	L ow H eating V alue
SCM	S hrinking C ore M odel
SNG	S ynthetic N atural G as
ST	S team T urbine
TIT	T urbine I nlet T emperature
TRL	T echnology R eadness L evels
WEO	W orld E nergy O utlook
WGS	W ater G as S hift

Nomenclature

A	reactor cross sectional area	m^2
a_v	particle surface area per unit reactor volume	$\text{m}_s^2 \text{m}_r^{-3}$
C	Concentration	mol m^{-3}
C_p	heat capacity	$\text{J mol}^{-1} \text{K}^{-1}$
\mathcal{D}	Diffusivity	$\text{m}^2 \text{s}^{-1}$
M_w	molecular weight	g mol^{-1}
\dot{m}, G	mass flow	kg s^{-1}
n	molar flow rate	mol s^{-1}
N	molar flow of gas reacted per pellet	mol s^{-1}
n_P	number of sorbent particle	
h	gas-solid heat transfer coefficient	$\text{W m}^{-2} \text{K}^{-1}$
ΔH	enthalpy of reaction	J mol^{-1}
P	Power	$\text{W (Js}^{-1}\text{)}$
r	radial coordinate	m
\mathfrak{R}	reaction rate	$\text{mol kg}_s^{-1} \text{s}^{-1}$
R	Ideal Gas Constant	$\text{J mol}^{-1} \text{K}^{-1}$
R_0	particle radius	m
T	temperature	K
t	time	s
X	conversion of the sorbent	
z	axial coordinate	m

Greek symbols

$\varepsilon, \varepsilon_b$	bed voidage
ε_0	particle porosity
η	efficiency

μ	viscosity	Pa s
ρ	density	kg m ⁻³
ω	mass fraction	

subscript

0	initial
<i>g</i>	gas or grain
<i>s</i>	solid
<i>cat</i>	catalyst

To my family
To my friends
and
To you, who are reading

Chapter 1

Introduction

During the last decades, the energy demand grew exponentially, together with the services provided and the technological development. In parallel, new challenges, i.e. climate change and natural source depletion, arose. Through market instruments, including green certificate, aid investments, tax reduction or exemptions, governments tried to promote renewable energy conversion systems, increasing their competitiveness towards fossil fuel technologies. This project, funded by the European Social Fund (FSE) and Calabria Region, is also one of the initiative to promote the research and the development of new technical concepts.

In spite of the Community Research efforts and the policy measures, the fossil fuel infrastructures, with their well established know-how, are deeply rooted in the energy market, contrasting the introduction of new technologies. In fact, according to the assertions of the World Energy Outlook (WEO) 2007, published by the International Energy Agency (IEA), widely recognized for global energy analysis and statistics in the medium/long term, more than 80% of the primary energy supply still comes from fossil fuels such as coal, natural gas and oil, and this dependence is likely to continue in the coming decades. These projections have been confirmed by the WEO 2014, which highlights an increment of 15% of coal already in the next decade. Thus, even if the development of renewable technologies is essential to produce energy in a sustainable way, reducing pollutant emissions, it is also worth to note that, because of the prevalence of fossil fuel infrastructures and carbon availability at low price, it is reasonable to expect that coal will represent one of the primary energy transitional sources during the development of renewable technologies. Hence, the improvement of *Clean Coal Technologies* is a key element to lower the emissions in the short and medium term.

Clean Coal Technologies (CCT) refers to all that strategies which allows to increase the efficiency of coal conversion plants, respecting the most strict regulations. Among these strategies, including Ultra Super Critical steam power plants, coal liquefaction and gasification, the latter is extremely attractive, with a wide range of possible applications,

as will be later highlighted.

Gasification of coal with air or oxygen produces the syngas, mainly composed of H_2 , CO , CO_2 , H_2O , CH_4 and various contaminants such as NH_3 , H_2S and COS , which must be removed before using. These contaminants in fact could seriously damage the downstream technologies and harm the environment; for this reason their emission is restricted by law. A large number of purification processes is available: traditional ones require syngas cooling, followed by a subsequent heating that reduces significantly the overall efficiency of the process. The development of purification processes at high temperature is a key step to increase energy efficiency of the gasification process and reduce costs of the final products.

This work is focused on the removal of sulfur compounds, especially hydrogen sulfide, which must be reduced to concentrations of a few ppm, to both non-damage the components of the plant and to reduce the environmental impact once the hydrogen sulfide is transformed into SO_2 .

The high temperature syngas desulphurization is still recent and more efforts are needed to reach a mature level. Hot Gas Desulphurization is based on the use of regenerable metal oxide to adsorb H_2S through a chemical looping process. This work will be focused on the investigation of this technology, as well as on its applications for:

1. direct electricity generation in Integrated Gasification Combined Cycle (IGCC)
2. high value energy carriers production, such as hydrogen or natural gas
3. synthesis of valuable products, like methanol, highly required in the chemical industry.

A preliminary analysis of the desulphurization process itself and its interaction with the components of the system in which it is introduced, is necessary. This particularly applies to chemical looping. In fact, even if the chemical looping process is quite known in chemical industry, its application to hot gas desulphurization is recent and still at an early stage of its technological development, according to the definition given by the *Technology Readiness Assessment Guide* published in 2011 by the US Department of Energy and adopted by the European commission in the work HORIZON 2020. In this document, the technology development is defined as:

“the process of developing and demonstrating new or unproven technology, the application of existing technology to new or different uses, or the combination of existing and proven technology to achieve a specific goal.”

Technology Readiness Assessment Guide, (DoE, 2011)

It is also worth noting that this definition includes new process design, seen as the combination of innovative and mature technologies. The above mentioned chemical

looping applications belong to this category. They are in fact a combination of several units interconnected to each other, with different maturity level, addressed to as *Technology Readiness Levels* (TRL). This aspect cannot be neglected when comparing different process designs, since the unit with the lowest TRL would introduce same uncertainty with regard to the overall system behavior.

In the *Technology Readiness Assessment Guide* a scale of nine TRL values is defined, from TRL1 to TRL9 which indicates a developed and proven technology, as described in more detail in table 1.1 at the end of this chapter. These guidelines assist the user through the whole research and development phases to the commercial plant, as the 'Grubb curve', in figure 1.1, highlights. It is actually at this stage that the high risk and cost involved impede the technology development. The continuous black line refers to the investments' cost which decrease to almost a constant value once the technology has reached a mature level, in gray instead, risks and uncertainty are represented. They are much higher in the early stages than later. This trend is due to the acquired know-how which reduces the risk derived from the low level of understanding of the process. Following the technological development of the chemical looping process and

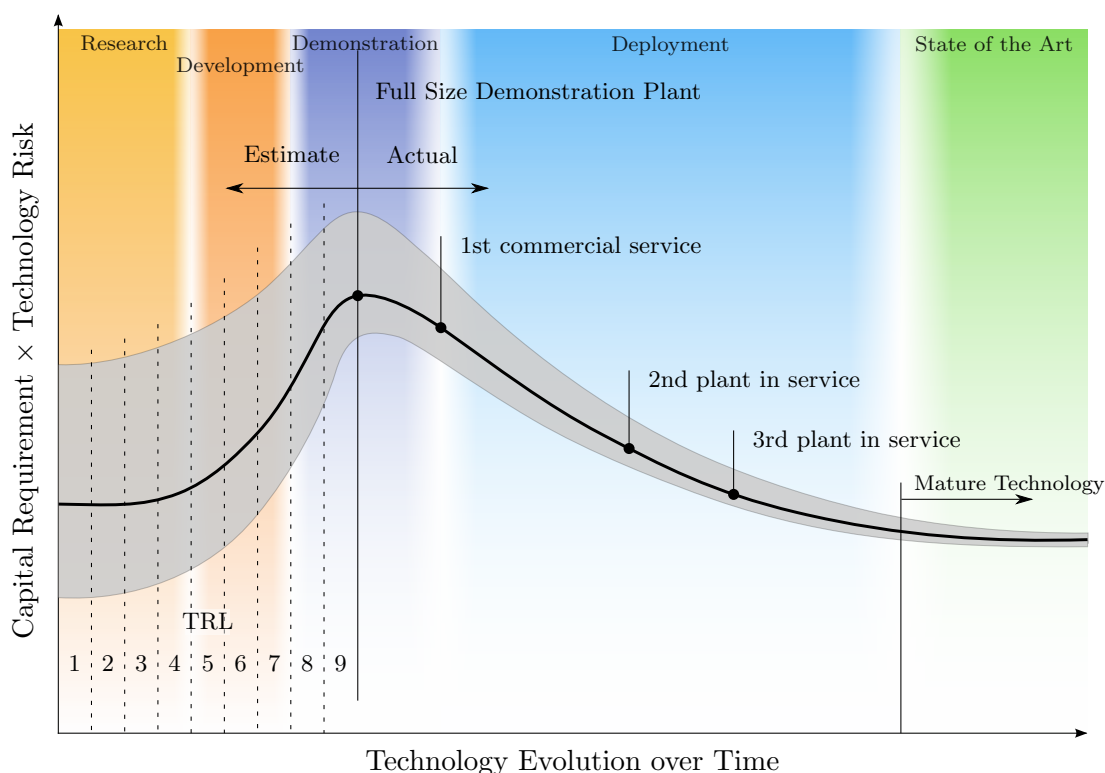


FIGURE 1.1: Grubb curve of the development of a new technology.
From: Teske, 2014

of its applications is beyond the scope of this thesis. The study will be limited to the first two steps TRL1 and 2, in which new technology concepts are identified, evaluated and selected based on literature review, modeling and simulation analysis. In fact,

Computational Aided Methods are particularly important in this phase, representing powerful tools for process analysis and optimization, process integration and cost estimation.

1.1 Thesis aims and objectives

On the basis of what has been said, the aim of this thesis will be to:

1. develop a model of the chemical looping desulphurization process with a good confidence level;
2. identify potential applications;
3. investigate the new process design through simulation analysis and the influences of the new technology on the operating conditions of the other component units, and vice versa;
4. compare the new process design with the previous one to evaluate if there is any potential advantage.

1.1.1 Methods and instruments

In order to achieve the above specified targets, an holistic approach has been used, according to the principles of the systems engineering method:

”The systems engineering method recognizes each system as an integrated whole even though composed of diverse, specialized structures and sub-functions. It further recognizes that any system has a number of objectives and that the balance between them may differ widely from system to system. The methods seek to optimize the overall system functions according to the weighted objectives and to achieve maximum compatibility of its parts.”

Systems Engineering Tools by Chestnut, 1965.

Even if there could be many objectives (minimize cost, maximize the output or the efficiency), in this context, the focus will be limited to the energetic requirements of the systems, optimized in order to increase their efficiency, respecting the technical constrains. The analysis has been carried out through modeling and simulations (M&S). Even if these words are often used as synonymous, they actually indicate different aspects:

”**Modeling** is the process of producing a model; a model is a representation of the construction and working of some system of interest. A model is similar to but simpler than the system it represents. One purpose of a model is to enable the analyst to predict the effect of changes to the system. On the one hand, a model should be a close approximation to the real system and incorporate most of its salient features. On the other hand, it should not be so complex that it is impossible to understand and experiment with it. A good model is a judicious tradeoff between realism and simplicity.”

”**A simulation** of a system is the operation of a model of the system. The model can be reconfigured and experimented with; usually, this is impossible, too expensive or impractical to do in the system it represents. The operation of the model can be studied, and hence, properties concerning the behavior of the actual system or its subsystem can be inferred. In its broadest sense, simulation is a tool to evaluate the performance of a system, existing or proposed, under different configurations of interest and over long periods of real time.”

Introduction to modeling and simulation

Maria, 1997

It is important to underline that models can mainly be divided into two categories: macroscopic models and CFD models. The CFD models are based on the conservation laws of mass, energy and momentum, giving a deep insight into the flow pattern. The mathematical model instead considers the object of study from a macroscopic point of view, with the implementation of the basic principles of mass and energy balances and/or empirical correlations. This way will be pursued to model the chemical looping process, due to the lower computational cost, which allows the integration of the model in the simulation of more complex systems.

In this work *Athena Visual Studio* has been used as modeling tool. Athena is a software package, developed to model chemical reactors, adsorption processes and catalytic reactions etc. It numerically solves sets of partial differential and/or algebraic equations with different boundary conditions. Suitable for both dynamic and steady-state analysis, it has the advantage of integrating in a single environment all tools that assist the user in the technology development phase: *modeling*, *parameter estimation*, *optimal experimental design* and *model discrimination*. Thus, the analyst is driven to a more active use of the model, not seen as a passive representation of experimental data but as an instrument which, based on the information step by step

implemented, leads to a better experimental planning. It also enables the direct link with other software (Excel, Aspen Plus, UniSim Design etc.), an extremely useful feature for subsequent simulations. As a consequence of the low maturity level of the analyzed technology and the subsequent lack of facilities, no experiments have been performed. Even if the model is based on literature data, sometimes not extremely recent due to confidential information and/or patent, it provides enough accurate results for a preliminary analysis. The chemical looping model, implemented in Athena, or more precisely, the two reactors that make up the chemical looping (as will be described in chapter 3), are later linked in UniSim Design to analyze their mutual influence and to simulate the overall system.

In *UniSim Design*, it was possible to automatically update all the inputs and outputs, allowing the user to control all the model parameter inside the UniSim environment. The latter is a commercial software, well known for system analysis and optimization. It has been used to simulate the overall plants for natural gas and methanol production and to investigate the effects of introducing the chemical looping on the whole system.

Furthermore, the use of this new technology for hot desulphurization has been evaluated in reference to an Integrated Gasification Combined Cycle. In this case, the amount of data required made the use of an other commercial software necessary, Thermoflex, specialized in simulation of power systems. Still based as UniSim on heat and mass balances, it enables the user to choose the components of the plant among the one actually available on the market, ensuring more accurate and reliable predictions.

1.2 Overview

This work is organized in two main sections. In the first part, the main focus is on chemical looping, in the second one, possible applications are discussed. Chapter 2 is a review of the technologies currently used for the desulphurization, whose limits and key strengths are underlined. In Chapter 3, the chemical looping process is described, different sorbents and reactor configurations are illustrated and compared in order to furnish a clear explanation of the factors leading to the choice of one rather than the other. Chapter 4 provides a detailed description of the developed model, analyzing the influence of the key variables on the reactor performance. The next three chapters deal with chemical looping applications: chapter 5 refers to Integrated Gasification Combined Cycles for electricity production, chapter 6 regards the production of methane by coal-syngas while chapter 7 suggests a new process design for the methanol synthesis. Finally, the most interesting results are summarized in chapter 8.

TABLE 1.1: Definition of the Technology Readiness Levels.
From: Teske, 2014 and DoE, 2011

Relative Level of Technology Development	Technology Readiness Level Definition	Description
Basic Technology Research	TRL 1 Basic principles observed and reported	This is the lowest level of technology readiness. Scientific research begins to be translated into applied R&D. Examples might include paper studies of a technology's basic properties or experimental work that consists mainly of observations of the physical world. Supporting Information includes published research or other references that identify the principles that underlie the technology.
Basic Technology Research or Research to Prove Feasibility	TRL 2 Technology concept and/or application formulated	Once basic principles are observed, practical applications can be invented. Applications are speculative, and there may be no proof or detailed analysis to support the assumptions. Examples are still limited to analytic studies. Supporting information includes publications or other references that outline the application being considered and that provide analysis to support the concept. The step up from TRL 1 to TRL 2 moves the ideas from pure to applied research. Most of the work is analytical or paper studies with the emphasis on understanding the science better. Experimental work is designed to corroborate the basic scientific observations made during TRL 1 work.
Research to Prove Feasibility	TRL 3 Analytical and experimental critical function and/or characteristic proof of concept	Active research and development (R&D) is initiated. This includes analytical studies and laboratory-scale studies to physically validate the analytical predictions of separate elements of the technology. Examples include components that are not yet integrated or representative tested with simulants. Supporting information includes results of laboratory tests performed to measure parameters of interest and comparison to analytical predictions for critical subsystems. At TRL 3 the work has moved beyond the paper phase to experimental work that verifies that the concept works as expected on simulants. Components of the technology are validated, but there is no attempt to integrate the components into a complete system. Modeling and simulation may be used to complement physical experiments.
Technology Development	TRL 4 Component and/or system validation in laboratory environment	The basic technological components are integrated to establish that the pieces will work together. This is relatively "low fidelity" compared with the eventual system. Examples include integration of ad hoc hardware in a laboratory and testing with a range of simulants and small scale tests on actual waste. Supporting information includes the results of the integrated experiments and estimates of how the experimental components and experimental test results differ from the expected system performance goals. TRL 4-6 represent the bridge from scientific research to engineering. TRL 4 is the first step in determining whether the individual components will work together as a system. The laboratory system will probably be a mix of on hand equipment and a few special purpose components that may require special handling, calibration, or alignment to get them to function.

Continued on next page

Continuation ...

Relative Level of Technology Development	Technology Readiness Level Definition	Description
Technology Development	TRL 5 Laboratory scale, similar system validation in relevant environment	The basic technological components are integrated so that the system configuration is similar to (matches) the final application in almost all respects. Examples include testing a high-fidelity, laboratory scale system in a simulated environment with a range of simulants and actual waste. Supporting information includes results from the laboratory scale testing, analysis of the differences between the laboratory and eventual operating system/environment, and analysis of what the experimental results mean for the eventual operating system/environment. The major difference between TRL 4 and 5 is the increase in the fidelity of the system and environment to the actual application. The system tested is almost prototypical.
Technology Demonstration	TRL 6 Engineering pilot-scale, similar (prototypical) system validation in relevant environment	Engineering-scale models or prototypes are tested in a relevant environment. This represents a major step up in a technology's demonstrated readiness. Examples include testing an engineering scale prototypical system with a range of simulants. Supporting information includes results from the engineering scale testing and analysis of the differences between the engineering scale, prototypical system/environment, and analysis of what the experimental results mean for the eventual operating system/environment. TRL 6 begins true engineering development of the technology as an operational system. The major difference between TRL 5 and 6 is the step up from laboratory scale to engineering scale and the determination of scaling factors that will enable design of the operating system. The prototype should be capable of performing all the functions that will be required of the operational system. The operating environment for the testing should closely represent the actual operating environment.
System Commissioning	TRL 7 Full-scale, similar (prototypical) system demonstrated in relevant environment	This represents a major step up from TRL 6, requiring demonstration of an actual system prototype in a relevant environment. Examples include testing full-scale prototype in the field with a range of simulants in cold commissioning. Supporting information includes results from the full-scale testing and analysis of the differences between the test environment, and analysis of what the experimental results mean for the eventual operating system/environment. Final design is virtually complete.
	TRL 8 Actual system completed and qualified through test and demonstration.	The technology has been proven to work in its final form and under expected conditions. In almost all cases, this TRL represents the end of true system development. Examples include developmental testing and evaluation of the system with actual waste in hot commissioning. Supporting information includes operational procedures that are virtually complete. An Operational Readiness Review (ORR) has been successfully completed prior to the start of hot testing.
System Operations	TRL 9 Actual system operated over the full range of expected mission conditions.	The technology is in its final form and operated under the full range of operating mission conditions. Examples include using the actual system with the full range of wastes in hot operations.

Chapter 2

Syngas desulphurization and sulfur recovery

Gasification processes using fuels with high sulfur content, such as coal, lead to a raw syngas rich in sulfur compounds, mainly H_2S . This component, once released in the atmosphere, reacts with oxygen forming SO_2 , responsible for acid rain. In consequence of this, the international environmental regulations and in particular the European directive 30/78/1980 impose strict emission limits. Moreover, sulfur compounds cause corrosion problems to both piping and plant components, catalyst poisoning, health and safety risk. Thus, removing H_2S impurities, in the most effective and efficient way, is essential. Many purification technologies are available, a review is presented in Wiheeb et al. 2013, while the most used ones are presented in the following sections.

They can be classified into:

- cold (low-temperature) gas desulphurization systems (CGD)
- hot (or high-temperature) gas desulphurization systems (HGD).

The former are proven technologies, at a mature level and commercially available. They operate below $300\text{ }^\circ\text{C}$, typically in a range of $20\text{-}60\text{ }^\circ\text{C}$ and some of them even require cryogenic stages. Physical and chemical absorption processes belong to this group. The main limits of cold wet technologies are the negative effect on the efficiency, caused by cooling and reheating duties, and the production of liquid effluent that must be treated.

Hot gas desulphurization systems are based on the adsorption of H_2S with sorbents. Compared to CGD, they are dry processes, operating above $400\text{ }^\circ\text{C}$. This determines an advantage in terms of both thermal efficiency and waste water treatments. These technologies are still under development and their reliability on a long term, is still not proven.

Once H_2S is removed from the syngas, it has to be recovered. Thus, the principal sulfur recovery strategies will be also described.

2.1 Cold gas desulphurization technologies

Currently, desulphurization of gas stream is mainly based on absorption systems, where the acid gas is transferred from the gaseous phase into the solvent. Depending on the interaction between component to be removed and solvent, the absorption processes can be classified into chemical and physical. In table 2.1, the most common and widespread chemical and physical absorption processes, are summarized.

TABLE 2.1: Cold desulphurization technologies

methodology	desulphurization technology	operating temperature
Absorption	Physical Absorption:	
	Selexol(DMPEG)	-40°C
	Rectisol (Methanol)	-10/-70 °C
	Purisol (NMP)	-20/40 °C
	Chemical Absorption:	
	(MDEA, MEA, DEA et.)	20/60 °C

Figure 2.2 shows a schematic representation of a gas absorption system. In the absorber, the raw syngas is washed with a regenerable solvent, exploiting the tendency of the acid components to pass into solution with particular solvents. The purified gas exits from the head of the column while the solvent saturated of the gaseous compounds previously absorbed is extracted from the bottom. Usually, this process is favored by high pressure (5-205atm) and low temperature (20-60°C). The absorption loading capacity is different whether a physical or chemical solvent is used. In the first case, the removal capacity depends on the solubility of the acid gas which, accordingly to Henry's law, is proportional to the partial pressure of the component that must be removed. Thus, for a given partial pressure, the amount of solvent required is proportional to the volumetric gas flow rate. Instead, when chemical absorption is used, the required solvent is proportional to the removed acid gas. For this reason, as figure 2.1 highlights, the use of physical processes is convenient when the compound to be removed is present

at high concentrations, thus with high partial pressure, in this case in fact, the volume of solvent required is less than that need in chemical processes for the same operation. In any case, the solvent, rich in acid compounds, must be regenerated, releasing the

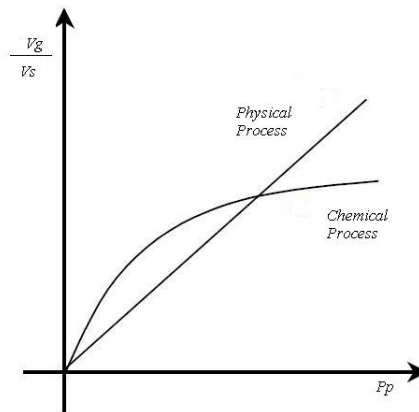


FIGURE 2.1: Equilibrium in chemical and physical absorption processes

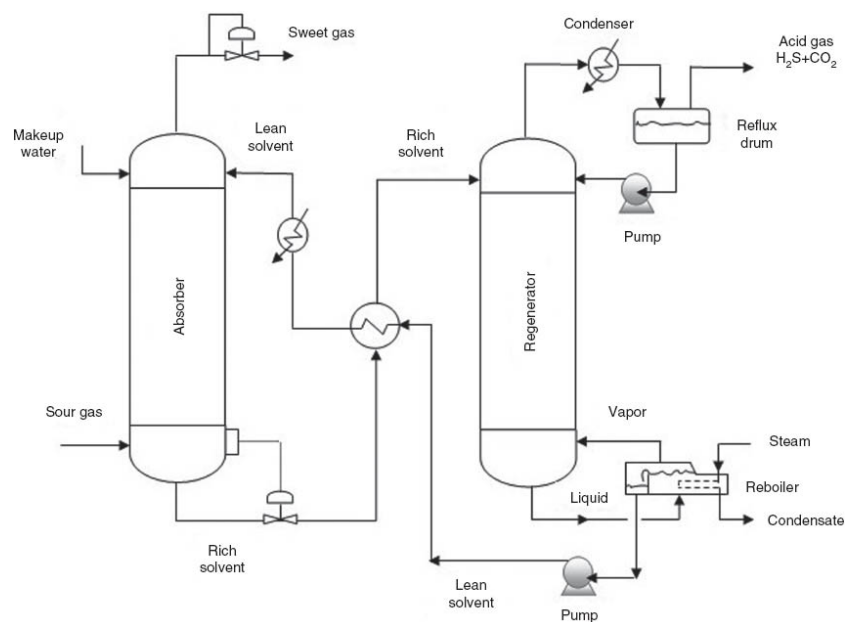


FIGURE 2.2: Schematic representation of the absorption process. Source: Wiheeb et al., 2013

acid components before being recycled to the absorber. This process is carried out at high temperature (115-130°C) and low pressure (1.4-1.7atm). There are three possible regeneration strategies:

- flash desorption
- stripping
- hot regeneration (reboiling)

The flash desorption represents the most economic method. It is based on pressure reduction, so that it will be the final pressure which determines the acid gas content in the regenerated solvent.

When stripping is used, the pressure reduction is followed by a desorption process where the rich solvent is contacted with an inert gas stream. In this way an almost pure solvent can be obtain. The drawback could be a diluted steam of contaminants leaving the regenerator.

The highest purity can be achieved with a reboiler. In this case in fact, the temperature increase reduces the solubility of the acid gas, which is released in the gas phase and acts as a "stripping stream". This represents the most expensive method, due to the heat required by the reboiler.

Flashing and stripping are usually applied for physical absorption while a reboiler is needed to break the bonds between solvent and solute in chemical absorption processes.

The regenerated solvent is then compressed, cooled and recirculated to the absorber, while the gaseous compounds extracted from the regeneration column are sent to a specific treatment section.

Physical Absorption

These are the principal physical absorption processes currently used:

1. Rectisol
2. Purisol
3. Selexol

The first two have been developed for high pressure syngas production, (Hochgesand, 1970). The Rectisol process was patented by Lurgi and Linde. Its first application was during the 1950s in the Sasol-Secunda CTL Plant, which further proved its suitability for H₂S and CO₂ removal. Moreover, it was observed that it allows to absorb many other contaminants like ammonia and cyanides.

The Purisol process instead has been developed by Lurgi. It was applied to natural gas sweetening, even if recent successful applications on high pressure hydrogen have also been developed. It showed to be very selective towards H₂S.

Chemical Absorption

Chemical processes differ for the use of solvent based on aqueous solutions of amines. Many chemical solvents are available for syngas sweetening: Monoethanolamine (MEA), diethanolamine (DEA), methyldiethanolamine (MDEA), di-isopropanol amine (DIPA), belonging to the group of alkanol-amines. The first alkanolamines, as sorbent for acid

gases removal, have been developed by RR Bottoms in 1930. Triethanolamine (TEA) were the earliest commercially available. Today MEA and DEA or a combination of both are widely used. MDEA shows an higher affinity with H_2S and is usually preferred for desulphurization process also because of its lower energy requirements for solvent regeneration. Often a combination of different solvents is used but should be considered that this makes the regeneration a more critical step.

As shown in table 2.1, typical absorption processes are carried out at temperatures of 20-60°C but the reduction of removal efficiency as a consequence of temperature increase has to be taken into account. In fact, as reported in Wiheeb et al. 2013, increasing the temperature from 20°C to 60°C, the H_2S removal efficiency decreases from 99% to 93% .

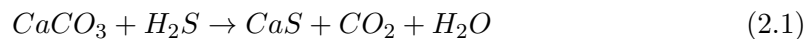
2.2 Hot gas desulphurization technologies

The increasing interest for high temperature sulfur removal is due to its potential in enhancing the efficiency, avoiding heat loss and reducing H_2S concentration below 1 ppm. Hot gas desulphurization is based on the adsorption of H_2S on solid compounds, mainly metal oxide which, under reducing conditions, are converted to their sulfide. Sorbents can be classified into non-regenerable and regenerable. The former are used for *in situ*, while the latter for external desulphurization, (Meng et al., 2010).

2.2.1 *In situ* desulphurization

In the *In situ* desulphurization, the sorbent is added directly into the gasification chamber at temperatures of 800-1000°C, (Abbasian et al., 1990b). Sorbents typically used for this application are alkali metals (Ca,Ba,Sr), as well as natural sorbents, containing high level of them, like dolomite ($CaCO_3MgCO_3$) and limestone ($CaCO_3$), (Abbasian et al., 1990a, Álvarez Rodríguez and Clemente-Jul, 2008, Borgwardt and Roache, 1984). Limestone, depending on the operating conditions, reacts with H_2S through two different mechanism:

direct sulphidation:



or for sufficiently high temperature, CaO is produced by calcination of $CaCO_3$, which then reacts with the hydrogen sulfide:



Studies performed by Fenouil and Lynn, 1995a,b Zevenhoven et al., 1996, 1998 and on limestone and dolomite highlight the influence of the temperature on the sulfur removal capacity.

The highest desulphurization level can be reached for temperature slightly above the calcination temperature, because of thermodynamical equilibrium. Furthermore, for pressure of 35 bar typical of many gasifiers, with already low CO₂ and H₂O concentration, it is difficult to reduce H₂S below 100 ppm, as figure 2.3 shows. The

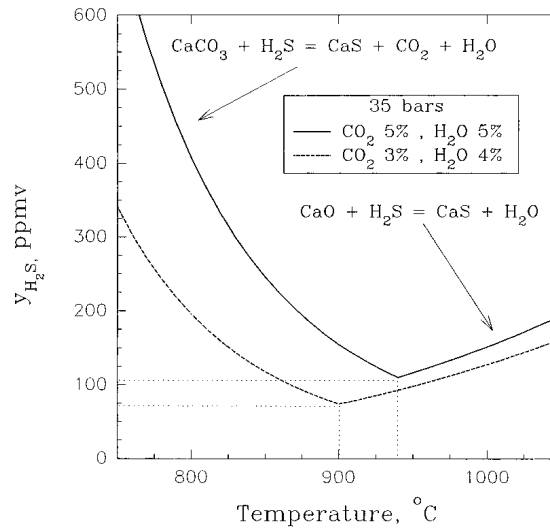


FIGURE 2.3: H₂S equilibrium concentration as a function of temperature, H₂O and CO₂ (from: Fenouil and Lynn 1995a)

equilibrium concentration of H₂S can be obtained through the correlation suggested by Fenouil and Lynn 1996:

$$y_{H_2S} = 0.00175 y_{H_2O} y_{CO_2}^{0.364} P^{0.364} \quad (2.4)$$

where P is expressed in bar. In spite of the low price of the CaO-based sorbents, the thermodynamic limitation previously discussed and disposal problems of the produced waste limit the use of *In situ* desulphurization.

2.2.2 External desulphurization

In contrast to the *in situ* desulphurization, the external desulphurization occurs in a subsequent step. The syngas, exiting the gasifier, is introduced in a reactor and put in contact with the sorbent, which reacts with H₂S and is converted in its sulfide. The sorbent is then regenerated with oxygen, steam or SO₂ to restart the cycle. Depending on the fluidizing agent, a stream containing SO₂ or H₂S will be obtained at the regenerator exit. This approach is also known as Chemical Looping Desulphurization Process and will be analyzed in detail in the next chapter.

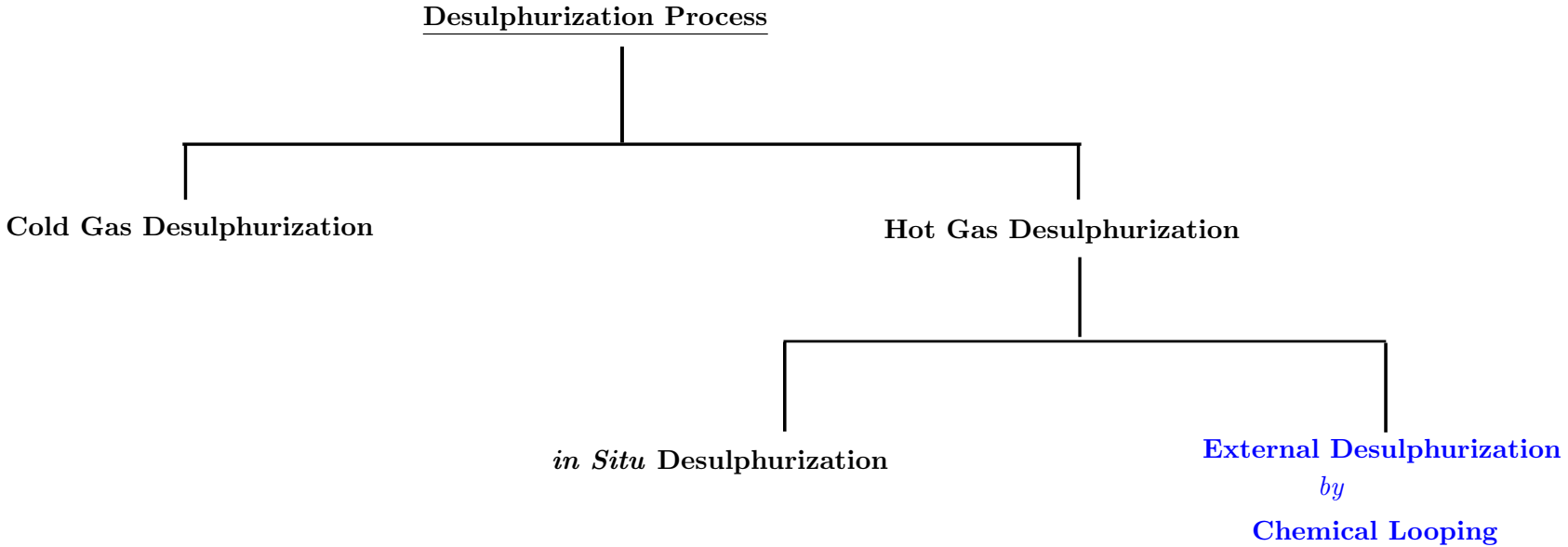


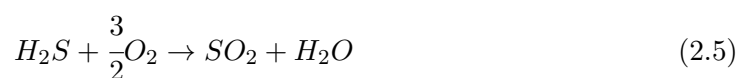
FIGURE 2.4: Sulphur Removal Technologies

2.3 Sulfur recovery

The gas stream rich in sulfur compounds, at the exit of the desorption column, is sent to the sulfur recovery unit to convert sulfur compounds to elemental sulfur. The aim of this recovery is two-fold: to obtain elemental sulfur salable on the market and to minimize pollutant emissions to the atmosphere. According whether H₂S or SO₂ is contained in the gas stream, different approach are used. Generally, H₂S recovery is obtained by the Claus Process, while SO₂ is treated with wet scrubbers.

2.3.1 Claus Process

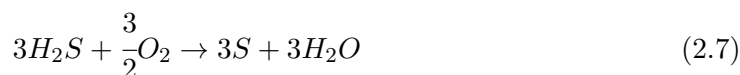
As described by Cau and Cocco, the Claus Process allows to recover 90-98% of the initial sulfur, converting it to elemental sulfur. The main reactions are the following:



A thermal reaction, where part of the H₂S is oxidized to SO₂



A catalytic stage, in which H₂S reacts with SO₂ to form elemental sulfur and water. Thus the global reaction will be:



The first step is represented by a fast and high temperature (1200-1400°C) oxidation carried out with an amount of air sufficient to oxidize about a third of the H₂S. Afterwards, the hot gaseous stream is cooled in a heat recovery steam generator producing medium pressure steam and sent to the catalytic reactor at a temperature of about 200-260°C. One or more of these thermal and catalytic stages could be necessary to promote further H₂S conversion. Finally, the gas is cooled to condense and remove the sulfur and the thermal energy released is recovered producing low pressure steam.

If the H₂S concentration is below 10-15% in volume, other processes, like Selectox and Stretford are used. They consist of a catalytic stage to convert directly H₂S into elemental sulfur.

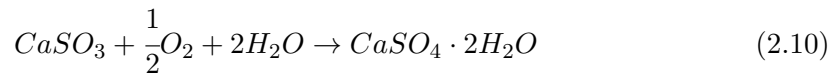
When high sulfur recovery is required, the exhaust gas of the Claus plant, known as "tail gas", is sent to an other unit for further treatment. This section is usually used to dispose waste gases from other sections of the plant.

The Scot process is the most widely used. It consists of a low temperature catalytic stage, which allows to convert the sulfur compounds present into H₂S, through a

cobalt and molybdenum based catalysts. The H_2S is then cooled from $150^\circ C$ to ambient temperature and sent to an absorption column operating with amines. The H_2S -rich gas, at the exit of regeneration column is recycled to the Claus section while the treated gas from the top of the absorption column are incinerated or directly released into the atmosphere.

2.3.2 Wet Flue Gas Desulphurization

SO_2 is produced by combustion processes as a consequence of the oxidation of sulfur compounds or, as for chemical looping, it derives from sorbent regeneration as will be described in chapter 3. There are many technologies to remove sulfur dioxide, one of these are the “wet scrubbers”. As described in Lozza 2006, they are used in at least 90% of the applications and allows to obtain very high removal efficiency, 92-95%. Moreover they represents a mature technology, with a well established know-how. They are based on absorption processes; the gas to be treated is put in contact with an aqueous solutions of calcium based sorbent which reacts with SO_2 producing gypsum or hydrated calcium sulphate ($CaSO_4 \cdot 2H_2O$), as equations 2.8 to 2.10 show. For an optimal sulfur recovery, an excess of sorbent should be used (Ca/S equal to 1.1/ 1.2).



The calcium based sorbents usually used are limestone ($CaCO_3$), dolomite ($CaCO_3 \cdot MgCO_3$) or hydrated lime ($Ca(OH)_2$). The former are usually preferred because of their low cost.

To ensure a commercial high quality product, as equation 2.10 show, a sufficient amount of oxygen, should be provided. This is obtained by blowing air on the bottom of the scrubber, as highlighted in figure 2.5.

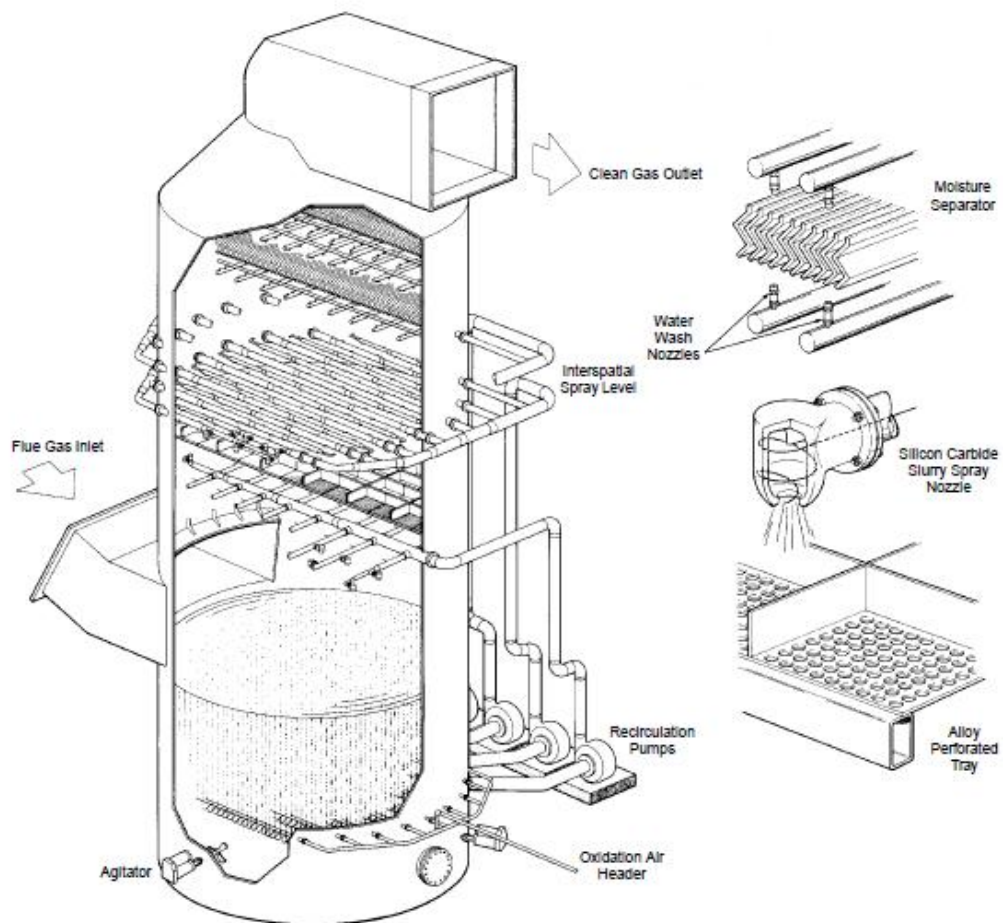


FIGURE 2.5: Wet FGD. From:Lozza 2006

Chapter 3

Chemical looping desulphurization process

Chemical looping has gained in few decades increasing attention of the scientific community, due to its many applications. From a general point of view, it is based on the mechanism of adsorption. The term *adsorption* refers to heterogeneous processes, in which bonds are established between the surface of the solid and the reacting component. Thus, the adsorption capacity is approximately proportional to the available surface area which, in case of porous sorbents, is not only the external surface, but also the one formed by the internal walls of the pores. For this reason, the solid can usually adsorb up to minimal traces of solute, making the process of adsorption ideal to treat dilute solutions.

The chemical looping system consists in two reactors: a fuel reactor where the sorbent is reduced and the regenerator where it is re-oxidized with a cycling process.

Based on this basic concept, a wide range of applications have been developed, analyzed and discussed:

- Chemical Looping Combustion (CLC), for combustion purpose delivering pure CO_2 in the dried flue gas that can be immediately captured and stored in CCS application; It includes Syngas-CLC process, *in situ* Gasification CLC, Chemical Looping with Oxygen Uncoupling (CLOU).
- Chemical Looping for H_2 production which includes Chemical Looping Reforming (CLR), Chemical Looping Hydrogen (CLH), Coal Direct Chemical Looping Process (CDCL), Syngas Chemical Looping Process (SCL).
- Calcium looping cycle for CO_2 capture

Detailed review of chemical looping are widely available in literature, (Adanez et al., 2012, Fan, 2011), as well as on the used intermediate material which, for the above

mentioned applications is known as oxygen carrier, as firstly introduced by Lewis and Gilliland 1954 in their patented work "Production of pure carbon dioxide".

Only later, in 1990s chemical looping has been applied for hot gas desulphurization.

3.1 Chemical looping desulphurization

In the chemical looping process for hot gas desulphurization, the sorbent, usually a metal oxide, is brought in contact with the syngas and is converted into its sulfide. In the next step, the sorbent is regenerated with air so as to restart the cycle. These reactions, represented schematically in figure 3.1, can be expressed in a general form as follow:

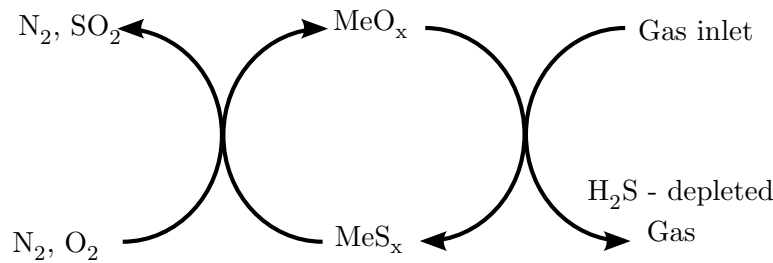
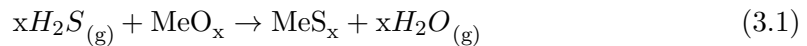
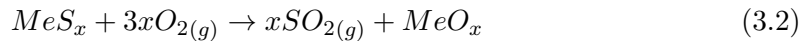


FIGURE 3.1: Scheme of Chemical looping desulphurization

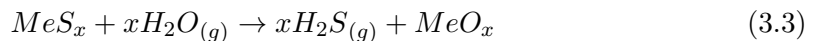
desulphurization:



regeneration:

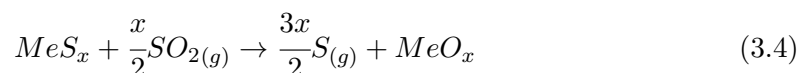


For the regeneration, reaction 3.2 considers oxygen as oxidizer, since this is the most common procedure, but also steam or even SO₂ can be used, depending on the particular sorbent. Using steam as oxidizer the reaction becomes:



Steam allows to operate at constant temperature, while the regeneration with oxygen leads to strongly exothermic reaction. Regarding the regeneration with SO₂, the main advantage is represented by the direct production of elemental sulfur but it is applicable

only to few sorbents: Iron, Cerium and Manganese, according to reaction 3.4



During the regeneration, side reactions could occur, as the formation of metal sulfate, an inert with respect to the desulphurization, which consequently reduces the sorbent reactivity:



Thus, it is important to determine the conditions under which reaction 3.5 occurs, in order to guarantee a satisfactory performance over many sulphidation and regeneration cycles.

Since the sorbent properties and reaction mechanisms change with temperature, pressure and/or syngas composition, it is essential to specify the operating conditions.

In particular, it would be advantageous to use an adsorption pressure close to the gasification pressure, usually of 20-30 bar, to avoid the use of compressors.

Similarly, the regeneration should be carried out at the same pressure of the absorption process, to reduce problems linked to pressure change.

Regarding the temperature, two different ranges could be identified:

- high desulphurization temperature, above 650 °C ensures high reaction rate but also increases the risk of sintering which leads to lower desulphurization efficiency
- low desulphurization temperatures, in the range of 350-550 °C, are characterized by lower reaction rate but present the advantage of a good compromise between thermal efficiency and technical and economical feasibility.

Lower temperatures reduce sintering problems ensuring good performance for longer periods, contemporary ensuring a wider sorbent choice, (Slimane and Abbasian, 2000b). Once the area of analysis is well defined, the subsequent step is a careful investigation of the sorbent characteristics.

3.2 Sorbent Screening

The development and commercialization of chemical looping desulphurization systems strongly depends on the improvement of sorbent materials properties. As underlined in Atimtay and Harrison 1998, the main features required to a sorbent are the following:

- selective reaction with H₂S and COS to guarantee a removal efficiency up to 99% in the temperature range of 400-650°C
- no side reactions such as sulfate formation or reduction to pure metal

- chemical stability and high reaction rate for both sulfidation and regeneration
- good thermal properties to avoid sintering as well as reduction of the sorbent porosity and of the contacting surface area
- mechanical strength to reduce attrition or cracking and ensure the lowest loss of sorbent over many cycles.

Not surprisingly, finding an element, that can fulfill all these requirements simultaneously, is not an easy task. Often a compromise is needed. To increase the rate of reaction for example, smaller particles with high porosity and large surface area could be used, but the resistance to attrition and deterioration decreases proportionally.

For a first screening, in order to identify the suitable sorbents, thermodynamic calculations have been performed by many authors, (Girard et al., 2014, Meng et al., 2009, Slimane and Abbasian, 2000b, Westmoreland and Harrison, 1976). Thermodynamic studies provide two important information:

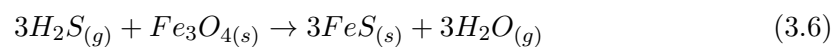
- operating conditions under which a reaction is promoted and its products are stable
- heat of reaction.

Westmoreland and Harrison 1976 analyzed the oxides of 28 elements and determined their sulfur removal at equilibrium, minimizing the free energy. From these results, considering as selecting criteria a removal efficiency of more than 95%, the most promising sorbents turned out to be Zn, Cu, Fe, Mo, Ba, Ca, Co, Mn, Sr, V and W. Every sorbent has its own advantages and limitations. Further studies tried to overcome the sorbent degradation by adding a supporting material, to increase the mechanical stability. Mixed oxides and natural sorbents containing high concentration of them have been also tested. As in Frau 2009, the most suitable for hot gas desulphurization are described: Iron oxide, cerium oxide, copper oxide, tin oxide, zinc oxide and mixed-metal oxide such as zinc titanate.

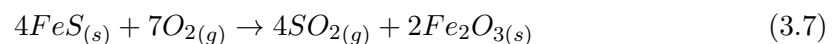
Iron oxide

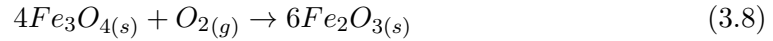
Iron oxide reacts with H_2S according to the following reactions:

desulphurization

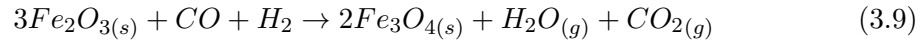


regeneration





As reactions 3.7 and 3.8 show, during the regeneration both the converted sorbent and the unreacted Fe_3O_4 are oxidized, producing Fe_2O_3 which reacts with CO and H_2 to produce again Fe_3O_4 .



This step represents a loss in term of valuable components in the syngas stream. Moreover, this sorbent is not suitable for desulphurization temperatures above 550°C, because of thermodynamic equilibrium leading to too low conversions. Nevertheless, in the temperature range of 400-450°C, it shows a high reactivity which makes it suitable for medium temperature applications.

Cerium oxide

Cerium oxide can be used for high temperature applications, above 600°C, where it shows a good removal efficiency and easy regeneration, which can be carried out using SO_2 as regenerating agent. The possibility to obtain elemental sulfur directly from the regeneration process, avoiding the recovery section, represents an extremely interesting property. Nevertheless, its limited success is due to the high cost and its low absorption capacity at low temperatures, which makes necessary more than one desulphurization step.

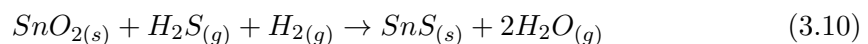
Copper oxide

The main limit of Copper oxide (Cu_2O) is the tendency to reduce to elemental copper. In recent studies to stabilize the sorbent and increase its sulfur removal efficiency the use of mixed metal oxide, in particular manganese, and alumina have been suggested in Slimane and Abbasian 2000a

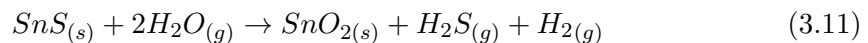
Tin oxide

Tin oxide SnO_2 adsorbs H_2S according to the following reaction:

desulphurization



regeneration

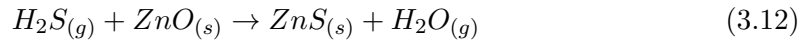


As reaction 3.11 shows, the regeneration is carried out using steam. This allows to avoid the strong temperature increase typical of air regeneration processes. In this way, it is possible to preserve the chemical and mechanical properties of the sorbent, over several sulfidation/regeneration cycles. According to the studies of Haldor Topsoe A/S, SnO_2 allows to obtain final H_2S concentrations below few ppm. However, the main drawback is represented by its stability, for temperatures above 231.9 °C, in fact, Sn is stable in liquid and metallic form.

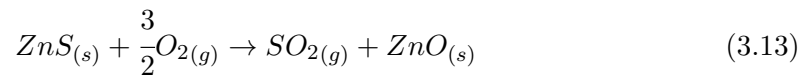
Zinc oxide

Zinc oxide reacts with H_2S as reaction 3.12 shows:

desulphurization



regeneration



As eq. 3.13 shows, oxygen is used as regeneration agent, because of the highly exothermic reaction and the risk of sulfate formation, diluted air is used. Regarding the desulphurization step instead, ZnO shows excellent performance:

- highly favorable thermodynamics
- fast reactions

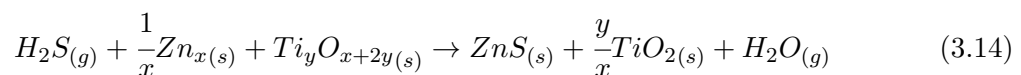
However, ZnO shows a strong tendency to volatilization with consequently loss of sorbent.

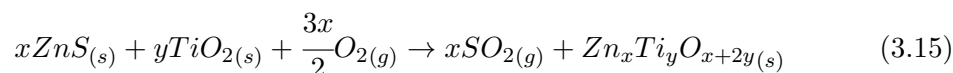
For this reason it is used in mixture with other metal oxide. According to Elseviers and Verelst 1999, among zinc-based sorbents, zinc titanate (Zn_2TiO_4) is the most effective for intensive desulphurization.

Zinc Titanate

Zinc Titanate (Zn_2TiO_4) is composed of zinc oxide and titanium dioxide, but only the former reacts with H_2S , while TiO_2 increases its stability and reduce its tendency to volatilization.

desulphurization



regeneration

The properties of this sorbent are strongly affected by the relative amount of the two compounds, since increasing the ZnO content the stability of the sorbent decreases, but its removal efficiency increases. An optimal ZnO /TiO₂ value of 1.5 has been obtained. Particularly important is the regeneration process carried out with dilute air to prevent sulfate formation. Moreover, the temperature has to be in the range of 725-760 °C; temperature above 725 °C prevents the formation of sulfates, while temperatures below 760 °C prevents ZnO sintering. Even if Zinc Titanate allows to obtain very high removal efficiency, it is quite expensive. In recent studies (Jun et al., 2001), Zn-Ti-based sorbents mixed with cobalt and nickel have been tested showing a good desulphurization capacity without deactivation over many sulphidation/regeneration cycles.

Due to its properties and ensuring low residual H₂S concentration of the order of few ppm at temperature of 500-650°C, zinc titanate will be used in the developed model.

It is worth pointing out that physical and mechanical properties, such as sorbent dimension, gas-solid interfacing surface area, attrition resistance are also influenced by the used reactor. This aspect will be analyzed in detail in the next section.

3.3 System Configuration

As previously mentioned, the hot gas desulphurization consist of two reactors, which could work in series or in parallel. The reactor types that can be used are:

- fixed bed
- fluidized bed
- transport reactor

Operating conditions as well as syngas composition have a strong impact on the choice of the reactor type, which on the other hand strongly affects the mechanical and physical properties of the sorbent. Table 3.1 summaries the main characteristic of the above mentioned reactors, discussed with more detail in the following sections, Frau 2009.

TABLE 3.1: Main characteristic of reactors used for hot gas desulphurization. Adapted from: Atimtay and Harrison 1998, Frau 2009

Reactor type	Fixed bed	Fluidized bed	Transport reactor
Reactor features:			
Operation mode	discontinuous	continuous	continuous
reactor dimensions	large	medium	small
pressure drop	high	medium	low
heat exchange	troublesome	good	good
temperature distribution	large temperature gradients	uniform	uniform
gas velocity (m/s)	0-0.7	0.01-0.4	2-20
solid hold-up	0.6	0.3-0.55	0.01-0.1
solid residence time	hours	minutes	seconds
sorbent characteristics:			
particle size	2-10 mm	50-500 μm	50-500 μm
particle utilization efficiency	small	high	maximal
particle attrition	low	medium	high

Fixed bed reactor

In early studies, the desulphurization process was based on the combination of two fixed bed reactors, as represented in figure 3.2a. The syngas is sent to one reactor while the other is regenerated. When the H_2S concentration reaches the breakthrough value, the valve switches the syngas to the regenerated reactor. Thus, in each reactor alternatively occurs regeneration and desulphurization processes. This is responsible of the discontinuous operating conditions. Because of the low attrition, high mechanical strength is not required but a pellet of large size (3-6mm) is needed to reduce the pressure drop. However this leads to higher diffusion resistance with consequently lower reaction rate.

Even if these problems could be reduced using egg-shell sorbent, where the active material is a layer on an inert core, the experiments with fixed bed reactors have shown unsteady SO_2 production, due to the low heat exchange which could lead to high temperatures, damaging the equipment and reducing the sorbent reactivity. As previously mentioned, in fact, the regeneration reaction can lead to significant temperature increase. For all these reasons, this configuration is not used.

Fluidized bed reactor

Compared to fixed bed reactors, fluidized bed ensures continuous operating conditions and higher flexibility since it enables to use different operating conditions for the regeneration and desulphurization. Two different units are used, one for each process step, in this case it is the sorbent which circulates between the two reactors. For this reason, higher sorbent resistance to attrition is required, compared to fixed bed but in any case lower than that necessary for the riser. The fluidized bed reactor offers a good compromise between the complexity of the entrained bed reactor and a good heat transfer which together with a uniform temperature allows to avoid hot spots and uncontrolled temperature increase. For this configuration, particles of low dimension are used, in the range of 100-300 μm . This ensures an optimal reactivity, with residence times in the order of minutes. Nevertheless, some important disadvantages, linked to bubble formation, should be considered:

- complex flow behavior, the gas moves both in bubble and emulsion phase
- by-passing of the gas in bubble phase, due to a limited mass transfer between the two phases.

Transport reactor

Similarly to bubbling fluidized bed, two units are used, one for the regeneration the other for the desulphurization, while the solid sorbent circulates between the two reactors. This systems are characterized by:

- reduced amount of sorbent in the reactor
- short residence times
- high throughput
- excellent gas-to-particle mass and heat transfer

In this systems, the sorbent is diluted. This allows to avoid temperature run away during the regeneration process, but higher sorbent reactive is required, moreover if considered the low residence time in the order of seconds. However, sorbent reactivity does not represent a problematic aspect if considered that small size particles ($<300 \mu\text{m}$) are used, but the high particle velocity imposes strict requirements on their mechanical strength.

Based on the above described reactor type, the different configurations considered for hot gas desulphurization are schematically represented in figure 3.2.

Usually reactors of the same type, dimension and constructing material are used for both desulphurization and regeneration reactors, while different operating conditions are chosen. However, since similar particle size are used for both bubbling fluidized bed and circulating fluidized bed reactors, hybrid systems are also developed. Further considerations are needed for a good technical choice. As reaction 3.5 shows during the regeneration side reactions leading to formation of sulfate occur. Even if sulfates decompose, when high temperature are reached, their formation and decomposition cause mechanical stress which leads to particle breakage i.e loss of sorbent. A critical step is represented by the regeneration where sulfates formation and sorbent deterioration increase proportionally with time, with a negative impact on the overall desulphurization process. A good solution to minimize and prevent this problem is to reduce the contact time between the sorbent and the regeneration gas. This aim can be achieved of course through fluid bed but even more with risers, where the residence time is in the order of seconds. Moreover, to meet economic requests, due to the high operating pressure, the use of small reactor diameter would be preferred. The stress that the material undergoes because of the pressurized fluid is directly proportional to the reactor diameter. Since usually a huge amount of gas is elaborated, if small reactor diameter are used, high gas velocities are required. For all these reasons, the chosen reactor type is a transport reactor, i.e. a riser, for both

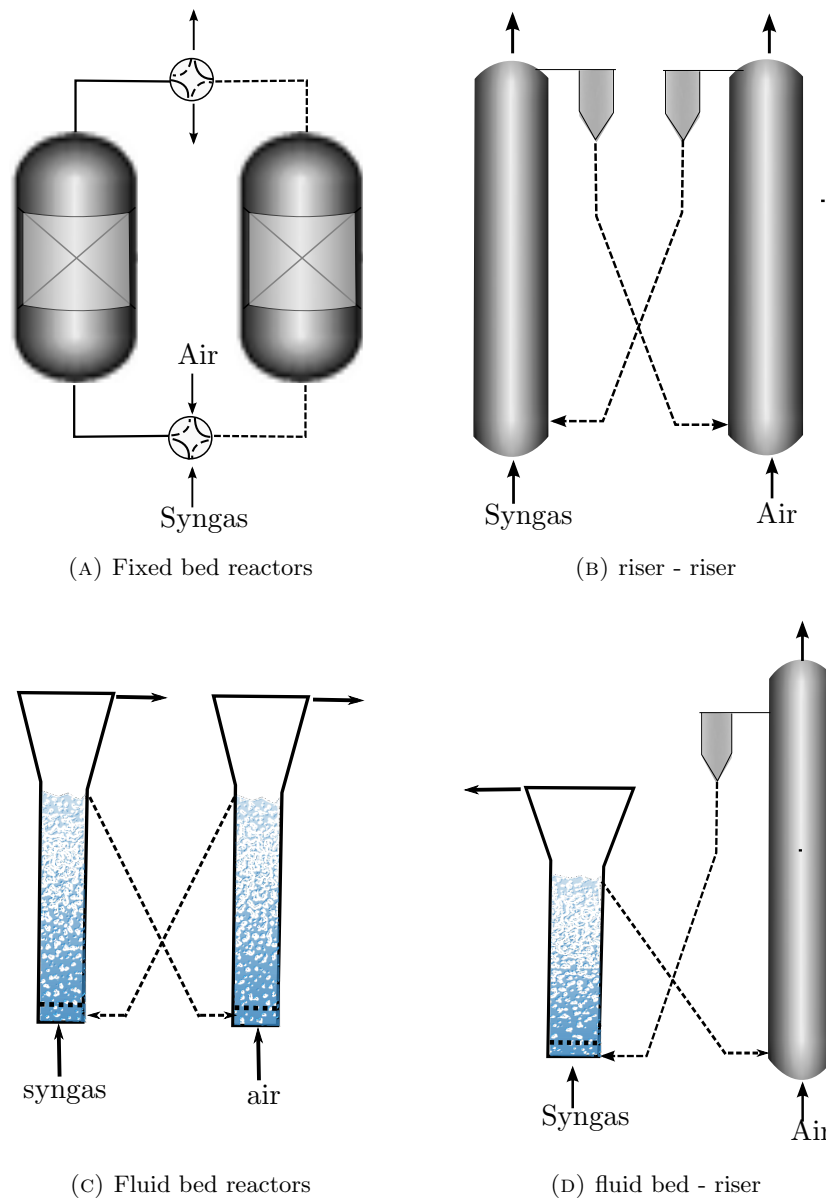


FIGURE 3.2: Reactor types and possible configurations

regeneration and desulphurization. A more detailed representation of these configuration is given in figure 3.3 for the particular case of zinc titanate. As shown in figure 3.3, the syngas is introduced in the desulphurization reactor, represented in yellow, from the bottom. The flue gas carries along with it the particles of zinc titanate sorbent due both to their small dimensions and weight and to the high gas velocity. During their residence time in the reactor, the particles react with H_2S as described by reaction 3.14. The reacting ZnO (TiO_2 is in fact inert as stated above) is, in this way, converted in its sulfide ZnS . In the upper region of the of the riser, the cyclone allows to separate from the gas stream the heaviest particles which fall to the hopper. Afterwards, they are sent to a second reactor, represented in blue, for the

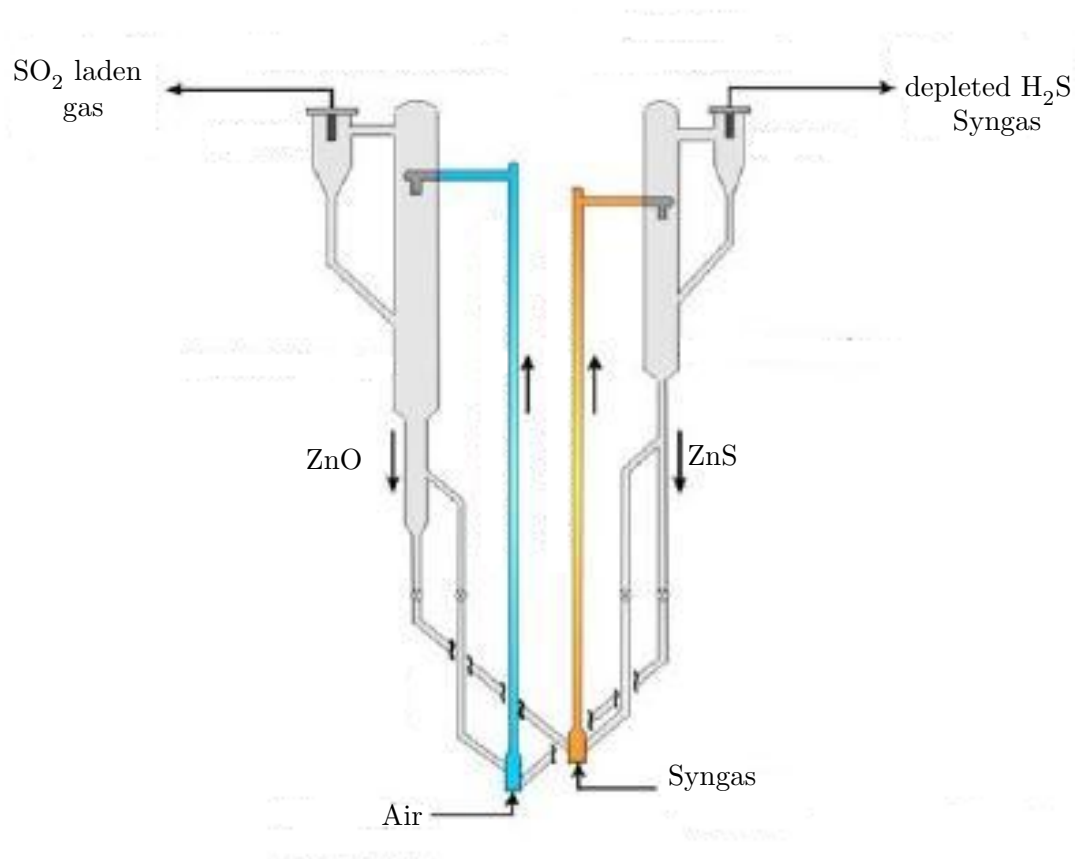


FIGURE 3.3: Chemical looping desulphurization by transport reactors. Adapted from: Monazam and Shadle 2005

regeneration. The process is similar from a hydrodynamic point of view, but as fluidizing agent air is used, or more precisely, air diluted with nitrogen reaching an O₂ concentration of 2% to avoid the formation of zinc sulphate. The regenerated zinc titanate is again separated from the gas containing SO₂ and recycled back to restart the process, while the SO₂ laden gas is recovered by wet scrubbing as gypsum, as described in chapter 2.

A model of these system has been developed. The two riser, highlighted in blue and yellow in figure 3.3 have been implemented in Athena Visual Studio, while the interaction between the two reactors has been realized in UniSim with a proper interface code. These aspects will be described in detail in the next Chapter.

Chapter 4

Chemical Looping Model

In order to model a chemical reactor, it is important to identify the main variables involved and all the aspects influencing the process.

With reference to syngas desulphurization through chemical looping, it must be considered the heterogeneous non-catalytic nature of the process. This being so, gas-solid interaction, gas-solid slip velocity, fluidization regime, as well as temperature distribution are key variables in order to determine the reaction rate.

Specifically, as figure 4.1 shows, kinetics, hydrodynamic and heat transfer effects should be considered simultaneously because of their mutual influence.

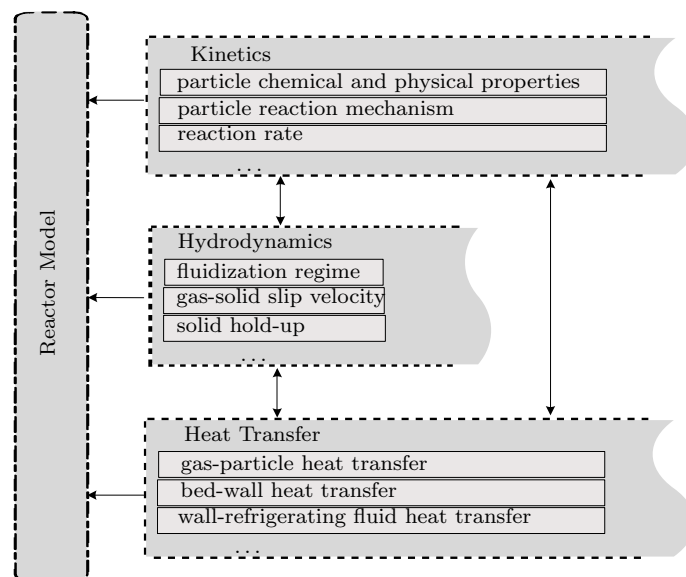


FIGURE 4.1: Chemical reactor model: influencing aspects

A deep understanding of all these aspects leads to a more reliable model, able to predict the reactor behavior under different operating conditions, also useful for reactor scale-up. On the other hand, the reactor model will allow to learn more about the involved variables and their complex interactions. A model is in fact, as precise

and accurate as its assumptions are. Even a model which fails to fit the data, would give important information, underlying, that the conceptual representation of the reality could not be enough close to the real phenomenon, and that, reconsider the main hypothesis, on which the model is based, could be necessary.

In the following sections, the main assumptions regarding kinetics, hydrodynamic and heat transfer will be discussed, with reference to the specific case of a transport reactor for syngas desulphurization.

4.1 Reaction Kinetics

To determine the reaction rate, a wide variety of models are available in literature. Every model describes the reality with a set of equations based on different assumptions, which try to describe the most relevant aspects of the particle reaction mechanism and neglect the non influential ones. More precise and detailed is this conceptual representation, more complex would be the mathematical formulation. To this complexity not always corresponds a more accurate solution which justify the effort and the much higher computational cost, and as Levenspiel states, "It is of little use to select a model which very closely mirrors reality but which is so complicated that we cannot do anything with it", (Levenspiel, 1999). Thus, it is advisable to use a model which is as simple as possible. In spite of the great variety of models, they are actually following two tracks: the grain model (GM) or the shrinking core (SCM). The shrinking core model, do not require specific information of the internal structure of sorbent, while the grain model, proposed by Szekely and Evans, 1970, requires more information, such as the specific surface area or the particle porosity to characterize the internal structure of the particle.

In the following sections, the progressive-conversion model, the Shrinking Core Model (Yagi and Kunii, 1955) and the Grain Model (Szekely et al., 1976) will be discussed and compared. To describe the above mentioned models, we will refer to the following generic reaction:



4.1.1 Uniform-Conversion Model

This model is based on the idea that the gas easily access through the particle. Thus, as figure 4.2 shows, the concentration of solid reactant changes gradually and homogeneously in the particle. This assumption is suitable for sorbents with high porosity but cannot be applied if the reaction is diffusion limited.

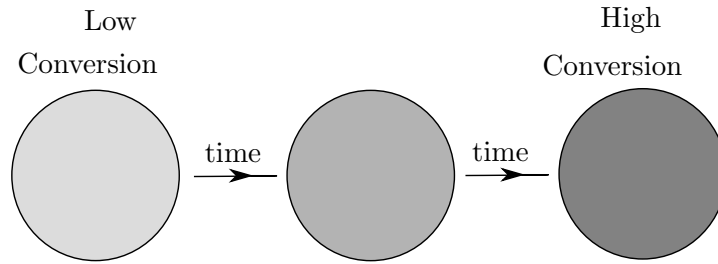


FIGURE 4.2: Uniform Conversion Model: schematic representation.
Adapted from: Levenspiel 1999

The rate of reaction can be expressed by the following equation:

$$\frac{dX}{dt} = k'(1 - X)C_A \quad (4.2)$$

where C_A is the concentration of the reacting gas in mol/m^3 , t the time, X the particle fractional conversion and k' the reaction rate constant in $\text{m}^3/(\text{mol s})$

A key parameter is the specific absorption velocity \mathfrak{R} , defined as the mol of gas reacted per second per kilogram of sorbent. It can be obtained by the following equation:

$$\mathfrak{R} = \frac{1}{b} \frac{\omega_B}{Mw_B} \frac{dX}{dt} \quad (4.3)$$

Where ω_B represents the kilograms of reacting compound B per kilogram of sorbent and Mw_B its molecular weight.

4.1.2 Shrinking core Model

In the Shrinking Core Model, proposed by Yagi and Kunii 1955, it is assumed that the reaction consists in a sequence of steps in series, as figure 4.3 shows:

1. Mass transfer from the bulk gas to the pellet surface
2. Penetration and diffusion of the reactant gas through the product layer to the reactant front
3. Reaction between gas and solid at the reaction surface
4. Diffusion of the product gas through the product layer
5. Diffusion of the product gas through the film

Since the last two steps do not contribute to the resistance to the reaction, they will not be further considered.

According to this conceptual representation, the reaction occurs at a narrow front. This leads to a sharp concentration profile in the solid reactant, while the front moves

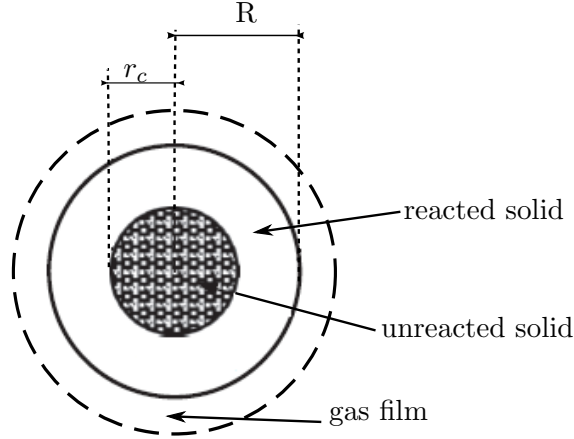


FIGURE 4.3: Schematic representation of the Shrinking Core Model. Adapted from (Monazam et al. (2008))

from the outer surface towards the inner particle. Thus, there will be an external completely-reacted zone known as "product layer" or "ash layer" and an internal non-reacted core, see figure 4.3. Considering a spherical particle of initial radius R_0 surrounded by reactant gas, the model equation representing the diffusive flux, as described by Carberry 1976, will be:

$$\frac{1}{r^2} \frac{d}{dr} \left(r^2 \mathfrak{D} \frac{dC_A}{dr} \right) = 0 \quad \text{for } r_c < r < R_0 \quad (4.4)$$

where r_c is the unreacted particle radius, C_A the concentration of the co-reactant gas and \mathfrak{D} the effective diffusivity inside the particle.

The boundary conditions are the following:

$$\text{at } r = r_c \quad \mathfrak{D} \frac{dC_A}{dr} \Big|_{r_c} = k C_{A_c} \quad (4.5a)$$

$$\text{at } r = R_0 \quad \mathfrak{D} \frac{dC_A}{dr} \Big|_{R_0} = k_g (C_{A_0} - C_{A_s}) \quad (4.5b)$$

C_{A_0} , C_{A_s} and C_{A_c} are respectively the concentration in the bulk gas, external pellet surface and reacting front. Solving eq. 4.4, with the specified boundary conditions eqs. 4.5, the concentration profile inside the product layer will be obtained:

$$C_A(r) = C_{A_c} + (C_{A_s} - C_{A_c}) \frac{r_c/R_0 - r_c/r}{1 - r_c/R_0} \quad (4.6)$$

The rate of reaction instead, expressed in terms of moles of reactant gas N_A , can be determined considering that, under pseudo steady state conditions, the gas film eq. 4.7a,

the ash layer eq. 4.7b and the chemical reaction eq. 4.7c resistances act in series:

$$\frac{dN_A}{dt} = 4\pi R_0^2 k_g (C_{A_0} - C_{A_s}) \quad (4.7a)$$

$$= 4\pi r_c^2 \mathfrak{D} \left. \frac{dC_A}{dr} \right|_{r_c} \quad (4.7b)$$

$$= 4\pi r_c^2 k C_{A_c} \quad (4.7c)$$

Moreover the product layer resistance can also be written as:

$$\frac{dN_A}{dt} = 4\pi r_c^2 \mathfrak{D} \frac{C_{A_s} - C_{A_c}}{1 - r_c/R_0} \quad (4.8)$$

In fact, differentiating and evaluating eq. 4.6 at $r=r_c$, it is possible to obtain:

$$\left. \frac{dC_A}{dr} \right|_{r_c} = \frac{C_{A_s} - C_{A_c}}{r_c(1 - r_c/R_0)} \quad (4.9)$$

Combining the equations from eq. 4.7a to eq. 4.7c, and eq. 4.8, it is possible to express the mol of reacted gas A, per pellet per second (dN_A/dt) in terms of C_{A_0} which, compared to C_{A_c} and C_{A_s} , is an easily detectable quantity

$$\frac{dN_A}{dt} = \frac{4\pi r_c^2 k C_{A_0}}{1 + \gamma^2 Da/Bi + Da\gamma(1 - \gamma)} \quad (4.10)$$

in this equation $\gamma = r_c/R_0$, Da and Bi are the Damköhler (kR_0/\mathfrak{D}) and Biot number ($k_g R_0/\mathfrak{D}$).

Considering the stoichiometry of reaction (see eq. 4.4):

$$\frac{dN_A}{dt} = \frac{1}{b} \frac{dN_B}{dt} = -\frac{4\pi \rho r_c^2}{b} \frac{dr_c}{dt} \quad (4.11)$$

where b is the stoichiometric coefficient, ρ is the molar density of the solid reactant B. In fact, if V is the volume of a particle, the amount of B in a particle will be $N_B = \rho V = 4/3 \rho \pi r_c^3$ which differentiated will give eq. 4.11. The comparison of eq. 4.11 and eq. 4.7c shows that:

$$\frac{dr_c}{dt} = -\frac{bkC_{A_0}/\rho}{1 + \gamma^2 Da/Bi + Da\gamma(1 - \gamma)} \quad (4.12)$$

All these equations are valid if the particle is assumed to be isothermal, if this is not the case the heat balance should be considered too (Carberry, 1976).

To obtain the specific absorption velocity \mathfrak{R} , one more mathematical manipulation is needed. Eq. 4.10 determines the number of mol of H_2S reacted per second per particle,

in order to calculate the amount reacted per second per reactor volume, the number of particle for unit of reactor volume is necessary and given by the following equation:

$$n_P = \frac{3(1 - \varepsilon)}{4\pi R_0^3} \quad (4.13)$$

Then, considering that the specific absorption velocity refers to kg of sorbent, it can be expressed as:

$$\Re = \left(\frac{4\pi r_c^2 k C_{A_0}}{1 + \gamma^2 Da / Bi + Da\gamma(1 - \gamma)} \right) \left(\frac{3(1 - \varepsilon)}{4\pi R_0^3} \right) \left(\frac{1}{\rho_s(1 - \varepsilon)} \right) \quad (4.14)$$

Shrinking Core Model with Changing Effective Diffusivity In order to account for the variation of the particle properties, direct consequence of the reaction, it was introduced the Unreacted Shrinking Core model with Changing Effective Diffusivity by (Konttinen, 1997, Konttinen et al., 1997). In the conventional SCM, \mathfrak{D} is only function of the temperature while in this case \mathfrak{D}_{eff} is also function of the conversion X:

$$\mathfrak{D}_{eff} = \frac{\epsilon_0 + (1 - \epsilon_0)X}{\frac{\tau}{\mathfrak{D}_{mol+Kn}} + \frac{Z(1 - \epsilon_0)X}{\mathfrak{D}_{pl}}} = \mathfrak{D}_{eff,0} \frac{1 + AX}{1 + BX} \quad (4.15)$$

where

$$A = \frac{1 - \epsilon_0}{\epsilon_0} \quad (4.16a)$$

$$B = \frac{A\mathfrak{D}_{eff,0}Z}{\mathfrak{D}_{pl}} \quad (4.16b)$$

τ is the tortuosity (assumed to be 3), \mathfrak{D}_{kn} the Knudsen diffusivity and \mathfrak{D}_{mol} the molecular diffusion coefficient obtained according to the relation for multicomponent gas mixtures proposed by Fairbanks and Wilke 1950, while the binary gas-phase diffusion coefficients have been estimated according to Fuller et al. 1966

$$\frac{1}{\mathfrak{D}_{mol+Kn}} = \frac{1}{\mathfrak{D}_{mol}} + \frac{1}{\mathfrak{D}_{kn}} \quad (4.17a)$$

$$\mathfrak{D}_{kn} = 97r_{av} \sqrt{\frac{T}{M_{w_{H_2S}}}} \quad (4.17b)$$

$$\mathfrak{D}_{eff,0} = \frac{\epsilon_0}{\tau} \mathfrak{D}_{mol+Kn} \quad (4.17c)$$

4.1.3 Grain Model

The grain model has been described by Szekely (Szekely and Evans, 1971, Szekely and Propster, 1975). It assumed that the particle is composed of a large number of non-porous grains, each of them reacting as in the Shrinking Core Model. According to this representation the reactant gas encounters four resistance in series. It undergoes mass transfer through the film surrounding the particle, successively, diffuses through the interstices between the grains and the product layer of each grain before reacting. As figure 4.4 underlines, if all the resistances are relevant, the gas concentration will show a progressive conversion towards the center of the particle.

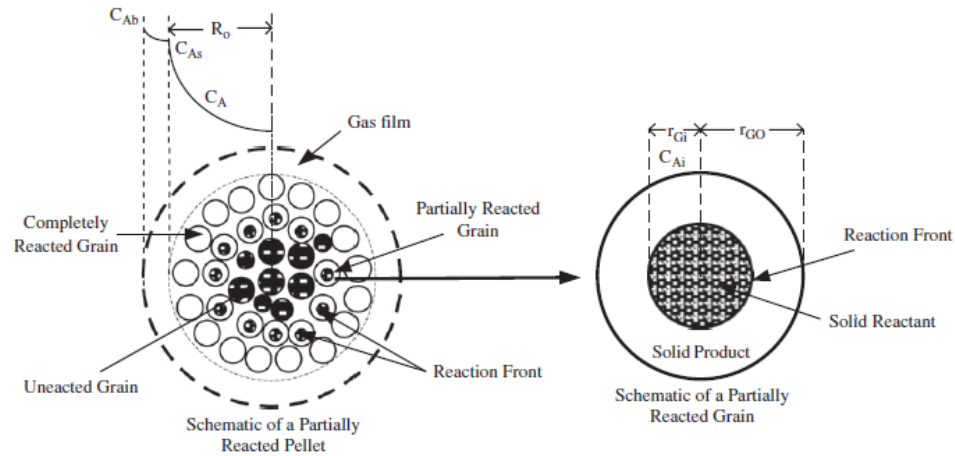


FIGURE 4.4: Schematic representation of the grain model.
(Source: Monazam et al. 2008)

Considering negligible the diffusion between grains, as in (Monazam et al., 2005, 2008), and with a procedure analogue to that presented for the Shrinking Core Model, the specific absorption velocity can be expressed as:

$$\mathfrak{R} = \frac{3(1 - \varepsilon_0)k'_s r_{gi}^2 C_{A_0}}{\rho_s r_{g0}^3 \left[1 + \frac{r_{g0}^2 k'_s}{k_g R_0^2} + \frac{r_{g0} k'_s}{D_e} [(1 - X)^{1/3} - (1 - X)^{2/3}] [Z + (1 - Z)(1 - X)]^{-1/3} \right]} \quad (4.18)$$

Z is a parameter which takes into account the different volume of product and reactant. It is defined as the ratio between the molar volume of reactant and that of the product.

Grain Model with variable properties Variation of the grain model are widely available in literature. A grain size distribution model has been proposed by Heesink et al. 1993. Turton et al. 2004 considered in their study a bimodal grain size model and

Ranade and Harrison 1981 modified the grain model to account for micro-structural changes which occur as a consequence of both reaction and sintering effect. Ranade and Harrison 1981 described the shrinkage and expansion of the grains, correlating the specific surface area of the grain, with the overall particle conversion and time:

$$r_{g0} = \frac{3}{A_g(X, t)\rho} \quad (4.19)$$

ρ is the grain density given by:

$$\rho = \rho_R + (\rho_P - \rho_R)X \quad (4.20)$$

where ρ_R is the density of the reacting sorbent and ρ_P that of the product.

$$\frac{A_g(X, t) - A_P(t)}{A_R(t) - A_P(t)} = (1 - X)^a \quad (4.21)$$

$A_g(t)$ represents the variation of the specific surface area of the grain with time, due to the high temperature which promote sintering of grains.

$$\frac{A_g(t) - A_e}{A_0 - A_e} = e^{K_j t} \quad (4.22)$$

where

$$A_e = A_0 e^{-d(T-623)} \quad (4.23)$$

and K_j , the sintering rate constant is given by:

$$K_j = K_{j0} e^{-E_j/RT} \quad (4.24)$$

Grain Model with variable properties, the porosity also change, due to sintering effects:

$$\varepsilon_0 = \varepsilon_R + (\varepsilon_P - \varepsilon_R)X \quad (4.25)$$

where ε_R is the porosity of the reacting sorbent and ε_P the porosity of the product.

Compared to the constant grain model, even if apparently the variable property grain model present the same equation, the parameter are not only function of the reactor operating conditions but also of the particle conversion.

The grain model has been used to describe the reaction of zinc titanium with H_2S , but no variation of the grain size and pellet is assumed to occur, neglecting the sintering effect. This is translated in mathematical terms considering a constant value for $A(X, t)$.

In table 4.1, the chemical and physical properties of Zinc Titanate and the values of the used parameter are summarized.

TABLE 4.1: Chemical and Physical properties of Zinc Titanate and model Parameters

Zn ₂ TiO ₂	
zinc oxide,% (weight)	60
particle density, g/cm ³	2.6
BET surface area, m ² /g	11
average size, μm	70
Estimated parameters	
porosity	$\varepsilon_0 = \varepsilon_R + (\varepsilon_P - \varepsilon_R)X$
ε_R	0.68
ε_P	0.45
D_e	$D_e = D_{e0} \exp(E/(RT))$
D_{e0} (cm ² /s)	4.9E-4
E (kcal/mol)	22
k'_s	$k_s = k_{s0} \exp(E/(RT))$
k_{s0} (cm/s)	0.333
E (kcal/mol)	31.4

Moreover the difference between the H₂S concentration and the H₂S equilibrium concentration ($C_{H_2S} - C_{H_2S}^{eq}$) has been used, rather than only C_{H_2S} , in order to consider the influence of thermodynamic aspects.

Regarding the regeneration, instead, according to the studies of Konttinen, the uniform conversion model can provide accurate predictions. Thus, as in , the value of the reaction rate constant was assumed to be:

$$k' = 8.36 \cdot 10^7 \exp(201740/RT) \quad (4.26)$$

4.2 Hydrodynamics

An other important aspect that has to be considered for a reactor model in general and for the chemical looping in this specific case, is the hydrodynamics, that is the gas motion and the forces acting on a solid particle immersed in it. Such analysis is important to determine the effective velocity of the solid particle. Two are the forces acting: the force exerted by the fluid, also known as drag force and gravity. The drag coefficient calculation, as well as the terminal velocity evaluation, has been analyzed by several authors. Many of them require an iterative process. In this work the correlation proposed by Haider and Levenspiel 1989 has been used. The authors defined d_* and u_* respectively the dimensionless particle diameter and terminal velocity:

$$d_* = \left(\frac{3}{4} C_D Re^2 \right)^{1/3} = d_P \left[\frac{g \rho_g (\rho_s - \rho_g)}{\mu^2} \right] \quad (4.27)$$

$$u_* = \left(\frac{4 Re}{3 C_D} \right)^{1/3} = u_t \left[\frac{\rho_g^2}{g \mu (\rho_s - \rho_g)} \right]^{1/3} \quad (4.28)$$

According to Levenspiel u_* can be estimated with good accuracy through the following correlation:

$$u_* = \left(\frac{18}{d_*^2} + \frac{3K_1}{4d_*^{0.5}} \right)^{-1} \quad (4.29)$$

where $K_1 = 2.335 - 1.744\phi$

The gas-solid relative velocity is often assumed equal to the terminal velocity. This hypothesis is acceptable for high gas velocities and dilute flows. Nevertheless, in many situations, this approach underestimate the slip velocity between gas and solid. Thus, it is often evaluated based on the solid fraction, ε_s . There is a direct link between the particle velocity and the solid fraction, as expressed in the following equation:

$$u_s = \frac{G_s}{\rho_s(1 - \varepsilon_s)} \quad (4.30)$$

For this reason, to determine the solid velocity, the axial voidage profile along the reactor has to be estimated. Because of the difficulty in determining this quantity directly, often the apparent axial voidage is used. It is obtained through the measurements of the pressure drop along the reactor, whose variation is assumed to be caused only by the solid fraction, as in eq. 4.31.

$$\frac{dP}{dz} = -g\varepsilon_s\rho_s \quad (4.31)$$

Experimental evidence suggests that the solid fraction is not constant along the reactor and is strongly affected by the solid mass flow, the solid gas velocity and not less important by the geometry of the riser.

It is possible to distinguish three regions: acceleration, fully developed and exit zone. In order to model the reactor, these zones should be properly described.

In this work, the empirical correlations proposed by Monazam and Shadle 2008 have been implemented, obtaining the voidage profile shown in figure 4.5 for different solid mass flux. These empirical correlations take into account six dimensionless groups: the Froude number, Reynolds number, Archimedes number, load ratio, riser to particle ratio

and gas to solid density ratio and are based on experiments designed to cover a wide range of value of the mentioned groups.

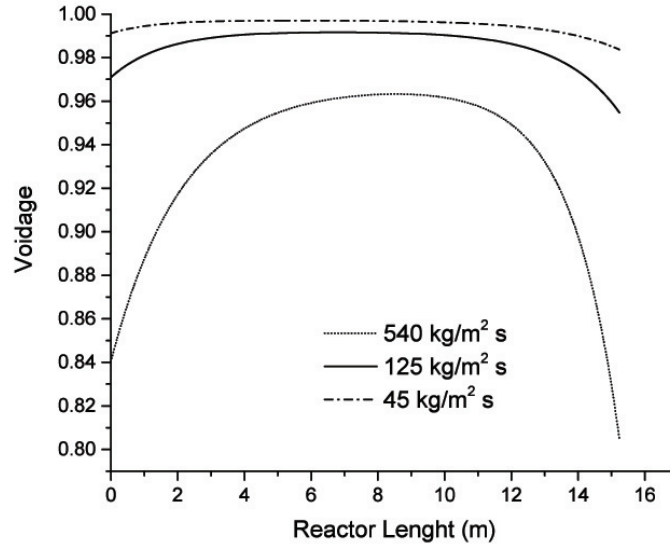


FIGURE 4.5: Voidage profile along the transport reactor

The C-shape profile, obtained in figure 4.5, is typical of reactor with abrupt exit.

4.3 Heat transfer

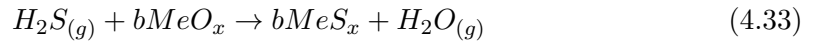
Both regeneration and desulphurization reactor are assumed to be adiabatic. Thus, the wall surface-bed heat transfer is neglected. However, considering the strong influence of the operating temperature on the kinetics, the gas-solid heat transfer has been analyzed with more detail. Different correlations are available in literature to predict the heat transfer coefficient. Many are based on the analogy between heat and mass transfer, like the correlation suggested by Hughmark 1967 . The Nusselt and Prandtl number are substituted by the Sherwood and Schmidt number. To predict the heat transfer coefficient between the particle and the gas, the correlation suggested by Gunn 1978 has been used:

$$Nu = (7 - 10\varepsilon + 5\varepsilon^2)(1 + 0.7Re_p^{0.2}Pr^{1/3}) + (1.33 - 2.4\varepsilon + 1.2\varepsilon^2)Re_p^{0.2}Pr^{1/3} \quad (4.32)$$

It presents the advantage of taking into account the bed voidage and the particle relative velocity, describing with good accuracy the variation of the heat transfer along the reactor.

4.4 Model assumptions

Due to the technical reasons clarified in chapter 3, the desulphurization and regeneration processes take place in a transport reactor. The transport reactor was assumed to be adiabatic, steady state and one dimensional. Both solid and gas phase hydrodynamics are considered as plug flow. For the particle dimension the mean value was assumed and, due to the small particle size ($< 70\mu m$), the thermal gradient inside the particle was neglected. To determine the concentration profile of the syngas components along the reactor, the mass and energy balance for both phases are solved within Athena Visual Studio software. Considering that a generic reaction, for a metal oxide is:



where $b = \frac{1}{x}$, the following equations describe the mass and heat balances for both phases.

Mass balance:

$$\frac{dn_g}{dz} = \Re \rho_s A (1 - \varepsilon) \quad (4.34a)$$

$$\frac{dn_s}{dz} = b \Re \rho_s A (1 - \varepsilon) \quad (4.34b)$$

\Re is the reaction rate, function of both particle geometry and kinetic model used. It is expressed in $kmol_{H_2S}/(kg_s s)$ and addressed to as specific absorption velocity.

Heat balance:

$$n_g C_{pg} \frac{dT_g}{dz} = h a_v A (T_s - T_g) - UA (T_g - T_{cool}) \quad (4.35a)$$

$$n_s C_{ps} \frac{dT_s}{dz} = \Delta H \Re \rho_s A (1 - \varepsilon) - h a_v A (T_s - T_g) \quad (4.35b)$$

Since these equations should be solved simultaneously, numerical methods are necessary. The equation set has been implemented in Athena Visual Studio, a software package whose advantage is represented by the possibility, the user has, to build a model without the duty to solve the underlying set of equations. In this specific case, it is a set of ordinary differential equations solved automatically in Athena with the DDAPLUS solver (Stewart and Caracotsios, 2008).

4.5 Model validation

To verify the accuracy of the model predictions, three are the possible methodologies:

- benchmarking: the predicted results, comparing to the predictions with that of another model, which hopefully is the best available.
- model verification: reproduce a model and the model predictions
- model validation: the aim is to reproduce the experimental results.

In the last case, a large number of experiments should be available, better if in Pilot scale. Because of the difficulty in Finding such data, the benchmarking was used. In particular the model predictions were compared with that obtained by the National Energy Laboratory Technology, whose model has been validated through experimental results.

As in the study of Monazam and Shadle 2005, a reactor with a diameter of 13.2cm and 15.24m height, has been considered. The inlet gas temperature has been assumed to be 844.5K, the pressure 2069 KPa and the H₂S concentration in the gas was 3400 ppm.

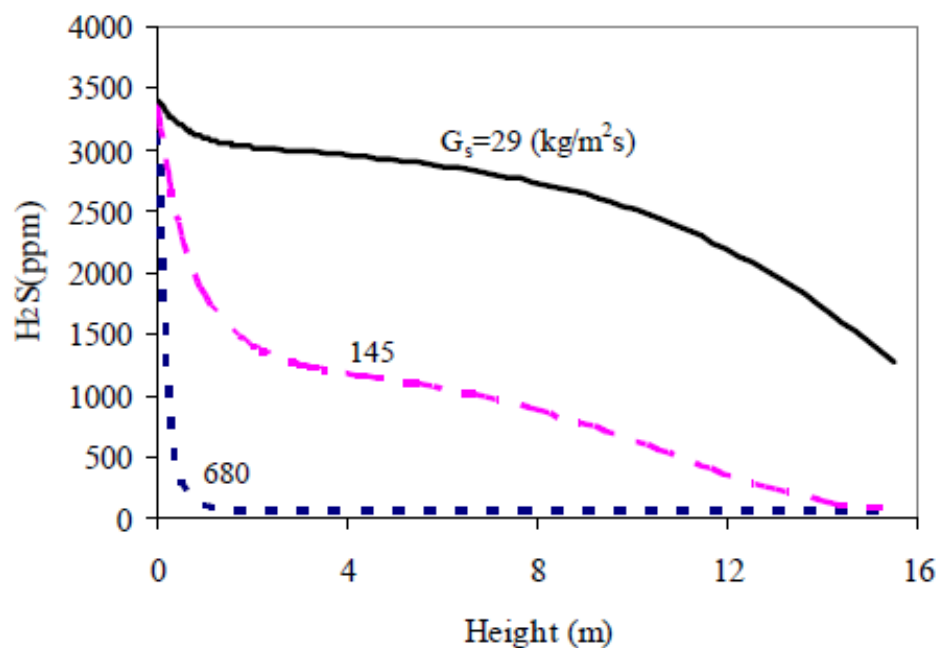


FIGURE 4.6: H₂S concentration along the reactor for solid mass flows of 680 kg/(m²s) 145 kg/(m²s) 29 kg/(m²s) at pressure of 2 MPa, temperature of 550°C and incoming H₂S concentration of 3400 ppm. Source: Monazam and Shadle 2005

Similar results are obtained. For a solid mass flux of 680 kg/m²s the reaction was completed already after 1.5 m. For lower solid mass flux the amount of removed sulfur also decrease until a breakthrough of H₂S is obtained for too low solid flux.

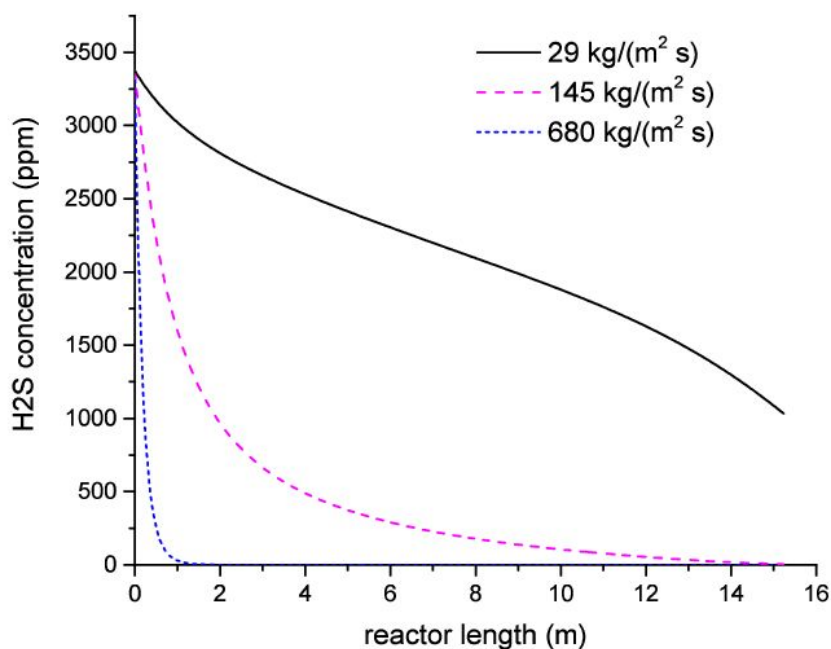


FIGURE 4.7: H₂S concentration along the reactor for solid mass flows of $680\text{kg}/(\text{m}^2\text{s})$, $145\text{kg}/(\text{m}^2\text{s})$, $29\text{kg}/(\text{m}^2\text{s})$ at pressure of 2 MPa, temperature of 550°C and incoming H₂S concentration of 3400ppm.

4.6 Sensitivity Analysis & Results discussion

On the basis of the described model, the performance of gas desulphurization in a riser has been analyzed. The operating conditions have been assumed to be pressure of 2.0 MPa and temperature of 550°C . To investigate the influence of the main parameters on the reaction rate and the desulphurization efficiency, a sensitivity analysis has been performed.

In figure 4.8 the effect of the solid flux on both H₂S concentration and ZnO conversion is shown.

It can be noted that decreasing the solid mass flux, ZnO conversion increases. This result is expected since the sorbent conversion is proportional to H₂S concentration, which is actually higher along the reactor when the amount of sorbent introduced decreases. It is also interesting to see that the sorbent conversion is lower than 2% in all cases.

Figure 4.9 shows the effect of the H₂S concentration in the syngas. For the same amount of solid flux, the reaction rate decreases at lower H₂S initial values. This represent an interesting results since even with high sulfur content is possible to obtain a final H₂S concentration well below 100ppm.

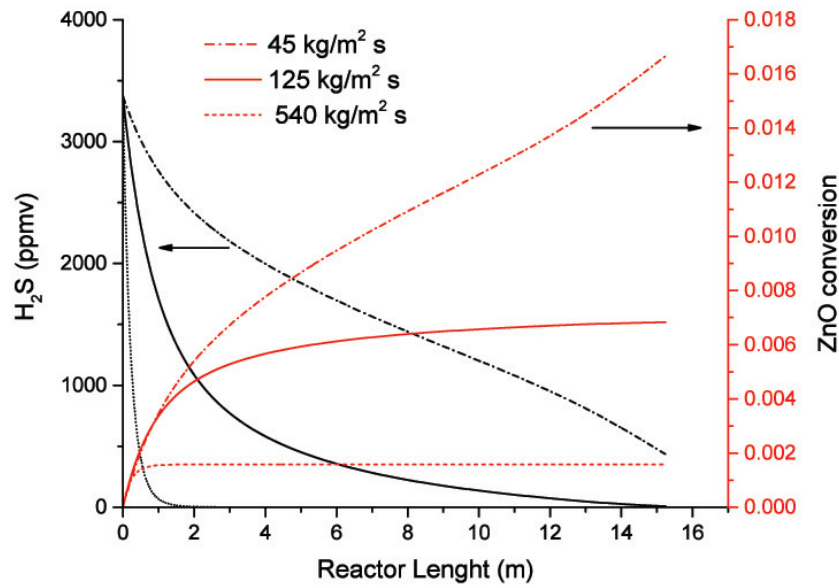


FIGURE 4.8: H₂S concentration and ZnO conversion along the reactor for solid mass flows of 45, 125 and 540 kg/m^2s , at a pressure of 2 MPa, temperature of 550°C and incoming H₂S concentration of 3400 ppm.

Figure 4.10 shows the influence of the operating temperature. Increasing the temperature also the reaction rate increase and a higher H₂S removal can be obtained.

The effect of the syngas composition, on the desulphurization process has been investigated. In particular, as figure 4.11 shows that the H₂S concentration increases under the same conditions increasing the water concentration. This can be explained considering the influence of thermodynamic equilibrium.

This result is not of little interest, since it has an impact on the gasifier and feeding system. The water slurry gasifier, for example, produces a raw syngas with a higher steam content.

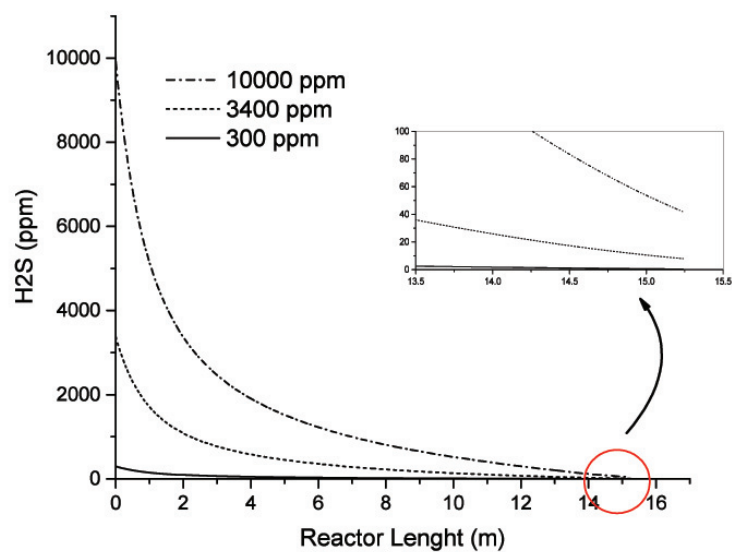


FIGURE 4.9: H₂S concentration for an initial value of 300, 3400 and 10000 ppm with a constant solid flux of $125 \text{ kg}/(\text{m}^2\text{s})$

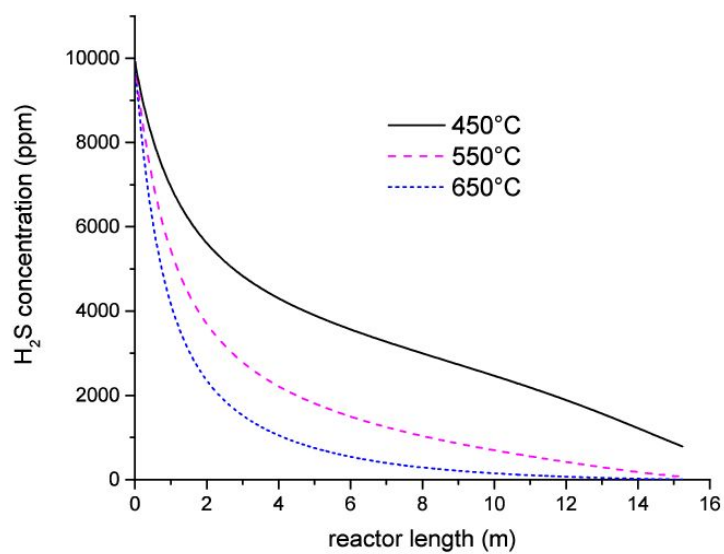


FIGURE 4.10: H₂S concentration along the reactor for solid mass flows of $125 \text{ kg}/(\text{m}^2\text{s})$, at a pressure of 2 MPa and incoming H₂S concentration of 10000 ppm.

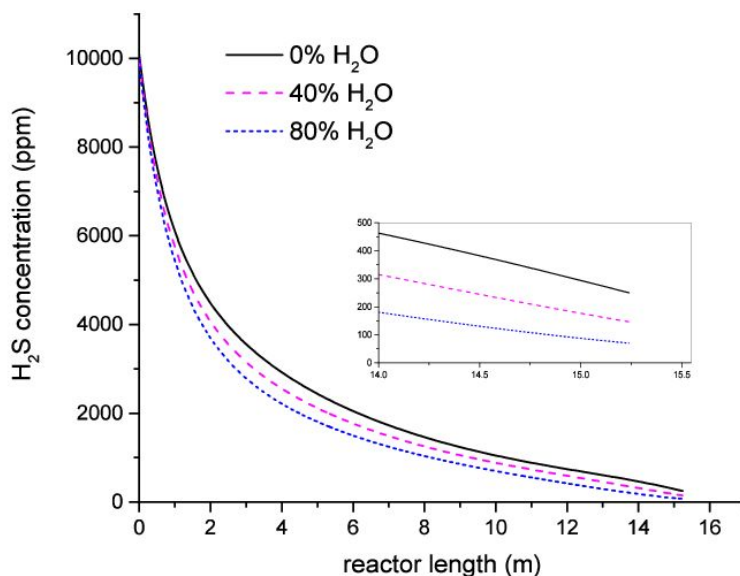


FIGURE 4.11: H_2S concentration along the reactor for solid mass flows of $125 \text{ kg}/(\text{m}^2\text{s})$ at a pressure of 2 MPa and incoming H_2S concentration of 10000 ppm.

4.7 Combination of *In situ* & external desulphurization

The results obtained and discussed in the previous section, highlighted the efficient desulphurization which is possible to obtain using Zinc Titanate. However, this sorbent is quite costly, for this reason other approach could be evaluated. As mentioned in chapter 2, a rather cheap alternative is represented by CaO based sorbents, stable in a temperature range of 800-1200°C. It is used as a non-regenerative sorbent, for an *in situ* desulphurization. Its main drawback, as underlined by Fenouil and Lynn 1996, is that, CaO reaction is limited by thermodynamic equilibrium. For typical gasification conditions, the H_2S concentration at equilibrium is around 300 ppm, not enough to satisfy the requirements. Thus, an external desulfurization process has to be added.

In this case a detailed economic analysis would be necessary in order to evaluate the two solutions: intensive external desulphurization with zinc titanate or *in situ* CaO for bulk H_2S removal followed by zinc titanate absorption of residual H_2S . In the former case, the main cost is represented by the sorbent, whilst in the latter, the cost will depend on the amount of zinc titanate still needed but also on the disposal problems of the large quantities of CaS produced, which is not stable at ambient conditions. A univocal answer is difficult to find, as it depends on the H_2S final concentration required and the gasification conditions, which strongly affect the inlet H_2S concentration in the riser and thus the reaction rate. In fact, as figure 4.12 shows, to obtain the same H_2S emission at the riser outlet, for an initial value of 300 ppm and 3400 ppm, even if

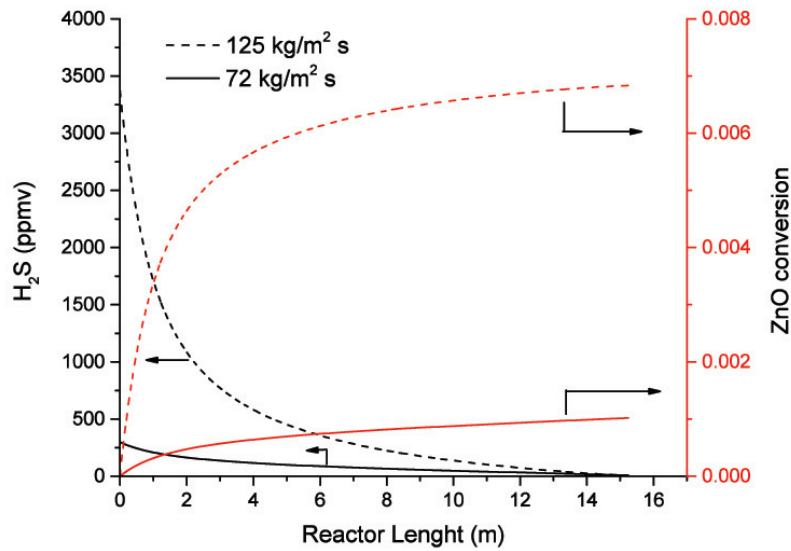


FIGURE 4.12: H_2S concentration and sorbent conversion along the reactor for an incoming concentration of 300 and 3400 ppm and solid mass flux respectively of 72 and $125 \text{ kg}/(\text{m}^2 \text{ s})$ in order to have the same H_2S exit concentration

the sulfur contented is reduced of 91%, the solid mass flux of zinc titanate required is reduced of the 40%. This results can be explained considering the strong influence of the H_2S concentration on the reaction rate, as underlined in figure 4.9.

4.8 Reactor Model Scale-up

The final aim of a reactor model is, generally, the scale-up to predict the performance of commercial reactors. In table 4.2, typical characteristic of a commercial riser are reported.

TABLE 4.2: Commercial riser characteristic. Source: Yang 2003

Superficial gas velocity:	2–12 m/s
Net solids flux through the riser:	10–1000 $\text{kg}/(\text{m}^2 \text{ s})$
Temperature:	20–950°C
Pressure:	100–3000 kPa
Mean particle diameter:	50–500 μm
Overall riser height:	15–40 m

The most critical aspects of the scale-up of the developed model is represented by the hydrodynamic. In figure 4.13, the predictions obtained by the empirical correlations of Monazam and Shadle 2008 and that obtained considering a constant solid fraction along the reactor (determined assuming the slip velocity equal to the terminal velocity) have been compared. In the latter case a reduction of the reaction rate is evident for the

same operating conditions, underlining the strong influence which the predicted axial voidage profile has on the overall reactor performance.

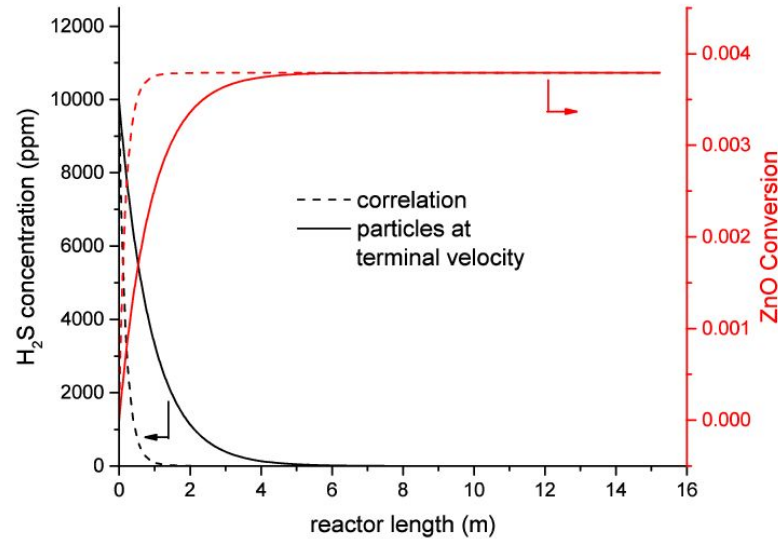


FIGURE 4.13: H_2S concentration and sorbent conversion along the reactor for solid mass flows of $125 \text{ kg}/(\text{m}^2\text{s})$ at a pressure of 2 MPa and incoming H_2S concentration of 10000 ppm, for different estimated particle velocities.

Several studies on reactor scale-up are available in literature, (Knowlton, 2013, Pallarès and Johnsson, 2006). A common and widely used approach to this problem is based on the introduction of a set of dimensionless groups to assure geometric and dynamic similarity between the laboratory scale riser and the commercial one, (Chang and Louge, 1992, Glicksman et al., 1994). According to Van der Meer E.H. et al. 1999 five are the main dimensionless groups that should be introduced: Froude number, dimensionless solids flux, density ratio, Reynolds number and reactor and particle diameter ratio. Other groups are sometimes used, like the Archimedes number in Mirek 2011. Even if, as stated in (Knowlton et al., 2005), it should be paid attention when scaling laws are applied, this scale-up approach gives a good starting point for further analysis, but experimental data on large scale are needed for the development of a reliable model.

Chapter 5

Application to Integrated Gasification Combined Cycle

Integrated Gasification Combined Cycle, also known with the acronym of IGCC, represents the most efficient way to produce electricity from solid fuels, such as coal and in a wider prospective also from biomass. IGCC are based on the gasification of coal with air or oxygen to produce the so called syngas or producer gas, mainly composed of H_2 , CO , CO_2 , H_2O , CH_4 and various contaminant compounds like particulate, NO_x , hydrogen sulfide, hydrogen Chloride and trace metals. In order to use the syngas for electricity production without harming the downstream technologies and the environment, removal of sulfur compounds is necessary.

Absorption processes are currently considered as state-of-the-art. In spite of their excellent desulphurization efficiency, this strategy is thermally inefficient, since it requires the gas to be cooled below the dew point and then reheated downstream. Thus, alternative solutions, operating at higher temperatures, would be interesting in order to avoid gas cooling and the related heat exchangers, with a consequent enhancement of the efficiency and simplification of the system configuration. In this chapter the use of chemical looping for hot gas desulphurization will be evaluate, and its influence on the conversion process analyzed.

5.1 IGCC with cold gas desulphurization

As described in Lozza 2006, an Integrated Gasification Combined Cycle is mainly composed of three sections, as shown in figure 5.1:

1. air separation section
2. gasification island
3. power generation section

In the air separation section, an almost pure stream of oxygen (95%) is obtained, using the cryogenic air separation process. Typically in fact, gasification with oxygen is preferred rather than with air, due to:

1. higher heat capacity of the syngas, which is not diluted with nitrogen, thus lower mass flow of syngas is required for the same output.
2. there is not the need to heat the nitrogen up to the gasification temperature, since this will increase the heat required and promote the oxidation of carbon, consequently reducing the lower heating value of the syngas.

The air separation unit, known with the acronym of ASU, could be stand alone or integrated with the gas turbine. The former option ensures higher flexibility and easier start-up, while the latter determines an increase of the efficiency. However, even if an 100% integration leads to the highest efficiency, the drawback is a lower power output. In fact, the fraction of air supplied by the compressor of the gas turbine compared to the amount of air required by the ASU represents the degree of integration. Higher is the integration level higher is the compressor bleed. In this work a stand alone ASU has been considered even if for future IGCC seems to increase the tendency towards partial integration. As shown in figure 5.1, representing the layout of the IGCC, object of this study, the N_2 produced by the ASU is used to:

- feed coal to the gasifier through the so called "lock-hoppers"
- dilute the syngas, introduced in the combustor, in order to lower the stoichiometric flame temperature and limit the formation of nitrogen oxides. In this way, in fact, NO_x emissions are reduced without the need to resort to other abatement systems.

The gasification section includes the storage, transport, grinding systems and the coal feeding system, as well as the gasifier itself. Many types of gasifier have been developed and are commercially available: fixed bed as the Sasol-Lurgi gasifier, fluidized bed and entrained flow like GE or its former Texaco gasifier, the Shell gasifier and ConocoPhillips E-gas. Among them, the entrained flow gasifiers are the most simple and cheap and therefore also the most widely used. Moreover, they operate at high temperatures to obtain very fast reaction kinetics and bring the ashes over the melting point, dropping them as slag. For all these reasons, an entrained flow, oxygen blown gasifier has been used and its specifics are summarized in table 5.1 while the properties of coal, used as feedstock, are reported in table 5.2.

The high gasification pressure allows to feed the gas turbine directly without the need of additional compressors. The only critical point is the efficient heat recovery required, due to the high outlet syngas temperature, 1560 °C. A good heat recovery is obtained through high pressure steam production, generated with syngas coolers which

TABLE 5.1: Gasifier specifics

Gasifier type	entrained flow
O_2 purity	95%
Gasifier pressure (bar)	39,34
Gasifier temperature ($^{\circ}C$)	1559
Gasifier efficiency (Cold gas efficiency)	81,9 %

TABLE 5.2: Coal Properties

Ultimate Analysis	(weight %)
Carbon	81,6
Hydrogen	4,8
Nitrogen	1,4
Sulfur	1
Oxygen	3
Moisture	2,1
Ash	6,1
Proximate Analysis (weight %)	
Volatile Matter	24,4
Fixed Carbon	67,4
LHV (at $25^{\circ}C$) kJ/kg	32184

reduce the syngas temperature to $350^{\circ}C$. Then, the cooled syngas is partially recirculated to the gasifier to lower the syngas exit temperature. Additional heat recovery is obtained pre-heating the clean syngas entering in the combustor.

In fact, before syngas can be fed to a gas turbine (GT), it must pass through a series of clean-up steps in order to remove species that would either harm the environment or the GT itself. Particulates are removed by “dry” processes such as a cyclone and filter or by “wet” processes such as a scrubber. Regarding sulfur species, IGCC allows an optimal desulphurization up to percentages even higher than 99%. The separation of acid gases occurs by absorption in chemical solvents, like MDEA. These processes are favored by high pressure and low temperature, as described in Chapter 2. For these reason syngas has to be cooled to ambient temperatures with consequently loss of energy, due to the irreversibility which are inevitable consequence of the cooling process. Moreover, the use of heat exchangers increase the system complexity. In figure 5.1 the traditional cleaning syngas steps are schematically represented. Cooled syngas is sent to a scrubber at about $200^{\circ}C$, for removal of dust and pollutants soluble in water, heated to allow the hydrolysis of COS to H_2S and cooled at near-ambient temperature to remove sulfur by means of chemical absorption using methyl-diethanol-amines.

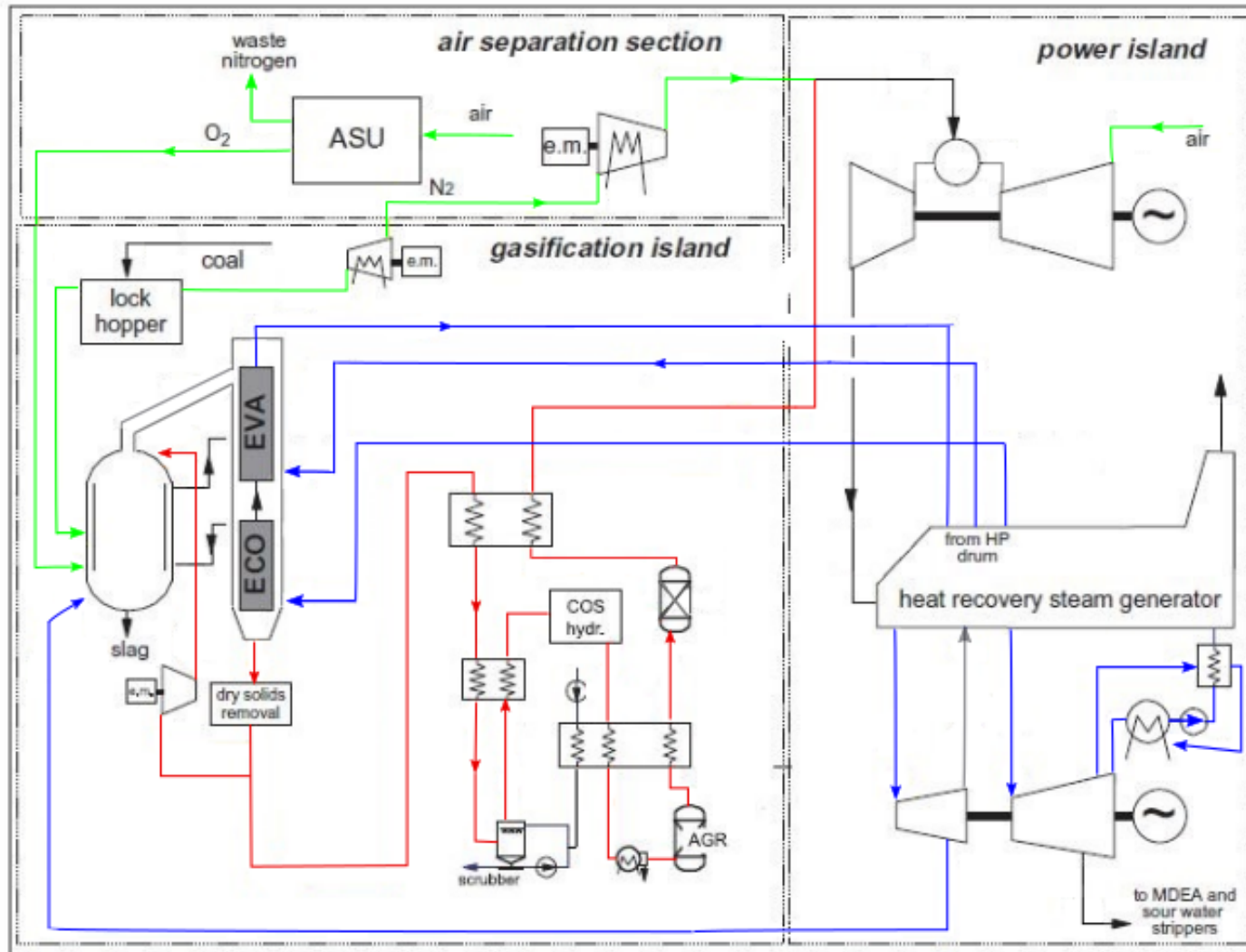


FIGURE 5.1: Scheme of an Integrated Gasification Combined Cycle with cold gas desulfurization. Adapted from: Giuffrida et al. 2010

In table 5.3 the main assumptions referred to the Acid Gas Removal unit (AGR) are summarized. The removed H_2S is sent to a Claus-Scot plant. This sulfur recovery section has not been modeled: it was assumed that the steam produced in the Claus plant balance that required in the scot section for solvent regeneration, as described in chapter 2.

TABLE 5.3: Acid Gas Removal specifics

H_2S removal strategy	chemical absorption (MDEA)
COS hydrolizer temperature ($^{\circ}\text{C}$)	180
Absorption tower temperature ($^{\circ}\text{C}$)	38
Absorption tower pressure (bar)	38,36

The purified syngas is finally humidified in a saturator, heated and sent to the combustor at a temperature of 250°C .

The clean syngas feeds a combined cycle plant in which the hot exhaust of a gas turbine, whose specifics are reported in table 5.4, operating by Brayton cycle, powers a steam power plant, operating by the Rankine cycle. The flue gas from the gas turbine

TABLE 5.4: Power Section specifics

Gas Turbine type	GE 9001H
Turbine inlet temperature ($^{\circ}\text{C}$)	1394
Pressure level (bar)	160/36
Condensing pressure (bar)	0.06
ΔT pinch point ($^{\circ}\text{C}$)	10

in fact are at high temperature, around 600°C . In the heat recovery steam generator (HRSG) the hot gas stream meets counter-currently and transfer its heat to the water to produce steam and superheated steam which later expands in the steam turbine. In the analyzed system, the steam cycle is a two pressure levels with re-heater, which ensures an already good heat recovery.

The collocation of the heat exchangers is chosen to reduce the temperature difference between the two fluids, reducing in this way the irreversibility of the process and is represented in figure 5.2. More pressure levels could be added but usually is not convenient to use a steam cycle with more than three levels, due to the increasing system complexity and the progressively lower increment of thermal heat recovery.

The integration of the described sections allows to obtain a good thermal recovery limiting the energy losses, as it happens for example in the purification section in which the energy, resulting from the thermal cooling of syngas, is recovered in the steam plant.

As regards the thermal exchanges, there is the possibility to further improve the integration, obtaining higher efficiency, (van der Ham, 2012). However an excessive increase of integration involves a much more complex power plant, which in turn causes increasing costs of installation and maintenance of the plant and a reduction of its

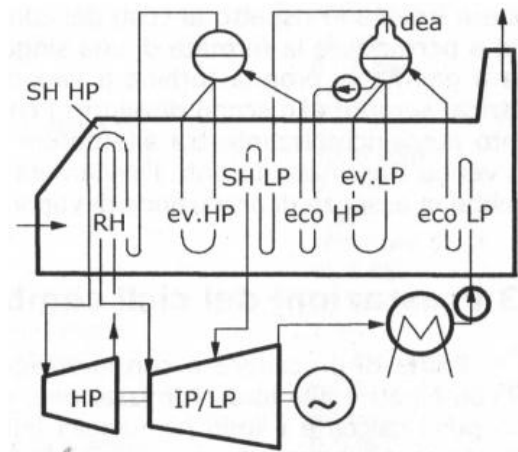


FIGURE 5.2: Scheme of a Heat Recovery Steam Generator. From: Lozza 2006

flexibility. Therefore, it is evident that it is necessary to find a compromise between the integration (and thus the energy efficiency of the plant) and the costs of installation and management.

Another way, to improve the performance of IGCC plants could be the development of new plant configurations, to simultaneously:

1. Simplify the structure of the system, with a consequent reduction in installation and management costs
2. Improve the energy conversion efficiency

This is the way that will be pursued though the use of chemical looping.

5.2 IGCC with hot gas desulphurization

In figure figure 5.3 the layout of the simulated IGCC power plant with hot gas desulphurization is shown.

In order to later compare this with the cold gas desulphurization case, gasifier specifics, as well as coal properties are kept constant. However, in this case, the syngas exiting the gasifier is cooled to 550°C producing high pressure steam, desulphurized and introduced in the combustion chamber at a temperature ideally equal to that of desulphurization about 550 °C instead of 250°C as in CGD. System simplification is evident. The heat exchanger are replaced by the chemical looping process for syngas desulphurization and high temperature filter.

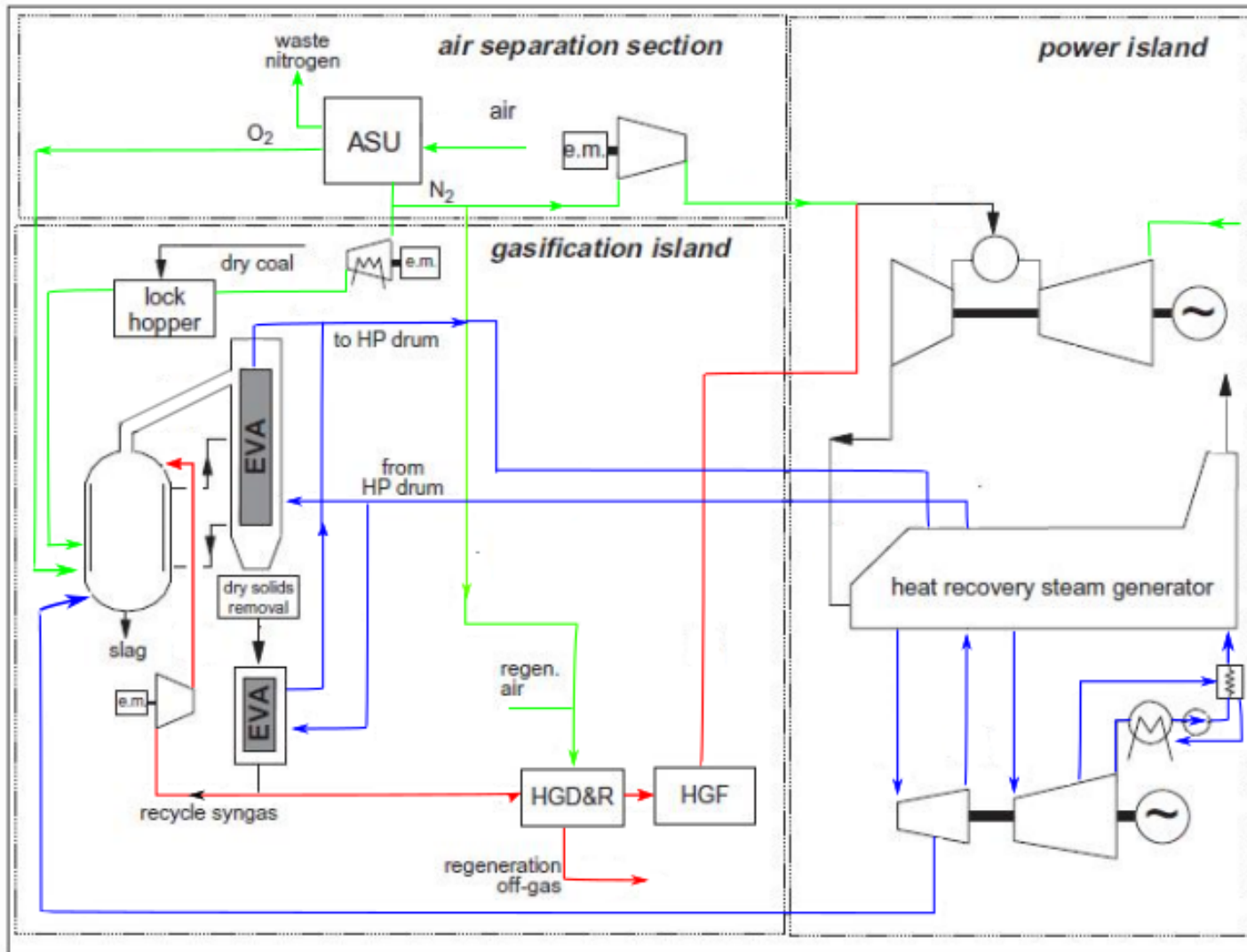


FIGURE 5.3: Scheme of an Integrated Gasification Combined Cycle with hot gas desulfurization. Adapted from: Giuffrida et al. 2010

The hot gas desulphurization section consists in two transport reactors for syngas desulphurization and sorbent regeneration as described in figure 5.4 and modeled in Athena Visual studio. A compressor is necessary to bring the regenerating agent at the desulphurization pressure, about 38 bar. Moreover the SO₂ laden gas exiting the regenerator at a temperature of 750°C expands in a turbine which drives the compressor, before being sent to a sulfur recovery unit. In this work sulfur recovery is obtained through a wet scrubber, as illustrated in chapter 2, with the production of commercial gypsum.

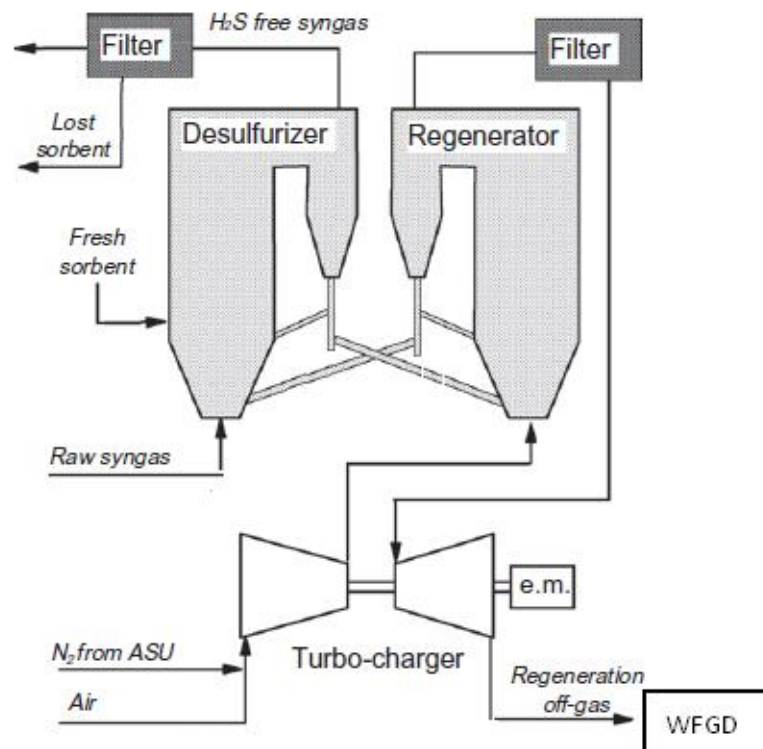


FIGURE 5.4: Hot gas desulphurization and regeneration unit. Adapted from: Giuffrida et al. 2010

It is worth noticing that the same gas turbine GE 9001H has been used, together with the same bottom cycle configuration and pressure levels. The additional syngas energy, due to the higher sensible heat, obtained with HGD, evolves inside both the power sections (Brayton cycle and Rankine cycle), rather than being dissipated as a result of heat exchanges and only partly recovered in the Rankine cycle at lower temperature, with lower efficiency.

5.3 Energy efficiency indicators

In order to compare the two described Process Design, some performance indicators will be defined. The Cold Gas Efficiency (CGE) is an important measure of the performance of a gasification process, although it should not be confused with the gasifier efficiency. It is defined as the fraction of feedstock's chemical energy, or heating value, which remains in the product syngas.

$$CGE = \frac{G_{syngas}LHV_{syngas}}{G_{coal}LHV_{coal}} \quad (5.1)$$

Most commercial-scale gasification processes have a cold gas efficiency of at least 65%.

Another important parameter that has to be considered is the Hot Gas Efficiency (HGE), introduced by Lozza et al. 2009, which evaluates the sensible heat in addition to the calorific value.

$$HGE = \frac{G_{syngas}LHV_{syngas} + \Delta H_s}{G_{coal}LHV_{coal}} \quad (5.2)$$

ΔH_s takes into account the difference in specific enthalpy of the syngas between the inlet gas temperature of the combustor and the temperature in standard conditions 15 °C. This parameter is important in order to compare the IGCC Power Plant using cold and hot gas desulphurization.

More common and widely used parameter, to compare the efficiency of different systems, are the net electric efficiency and the gross electric efficiency.

$$\eta_{net} = \frac{P_{TG} + P_{ST} - P_{aux}}{G_{coal}LHV_{coal}} \quad (5.3)$$

P_{TG} represents the Power generated by the gas turbine, P_{ST} the one obtained by the steam turbine and P_{aux} is the power required by the auxiliaries.

$$\eta_{gros} = \frac{P_{TG} + P_{ST}}{G_{coal}LHV_{coal}} \quad (5.4)$$

The efficiency of each cycle can be also calculated. The efficiency of the topping cycle refers to the output generated only by the gas turbine, while the bottoming cycle refers only to the steam turbine.

$$\eta_{TC} = \frac{P_{TG}}{G_{coal}LHV_{coal}} \quad (5.5)$$

$$\eta_{TB} = \frac{P_{ST}}{G_{coal}LHV_{coal}} \quad (5.6)$$

5.4 Cold gas clean-up vs. Hot gas clean-up

In order to compare the two described IGCC configurations, a simulation of the overall system is necessary. The simulations have been developed in Thermoflex, a software package which allows to built the scheme of complex systems, mainly power systems, as an assembly of single units solved through mass and heat balances. The great potential of this tool relies in the possibility the user has to choose among commercially available unit, which enable a more accurate comparison.

In table 5.6 and in table 5.5 the main results are summarized. Since the same gas turbine is considered and the TIT is kept constant, different syngas input are predicted, because of its different properties. This turns out into a lower amount of coal required. Moreover, even if the Cold Gas Efficiency is the same, the Hot Gas Efficiency is higher when HGD is used, due to the higher temperature of the syngas entering in the combustor.

TABLE 5.5: Gas Turbine specifics

	Gas Turbine Type GE 9001H	
	TIT °C 1394	
	CGD	HGD
Mass flow kg/s	66,84	64,77
Temperature °C	250	550,4
LHV+sensible heat	12778	13177
HGE %	83,9	86,7

Additionally, as reported in table 5.6, the overall net efficiency of the plant increases of 1-2 point percent, but the generated power decreases. The power output of the gas turbine is only slightly affected, its reduction could be explained considering that in the CGD case, the N₂ separated in the ASU is used to dilute the syngas, while in the HGD part of it is used as regeneration agent.

However the main reduction in term of power output is registered in the steam section, because of the less high pressure steam produced in the syngas coolers.

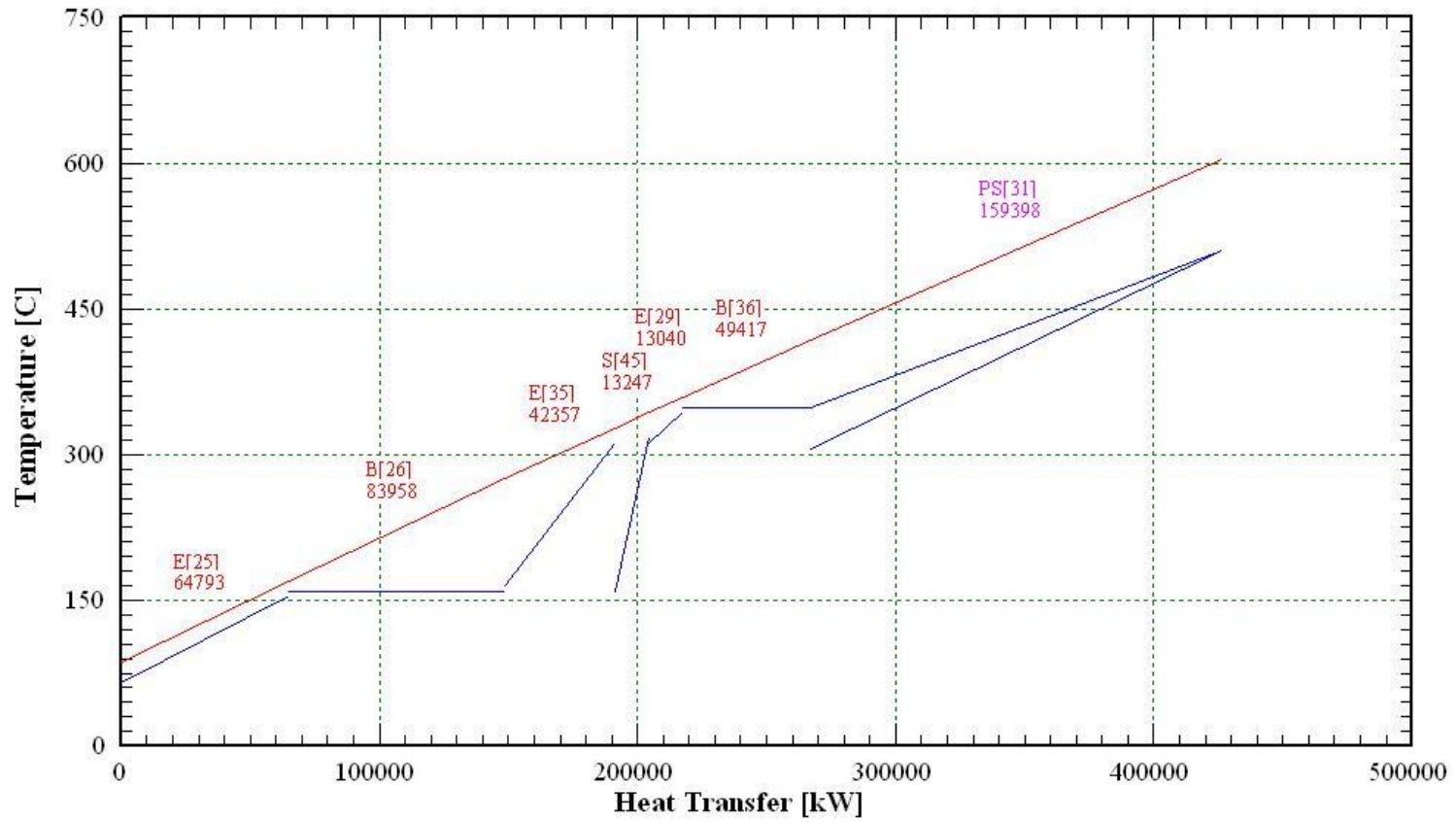
The power required by the auxiliaries also decreases, except for that needed by the recycling compressor of the gasifier, because of the higher temperature of the syngas recycled.

TABLE 5.6: Performance of IGCC with Cold Gas Desulphurization

	Cold gas cleaning		Hot gas cleaning	
Net fuel input [MW]	101.9		98.43	
Gross electric efficiency [%]	51.6		52.69	
Net electric efficiency [%]	45.77		46.9	
Gross power [MW]	525.7		518.7	
Net power [MW]	466.4		461.6	
Total auxiliaries [MW]	59.4		57	
POWER DEVICE(S)				
	shaft	generated	shaft	generated
Gas Turbine (GT PRO)	346.1	341.3	345.6	340.8
HP Steam Turbine	42.8		40.9	
IP Steam Turbine	60.2		57.5	
LP Steam Turbine	83.8		81.3	
Steam Turbine Group	186.8	184.4	179.8	177.4
Gas/Air Turbine HGD			7.12	
Gas/Air Compressor HGD			-6.64	
Total HGD			0.488	0.463
Total Generator(s)		525.7		518.7
AUXILIARY DEVICE(S)				
Air Separation Unit		42.4		41.4
Gas Cleanup System		2.04		
Wet FGD:				0.594
Gas Turbine (GT PRO) aux:		0.662		0.662
Gasifier aux:		3.11		3.57
Overall Water Pump		6.16		5.93
Steam turbine aux.		677.8		652.1
Total components auxiliaries		55.06		52.8
Total miscellaneous auxiliary		4.3		4.23
Total plant auxiliary		59.35		57.03

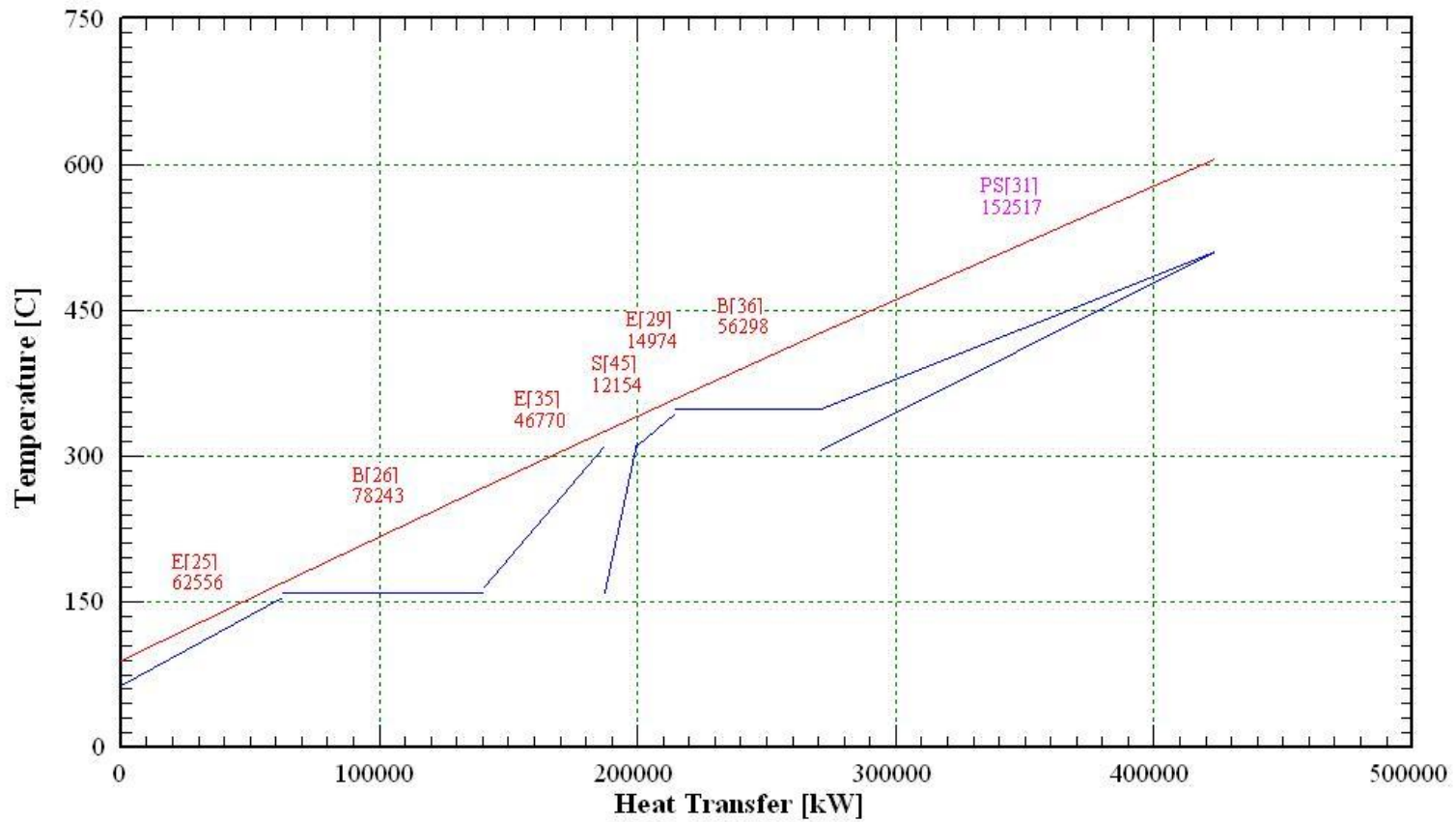
In figure 5.5 and figure 5.6, the T-Q diagram have been reported. These diagrams highlight the heat transfer between the hot exhaust of the gas turbine, indicated by the red line, and the water/stream in the bottom cycle. The heat transferred in each heat exchanger is shown.

The comparison of the T-Q diagrams, confirm an higher heat recovery in the cold gas desulphurization case, except for the HP-EVA (High pressure evaporator) and the two HP-ECO (high pressure economizer). This can be explained considering that the heat provided by the syngas cooler is higher, in fact, the temperature of the syngas at the exit is 350°C rather than 550°C as in the hot gas desulphurization.



THERMOFLEX Version 24.1

FIGURE 5.5: Heat recovery from the hot exhaust of the gas turbine for cold gas desulphurization.



THERMOFLEX Version 24,1

FIGURE 5.6: Heat recovery from the hot exhaust of the gas turbine for hot gas desulphurization

5.5 Effect of the desulphurization temperature

In early studies, an higher desulphurization temperature was associated to a beneficial effect on the overall IGCC plant.

Recent studies (Giuffrida et al., 2010, 2013) instead, suggested a lower optimal temperature range (400-600°C), due to the lower plant cost and higher hot gas clean-up system reliability. An analysis to determine the effect of the desulphurization temperature has been performed. The results discussed in the previous section, were based on a desulphurization temperature of 550°C. This case has been assumed as the reference case and for the same gas turbine and TIT, the desulphurization temperature has been varied from a value of 450°C to 650°C. The results of this analysis have been summarized in table 5.7.

It is interesting to notice that higher desulphurization temperatures lead to higher net electric efficiency but lower power output.

Not only the trade-off between the increase of energy efficiency and costs of the constructing materials have to be considered, but also the effects of the desulphurization temperature on the other contaminants, mainly on trace metals, since they could volatilize during coal gasification and consequently be transported with the syngas through the downstream technologies and finally released in the atmosphere. Some toxic metals like selenium, arsenic and mercury could cause environmental problems. Through thermodynamic calculations, four different categories have been identified, as described in Ian R Fantom and Sage 1998:

1. trace metal which condense at gasifier conditions like chromium, calcium, vanadium, and nickel
2. metals which condense once syngas is cooled at 600°C like sodium and zinc
3. elements which require temperature of 400°C to condense such us lead
4. metals which even at 400°C show an high vapor pressure and do not condense

Operate at temperature of 600°C or below allows to condense many alkali metals which can be easily collected and removed. Even if several studies have been performed on high temperature systems for trace metal removal, an example is the use of activated bauxite at temperature of 900°C to remove sodium and potassium, responsible of the deposit of liquid sulphates in the turbine, which promote corrosion effects.

TABLE 5.7: IGCC desulfurization temperature variation

PLANT SUMMARY Unit	Case 1 450°C	Case 2 500°C	Case 3 (Base Case)	Case 4 600°C	Case 5 650°C
Gross power MW	523	520.8	518.7	516.6	514.5
Gross electric efficiency(LHV) %	52.49	52.59	52.7	52.8	52.91
Net power kW	465.7	463.7	461.6	459.6	457.4
Net electric efficiency(LHV) %	46.74	46.82	46.9	46.98	47.05
Net fuel input(LHV) MW	996.4	990.3	984.3	978.28	972.3
Sorbent to desulfurizer kg/s	47.5	44.1	41	38.2	36.2
Plant auxiliary MW	57.3	57.15	57.03	56.97	57.03
Net electric efficiency(HHV) %	45.19	45.27	45.35	45.42	45.49
Net fuel input(HHV) MW	1030	1024	1018	1012	1006
Gas Turbine (GT PRO) Power MW	340.98	340.88	340.77	340.66	340.5
Steam Turbine Power MW	181.6	179.5	177.5	175.4	173.5
Air Separation Unit MW	41.8	41.6	41.4	41.2	41
Gasifier aux. MW	3.2	3.4	3.57	3.8	4.2
total auxiliary MW	0.667	0.66	0.65	0.64	0.637

For the sake of completeness, in table 5.8 the typical ranges of concentration of the main contaminants in raw syngas and the allowed limits are showed.

TABLE 5.8: Contaminants and emission limits

contaminants	typical range values	limits
H ₂ S [ppm]	1,000-14,000	<20 (<1ppm for MCFC)
HCl [ppm]	40-700	<-
Dust [<i>mg/m</i> ³]	8,300-17,000	30
Alkali metals [<i>mg/m</i> ³]		0.25

Wet scrubbing, synthetic-fibre filters represent the state of the art for low temperature gas clean-up. In table 5.9, they are compared with the hot cleaning techniques.

TABLE 5.9: Clean-up systems for hot gas desulfurization

contaminants	traditional techniques	hot gas cleaning techniques
Halogens	wet scrubbers	calcium and sodium based sorbents
Dust	cyclones fabric filters electrostatic precipitators wet scrubbers	cyclones ceramic filters
Trace metals	condensation	condensation (Cr,Ni, V, Ca) sorbent (ex:activated bauxite)

Hydrogen chloride, whose concentration can vary in quite wide range, could be removed in a temperature range of 300-600°C through calcium and sodium based sorbents, ensuring a final HCl concentration below 1 ppm, (Dou et al., 2012). However the reliability of this system has still not been proven on a significant scale.

As it is possible to notice, the hot gas cleaning techniques cover a quite large area and the need to obtain the same or higher removal efficiency, compared with the corresponding cold gas systems, see table 5.9, with a good reliability is the key element for the commercial success of these new technologies.

5.6 Outlooks & perspective

The interest in developing hot gas clean-up systems is understandable, since they allow to simplify the system configuration reducing the importance of heat recovery equipment

and enhance the energy efficiency of 1-2 point percent, because of the lower energy losses and the sensible heat of the syngas, which contributes directly to the combustion process (inlet temperature of 550°C vs. 250°C). Contemporary the power output decreases, mainly because of the lower steam produced and consequently expanding in the steam turbine. A parametric analysis to evaluate the effect of the desulphurization temperature has been performed to determine its effect on the overall plant performance. The trend obtained shows that to a temperature increase corresponds a lower power output and a higher net electric efficiency. Thus, an economic analysis could be performed to determine the optimal operating conditions.

However, some consideration would allow to define and delimit the operating range.

Many metals present in trace, such as lead, which cause faster turbine corrosion, can be condensed for desulphurization temperature above 600°C.

Low desulphurization temperatures reduce the reaction rate of the sorbent, so the amount of sorbent required increase.

For these thermodynamic reasons, the best option could be to operate at 500-550°C.

Chapter 6

Application to Coal-to-SNG Process

In Figure 6.1, the main process steps of Coal-to-SNG processes are highlighted. Coal is fed to the gasification unit to be converted through the addition of a gasification agent (air, oxygen and/or water steam) into the so called syngas or producer gas. This gas consists mainly of H_2 , CO , CO_2 , H_2O , CH_4 , and N_2 if air is used as gasification agent. Additionally, impurities like sulfur compounds and tars are also produced. However, the high temperatures reached by entrained flow gasifier allow to obtain syngas with an extremely low tar level. Sulfur compounds instead, whose concentration depends on the initial coal sulfur content, have to be removed to avoid deactivation of the catalyst caused by irreversible sulfur adsorption on the active sites. Therefore, a gas cleaning step is necessary. The use of well established cold gas desulphurization technologies will be compared to that of more advanced hot gas desulphurization. However if the former can be classified as mature technologies, the latter are still in the development & demonstration phase (with TRL 7). In the following step, methane is produced from CO and H_2 through the methanation reaction favored by the use of nickel based catalyst. The methanation process could be carried out in different reactor types: isothermal bubbling fluidized bed, as that developed by PSI (Kopyscinski et al., 2011), cooled fixed bed reactors and adiabatic fixed bed in series with intermediate cooling. The final step is the gas upgrading, where usually CO_2 and H_2O are separated to adjust the gas mixture to respect the gas quality requirements for being directly injected into the gas grid. In the following sections, the cleaning and conversion processes adopted will be discussed with the main focus on modeling & simulation aspects and their effect on the methanation process design analyzed.

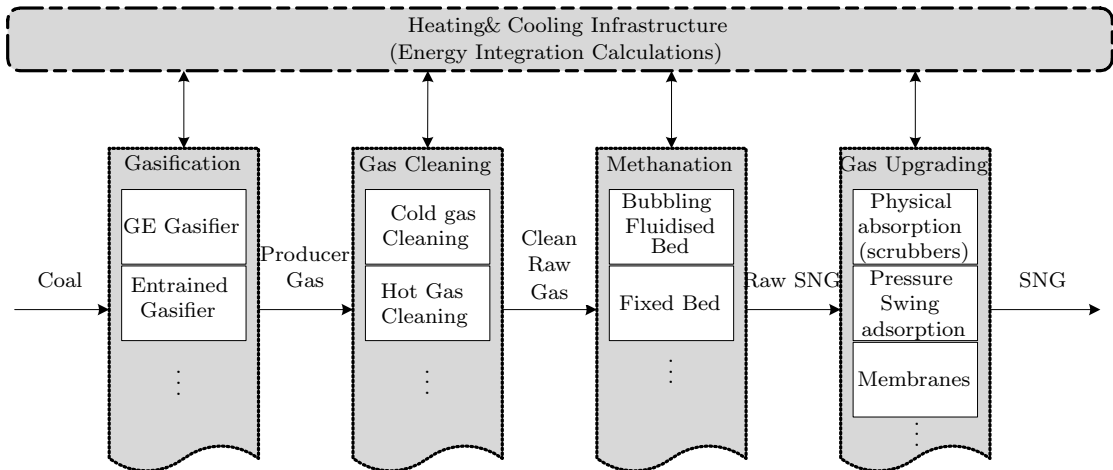


FIGURE 6.1: Alternative process unit technologies for each step of the Coal-to-SNG (Synthetic Natural Gas) process with illustration of the energy integration system. Adapted from: Teske 2014

6.1 Syngas Cleaning & conditioning

The syngas exiting the gasifier does not present the stoichiometric mixture required by methanation processes (H_2/CO ratio of three). The carbon monoxide content is usually higher than required, making it necessary to use the water gas shift reaction to adjust its value:



This reaction is not significantly affected by pressure, since the number of moles do not change, while the temperature has a strong influence. Low temperatures shift the equilibrium of the reaction towards the products but the reaction rate is slow, conversely high temperatures increase the reaction rate but the equilibrium shifts towards the reagents (according to the principle of Le Chatelier). There are two temperature ranges used for the conversion, (Twiggs, 1989):

- High-Temperature Shift - HTS (340-510°C). The active catalyst usually used is a chromium catalyst with iron oxide as a promoter. This type of catalyst has the advantage of not being affected by the presence of sulfur compounds.
- Low-temperature shift - LTS (175-270°C), using copper-zinc catalysts. It is used when low concentration of carbon monoxide are required. It allows, in fact, an almost complete conversion, in the order of 99%, but it has the disadvantage of being extremely sensitive to the presence of sulfur compounds, which must be removed to avoid catalyst poisoning.

Since low temperature catalysts are more expensive and the reaction rate is lower, when high conversion is required, an economically advantageous solution is to use a combination of both HTS and LTS. In the high temperature stage, 80-95% of the

conversion is obtained, while the remaining CO is converted at low temperature reaching concentrations below 1%.

Therefore, the WGS reaction can be conducted either before sulfur removal, known as sour shift, or after sulfur removal, known as sweet shift and at different temperatures according to the final target. Since a high conversion of CO is not required, high temperature sour shift has been considered and modeled in UniSim Design through an equilibrium reactor. Moreover, it is important to underline that sour WGS is able to convert organic sulfur compounds and mainly carbonyl sulfide (COS) into hydrogen sulfide (H₂S) which is removed in the subsequent step.

As already mentioned, two strategies for sulfur removal will be compared: cold gas desulphurization using Rectisol and hot gas desulphurization based on chemical looping. The flowsheet of the Rectisol, modeled in UniSim Design is shown in figure 6.2. It is based on the scheme proposed in Gatti et al. 2014, where a detailed description of the process is available and whose results have been closely reproduced. Only few aspects will be highlighted here. The solvent used in this process is methanol, which is able to remove both H₂S and CO₂. However, they present different solubility and this characteristic is exploited in the scheme reported in figure 6.2. The Absorber T-100 actually consists of two columns, one on top of the other. In the bottom column, due to the higher solubility of H₂S, sulfur compounds are removed together with a lower CO₂ percentage. The H₂S depleted syngas is then introduced at the bottom of the top column, in which, the pure methanol from the top removes the CO₂ remained in the gas stream. In this way, part of the methanol (A4), containing mainly CO₂, and other valuable compounds like CO and H₂ (recycled back to the absorber), is sent directly to the CO₂ desorption column indicated with T-101, while the other part of methanol rich in CO₂ enters in the bottom column from the top, meeting counter-currently the raw syngas and removing H₂S as previously underlined, producing methanol rich in both CO₂ and H₂S which has to be further treated to obtain a CO₂ pure stream which can be stored and a concentrate H₂S stream that can be sent to the Claus plant.

In the hot gas desulphurization case instead, the chemical looping process has been applied, as schematically represented in figure 5.4, considering again the air compressor driven by the turbine where the SO₂ laden gas expands.

The Clean syngas composition obtained in both cases is reported in table 6.1.

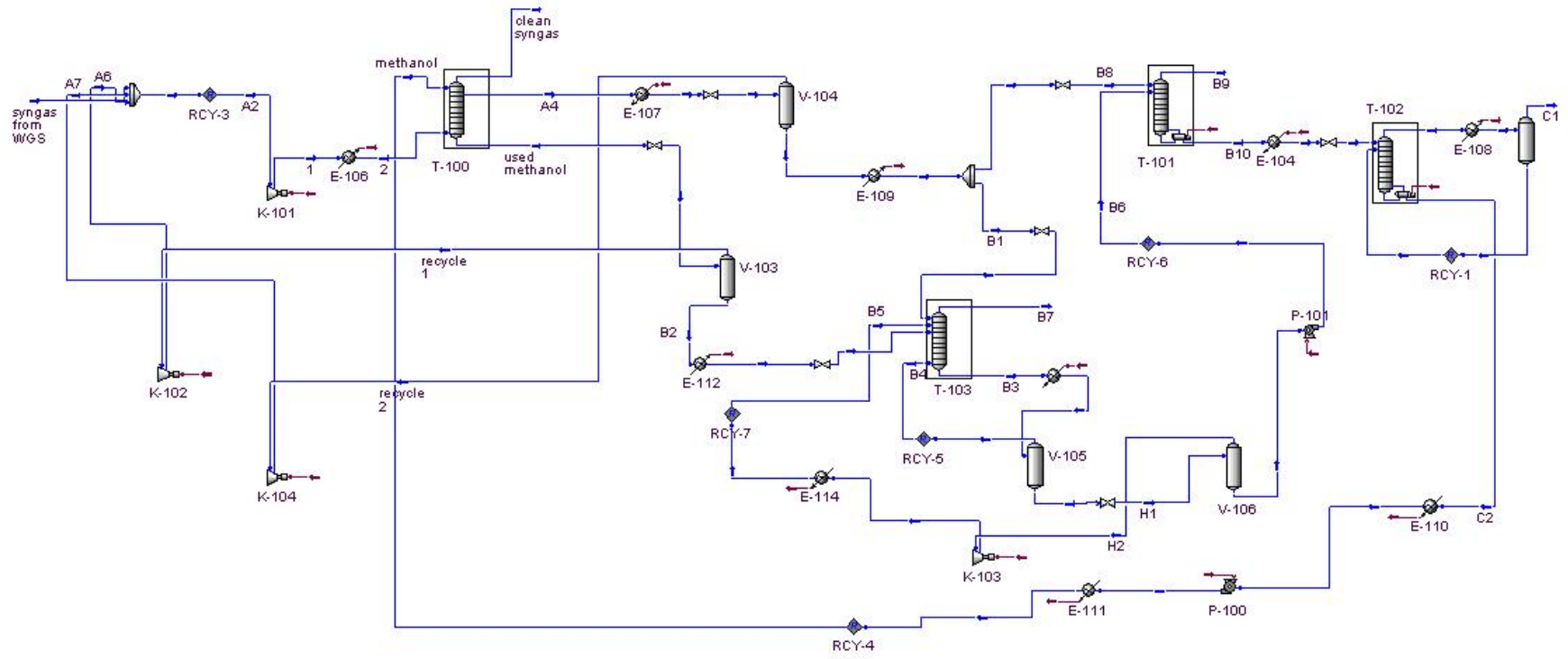


FIGURE 6.2: Flowsheet of the Rectisol Process in UniSim Design

TABLE 6.1: Clean syngas composition after Rectisol/chemical looping processes

	Clean Syngas	
	CGD	HGD
Methane	0.0	0.0
Nitrogen	0.001	0.0006
Water	0.0	0.176
CO	0.249	0.136
CO ₂	0.0007	0.279
Hydrogen	0.749	0.408

6.2 Methanation reactor

In the methanation reactor, two main reactions are occurring:

methanation



water gas shift



Even if, as already stated, different reactor types can be used, in this work, the well-known state-of-the-art adiabatic fixed bed reactor as been modeled and investigated.

6.2.1 Adiabatic fixed bed reactor model

The methanation reactor model reproduces that suggested by Parlikkad et al. 2013 validated through experimental results.

The reaction rate is expressed through the following equations, and the parameters estimated by Xu and Froment 1989 have been used:

$$r_{SMR} = \frac{K_{SMR}}{P_{H_2}^{2.5}} \frac{\frac{P_{H_2}^3 P_{CO}}{k_{SMR}} - P_{CH_4} P_{H_2O}}{1 + K_{CO} P_{CO} + K_{H_2} P_{H_2} + K_{CH_4} P_{CH_4} + K_{H_2O} P_{H_2O} P_{H_2}^{-1}} \quad (6.4)$$

$$r_{WGS} = \frac{K_{WGS}}{P_{H_2}} \frac{P_{CO} P_{H_2O} - \frac{P_{H_2} P_{CO_2}}{k_{WGS}}}{\left(1 + K_{CO} P_{CO} + K_{H_2} P_{H_2} + K_{CH_4} P_{CH_4} + K_{H_2O} P_{H_2O} P_{H_2}^{-1}\right)^2} \quad (6.5)$$

It is a one dimensional model based on pseudo-homogeneous plug flow assumptions solving mass and energy balance and Ergun equation to account for the pressure drop

along the reactor.

Mass balance:

$$G \frac{dw_i}{dz} = M w_i \rho_{cat} A (1 - \epsilon) \sum (\nu_i r_j) \quad (6.6)$$

Heat balance:

$$G c_P \frac{dT}{dz} = \rho_{cat} A (1 - \epsilon) \sum (-\Delta H_j^{react} r_j) + \pi U_{shell} (T_{shell} - T(z)) \quad (6.7)$$

Since the reactor is adiabatic the second term has been neglected.

Pressure Drop:

$$\frac{dP}{dz} = - \left(1.75 + 150 \left(\frac{1 - \epsilon}{Re} \right) \right) \frac{u^2 \rho_g (1 - \epsilon)}{d_p \epsilon^3} \quad (6.8)$$

This set of equations has been implemented and solved in Athena Visual Studio.

The model has been verified reproducing the results of Parlikkad et al. 2013 as figure 6.4 and figure 6.3 highlights.

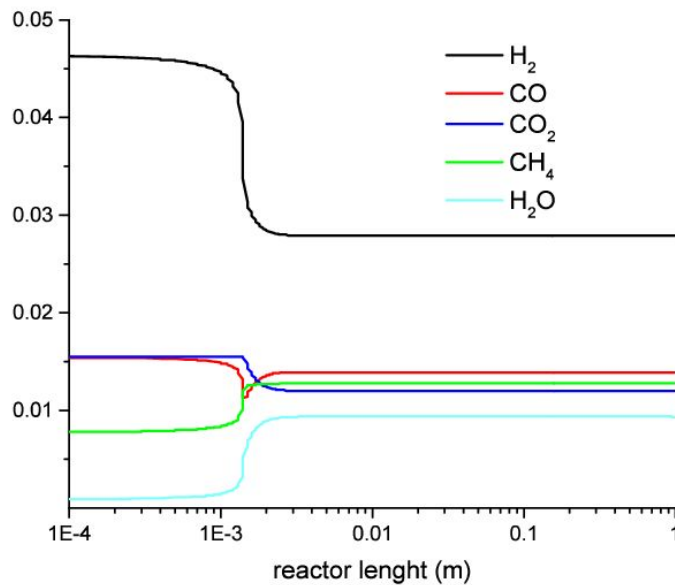


FIGURE 6.3: Concentration of the main reactant under adiabatic conditions for a Pressure of 1 atm, temperature of 550 K and H_2/CO equal 3.

The obtained results show that the reaction is already completed in the first few mm of reactor leading to thermodynamic equilibrium, no further conversion occur. This reaction is accompanied by a sudden temperature increase, as shown in figure 6.4.

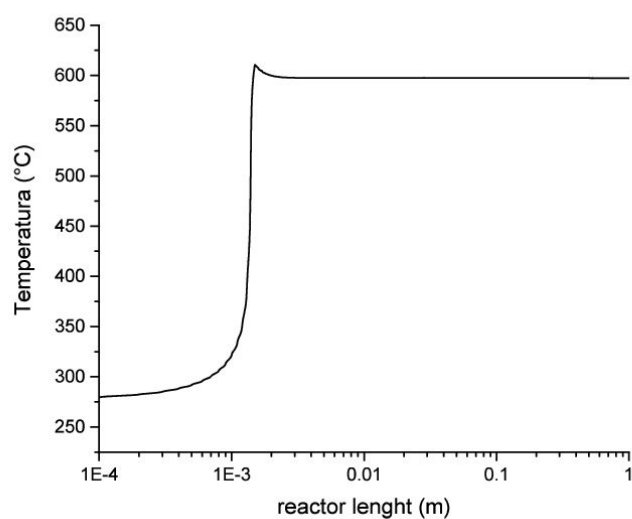


FIGURE 6.4: Temperature profile under adiabatic conditions

Figure 6.4 highlights the temperature run away, due to the exothermic reaction occurring. This temperature peak cannot be avoided even using cooled fixed bed reactors Schildhauer et al.. For this reason alternative strategies, like the recycle of reacted gas and a series of reactors with intermediate cooling are generally needed.

The effect of pressure has been also analyzed.

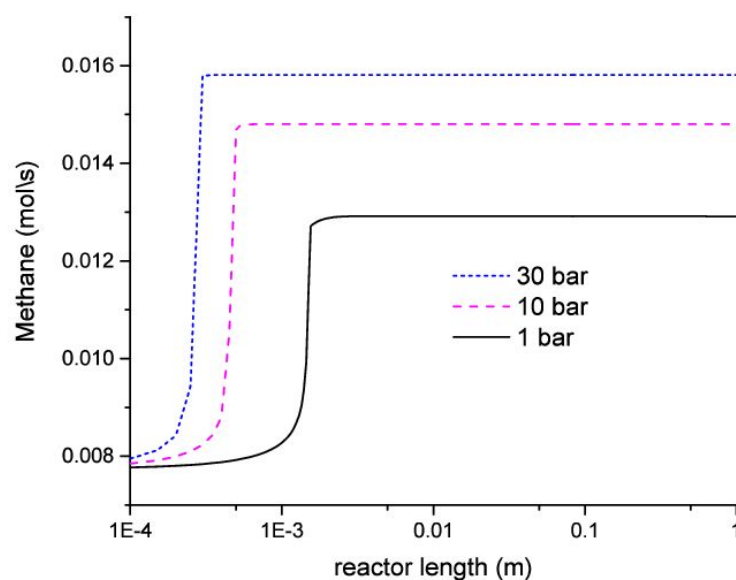


FIGURE 6.5: Methane conversion under adiabatic conditions at 1-10-30 bar

As figure 6.5 shows, a pressure increase determines an increase of the reaction rate but also a temperature increase, as figure 6.6 underlines. For this reason, higher recycles

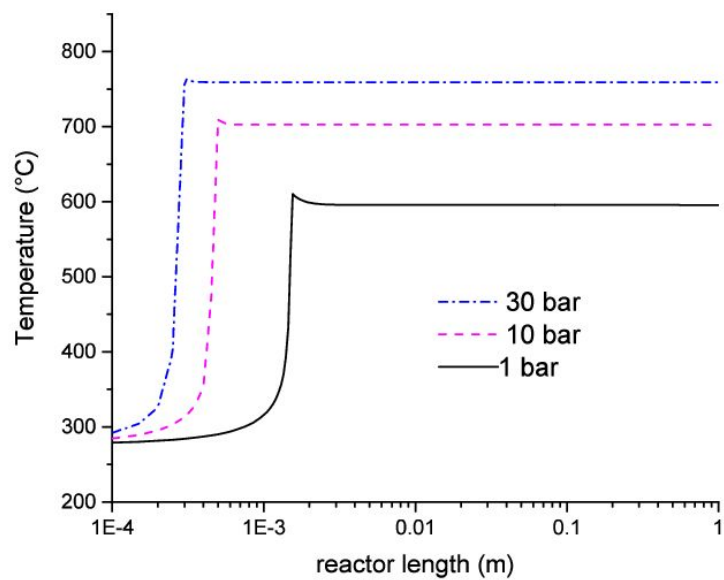


FIGURE 6.6: Temperature profile under adiabatic conditions at 1-10-30 bar

are necessary when the operation occurs at higher pressures to avoid too high reactor temperature which could damage the catalyst.

6.3 Methanation Process

Because of thermodynamic equilibrium, it is not possible to obtain a complete conversion in a single adiabatic fixed bed reactor. 4 or 5 with inter-cooling are usually required to obtain a satisfactory percentage of methane in the final gas stream. As highlighted

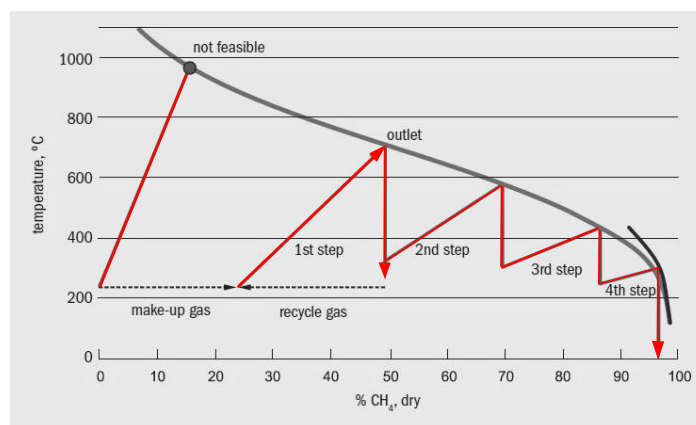


FIGURE 6.7: Equilibrium Curve for methanation process. Modified from: Jensen et al. 2011

in the previous section, the most critical parameter is represented by the temperature. The methanation reaction has a reaction enthalpy of -206 kJ/mol, which is responsible for the temperature run away and consequently for the risk of hot spot and catalyst deactivation due to sintering effect. The methanation plants are usually designed to not exceed the temperature of 600 - 700 °C. The first reactor is the most problematic, and a high recycle is needed to keep the temperature peak under control.

In the case study, the required recirculation rate is 72% , determining a not negligible effect on the recirculation costs, due to compressor K-100.

The flowsheet of the methanation plant, simulated in UniSim Design, is reported in figure 6.8, based on the TREMP process developed by Haldor Topsoe. It is also worth noticing that a drying step has been introduced followed by two adiabatic fixed bed reactors, to further increase the methane conversion.

It is important to underline that these results refer to the the desulphurization obtained by Rectisol and more detailed information is reported in Appendix A.

Regarding hot gas desulphurization, in a preliminary phase, the methanation process has been kept the same. However, the observation of the outlet temperature of the first reactor, 500 °C well below 700 °C, that represents the maximum temperature of stabilized catalyst, introduced the possibility to avoid the recycle.

The recycle, in fact, is needed in the cold case to dampen the reactor temperature: a $72,5\%$ of the gas has to be recirculated to lower the reactor temperature to 680 °C.

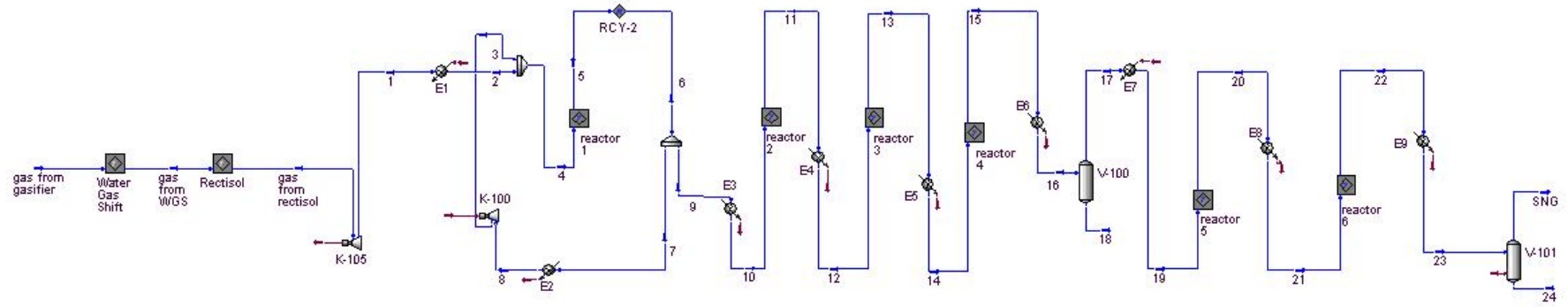


FIGURE 6.8: Flowsheet of the methanation plant in UniSim Design

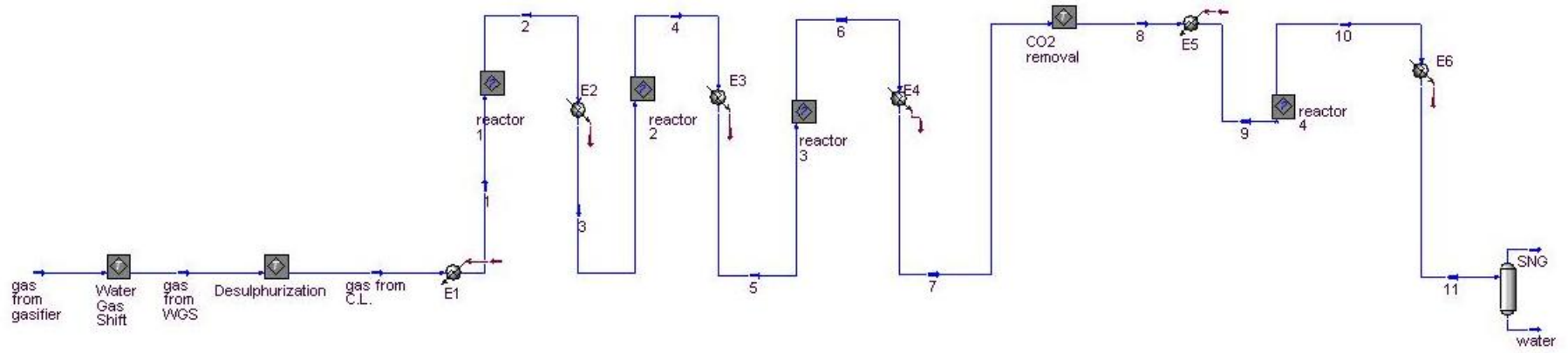


FIGURE 6.9: Flowsheet of methanation process with hot gas desulphurization in UniSim Design

In the HGD case instead, the CO_2 , not removed from the gas stream (see table 6.1), avoids the run away as suggested by Foster Wheeler in the methanation process known under the name of VESTA process (Romano et al., 2014), still at pilot scale. This process design, modeled in UniSim is reported in figure 6.9.

Advantage of this solution is not only the evident technical simplification, but also the cost ascribable to the recycle are decreased, like the cost of installation and operation of the recycling compressor.

6.4 Gas upgrading

The gas leaving the methanation reactor does not fulfill all the requirements for being directly injected into the gas grid. In fact, strict specifications should be respected, with main reference to syngas composition, Wobbe index, higher heating value (HHV) and relative density (ρ_{SNG}/ρ_{air}) at standard conditions (1atm, 15°C). In order to have comparable results, the methods to calculate the above mentioned properties, once the gas composition is known, are standardized in the ISO 6976. In particular the Wobbe index, which represents the most important interchangeability parameter, is defined as:

”The superior calorific value on a volumetric basis at specified reference conditions, divided by the square root of the relative density at the same specified metering reference conditions.”

$$WI = \frac{\cdot HHV_{SNG}}{\sqrt{\rho_{SNG}/\rho_{air}}} \quad (6.9)$$

Due to its definition, the WI is important to evaluate if the SNG quality is good enough for commercial purpose. In particular, its value should be in a range of 47.2 – 51.41 MJ/Nm³.

In the cold case, where the final products are essentially methane and water only a drying step is necessary to fulfill the specifics. In table 6.2, syngas composition and properties are reported.

TABLE 6.2: Gas composition before and after upgrading

	Before gas upgrading		After gas upgrading	
	CGD	HGD	CGD	HGD
Stream name	23	7	SNG	8
Methane (mol%)	92	18.4	96	93
Nitrogen	0.4	0.07	0.4	0.4
Water	4.2	42.3	0.06	0.2
CO	0.02	0.01	0.02	0.06
CO_2	0.6	38.4	0.7	2.78
Hydrogen	2.7	0.7	2.8	3.6

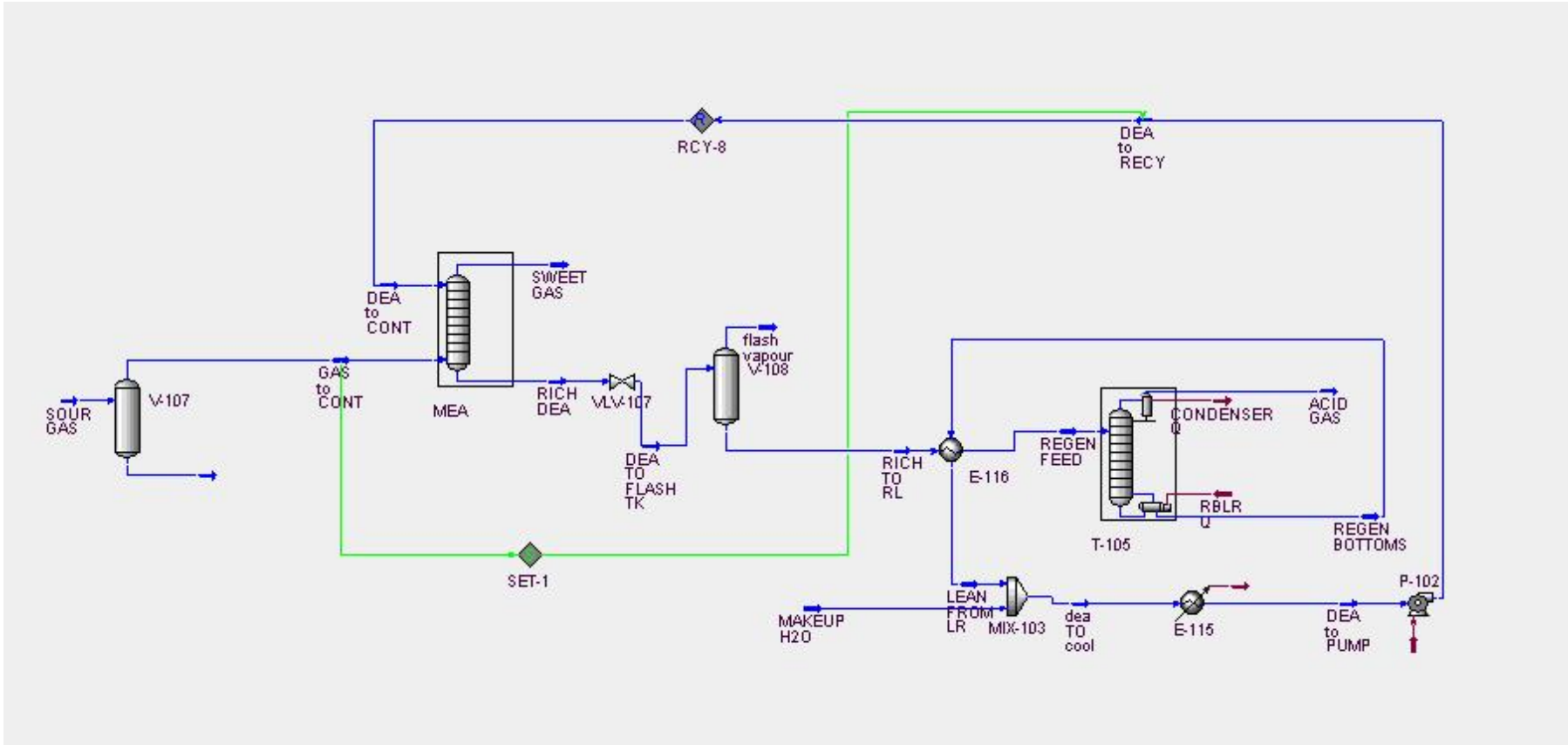


FIGURE 6.10: Flowsheet of the Amine Process in UniSim Design

Different is for the hot gas desulphurization, in this case in fact, the gas fed to the methanation reactor is not a stoichiometric mixture, this leads to high CO₂ concentration in the final gas, which has to be removed. Moreover in the HGD case, a methanation reactor is added after CO₂ removal in order to enhance the conversion and obtain a commercial SNG. CO₂ can be separated through physical absorption with rectisol or chemical absorption with amines, whose process, simulated in UniSim, is reported in figure 6.10.

The most problematic aspect of amine based absorption processes is the high energy required for solvent regeneration. In the modeled system, it assumes a value of 200 MW, which could be reduced through the optimization of the desorption column. This is beyond the object of the present thesis. Thus, the desorption column has been dimensioned according to the recommended values reported in the User Guide of UniSim (Honeywell, 2010). Moreover, considering the high amount of CO₂ that has to be removed, physical absorption could be preferable. By methanol wash in fact, it would be possible to remove the acid gas with an overall power consumption of 76 MW.

6.5 Results discussion & comparison

In order to compare the two analyzed cases with cold and hot gas desulphurization, some efficiency parameters, like the process efficiency, and /or efficiency indicators should be considered. The power output, P (kW), can be expressed through eq. 6.10

$$P = \dot{m}_{SNG} \cdot LHV_{SNG} \quad (6.10)$$

where \dot{m}_{SNG} represents the SNG mass flow rate (kg/s) and LHV_{SNG} its lower heating value (kJ/kg).

An interesting parameter is the process efficiency ($\eta_{process}$), i.e. the energy efficiency of syngas conversion to SNG, referred to the lower heating value.

$$\eta_{process} = \frac{\dot{m}_{SNG} \cdot HHV_{SNG}}{\dot{m}_{syngas} \cdot HHV_{syngas}} \quad (6.11)$$

A global efficiency (η_{global}) could also be defined. It represents the energy efficiency of coal conversion to SNG.

$$\eta_{global} = \frac{\dot{m}_{SNG} \cdot HHV_{SNG}}{\dot{m}_{coal} \cdot HHV_{coal}} \quad (6.12)$$

However, since the gasification process used is supposed to be the same in both situations, this parameter would not provide additional information.

TABLE 6.3: Efficiency indicators & produced SNG

	CGD	HGD
Power output (MW)	724	720.7
Process efficiency (%)	72.2	72
syngas molar flow (kmol/s)	5.271	5.271
syngas LHV (MJ/kmol)	190.1	190.1
SNG molar flow (kmol/s)	0,9313	0.9311
SNG LHV (MJ/kmol)	777.4	774
Wobbe Index SNG	49.39	48.18

In table 6.3, the values of the power output and the process efficiency are summarized, as well as the characteristic of the produced SNG. These efficiency indicators assume values close to each other in both HGD and CGD, as table 6.3 shows, but in the former case, it is obtained with a system simplification and lower cost due to the avoided recycle cost.

From an energetic point of view, it should be considered that even if the downstream CO₂ removal reduce the potential benefit of using hot gas desulphurization, important advantages should be underlined:

- H₂S is removed without any penalty on the system efficiency, because no syngas cooling is required. Moreover, the the overall energy balance of the desulphurization unit, including the sulfur recovery system, is nil, since the energy required by the air compressor is provided by a turbine were the SO₂ laden gas, from the regenerator, expands, according to the scheme presented in figure 5.4.
- the CO₂ produced presents a higher purity since the contaminants are removed upstream
- even if Rectisol is used for CO₂, its configuration would be simplified compared to the one removing both H₂S and CO₂, reported in figure 6.2.

6.6 Outlooks & perspective

The use of hot gas desulphurization by chemical looping, applied to methanation systems allows to: simplify the system configuration, avoiding the recycle because of the damping effect of the CO₂ in the gas stream. This determines a reduction of the costs, both the cost of installation and operation of the recycling compressor are decreased. Contemporary, a purer CO₂ stream can be separated, ensuring a high quality SNG (Wobbe index in the range of 47.2-51.41 MJ/Nm³) in both cases.

The analyzed system presents potential elements for further improvement, optimizing the CO₂ removal unit.

Chapter 7

Application to Methanol Production

Methanol is widely used in the chemical industry as additive or reactant. Common practice is to convert methanol to formaldehyde for plastics, paints and semiconductor production. It is also an excellent antifreeze and according to some researcher (Biedermann et al., 2006, McGrath et al., 2004, Olah, 2005) its environmental benefits (half-life 1 to 7 days) and low cost make methanol a suitable energy carrier.

Methanol (CH_3OH), also known as wood alcohol, since it was initially produced by wood distillation, is currently obtained through highly pure producer gas (or syngas), generated from gasification processes as well as from steam methane reforming. In this analysis, coal gasification derived syngas has been considered.

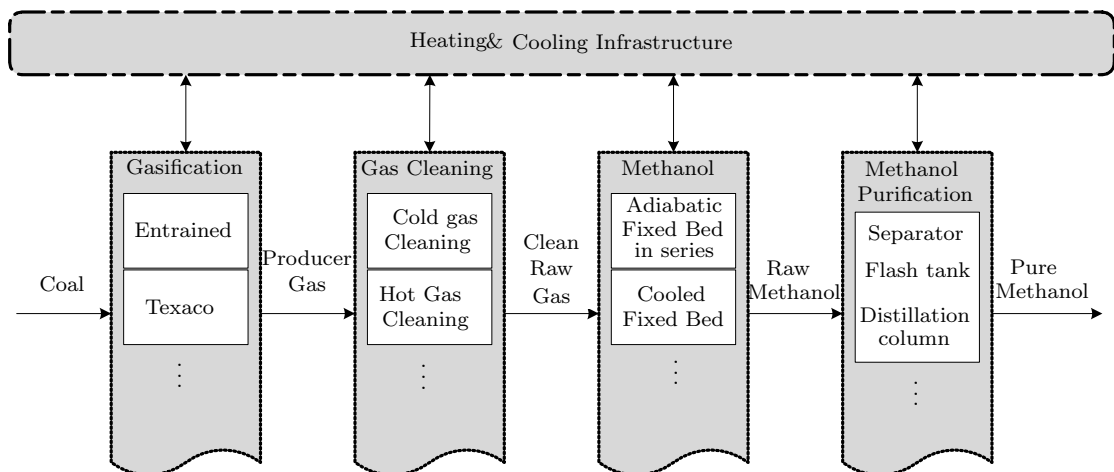


FIGURE 7.1: Alternative process unit technologies for each step of the Methanol Production. Adapted from: Teske 2014

As figure 7.1 shows, four are the main steps:

1. syngas production and conditioning

2. syngas clean-up
3. methanol synthesis
4. methanol purification and storage

With reference to syngas production, a GE gasifier has been considered. Syngas conditioning is necessary, since an H_2/CO ratio of 2 is required for methanol synthesis. This target is achieved through the water gas shift, as illustrated in chapter 6. Here, only the outlet syngas composition and the main process variable are reported in table 7.1

TABLE 7.1: Gasification & Conditioning process

Gasifier specifics		Raw syngas	
Gasifier type	GE Gasifier	Carbon monoxide (CO)	43.0%
O_2 purity	95%	Carbon dioxide (CO ₂)	9.4%
Gasifier pressure (bar)	40	Hydrogen (H ₂)	26.7%
Gasifier temperature (°C)	1589	Hydrogen sulfide (H ₂ S)	0.9302%
Carbon Conversion	99%	Nitrogen (N ₂)	0.4%
Coal/slurry ratio (mass%)	66%		
Cold gas efficiency	75,4		
Syngas after WGS & water condensation			
		Carbon monoxide (CO)	23.2%
		Carbon dioxide (CO ₂)	29.1%
		Hydrogen (H ₂)	46.4%
		Hydrogen sulfide (H ₂ S)	0.93%
		Nitrogen (N ₂)	0.4%

Syngas obtained through coal gasification is usually more rich in contaminants than that derived from methane reforming. The cleaning process is then even more critical. The concentration of sulfur compounds in particular has to be below 1ppm. Once again, the influence of using two different desulphurization processes, carried out at different temperature range will be analyzed:

- cold gas desulphurization
- hot gas desulphurization by chemical looping

The clean syngas is then sent to the plant for methanol synthesis, where it is converted into methanol and water. However, the conversion rate is so low that the recycle of unreacted gas is absolutely necessary as well as a purge line to avoid inert gas accumulation. Afterward, the produced methanol has to be purified to obtain a pure methanol stream (99% or more). Following the ASTM standard, methanol can be classified according to its purity level in A and AA. The former is generally used as solvent, while the latter requires a purity of at least 99.95% and represents the

standard usually observed in the chemical industry. Due to its central role, initially the focus will be on the methanol synthesis reactor, modeled with Athena Visual Studio, while the whole plant will be analyzed with more detail in a following step and simulated in UniSim Design.

7.1 Methanol synthesis reactor

The earliest methanol plants, introduced in 1923 by the Badische-Anilin & Soda-Fabrik (BASF), were based on high pressure processes (250-300 atm) and temperatures of 300-400°C, using manganese chromium oxide catalysts. It was only in 1960s, that the methanol process became more effective from both an economical and energetic point of view through the development of copper zinc oxide catalysts, which enabled to operate at lower pressures (40-120 atm). All the methanol synthesis technologies are currently based on low-medium pressure processes and use Cu/Zn based catalysts. In spite of these similarities different designs of methanol synthesis reactors have been developed and are commercially available:

- Quench reactor
- Adiabatic reactors in series
- Boiling water reactors (BWR)

The quench reactor consists of a certain number of adiabatic catalyst layers, as represented in figure 7.2. The main portion of reactor feed is preheated and sent at the top of the reactor, while the remaining part is split into smaller fractions and distributed below the catalyst layers, through lozenge distributors, to remove the heat of reaction.

The quench reactor represents one of the earliest reactor design, today overcome by more advantageous reactor design.

An alternative design is represented by adiabatic fixed bed reactors, generally two or four in series with a cooling step after each reactor. The heat is usually recovered by producing medium pressure steam or preheating the gas fed to the first reactor.

The main advantages of adiabatic reactors are their mechanical simplicity with consequently low investment costs and their easy scale up.

The most widely used reactor is the Boiling Water Reactor (BWR), represented in figure 7.3, whose design is similar to a shell and tube heat exchanger, with the catalyst on the tube side where the reaction takes place and steam on the shell side to keep the operating temperature under control.

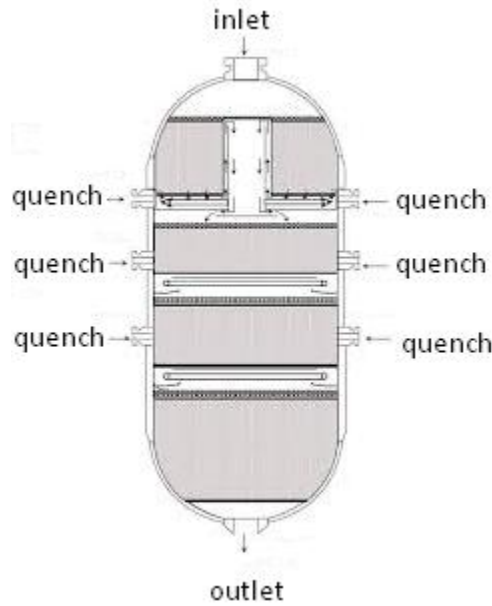


FIGURE 7.2: Scheme of a Quench Reactor. Source:Ray et al. 2015

The heat of reaction is in fact transferred to the boiling water on the shell side, allowing to operate with almost isothermal conditions, obtaining good conversion rate in comparison to other solutions, above all for temperatures of 200-260°C.

For these reasons, the boiling water reactor is analyzed and modeled as will be described in the following section.

7.1.1 Boiling water reactor model for Methanol synthesis

To model the boiling water reactor a pseudo-homogeneous approach has been used. As proven by Manenti et al. 2011, this allows to obtain results similar to the heterogeneous model but in a more efficient way, because less parameter have to be known. Since the reactor is designed to ensure that each tube behaves in the same way, the model of only one tube is sufficient to predict the behavior of the whole reactor, by solving mass and energy balance and Ergun equation to account for the pressure drop along the tubes.

Mass balance:

$$G \frac{dw_i}{dz} = Mw_i \rho_{cat} A (1 - \epsilon) \sum (\nu_i r_j) \quad (7.1)$$

Heat balance:

$$G c_P \frac{dT}{dz} = \rho_{cat} A (1 - \epsilon) \sum (-\Delta H_j^{react} r_j) + \pi U_{shell} (T_{shell} - T(z)) \quad (7.2)$$

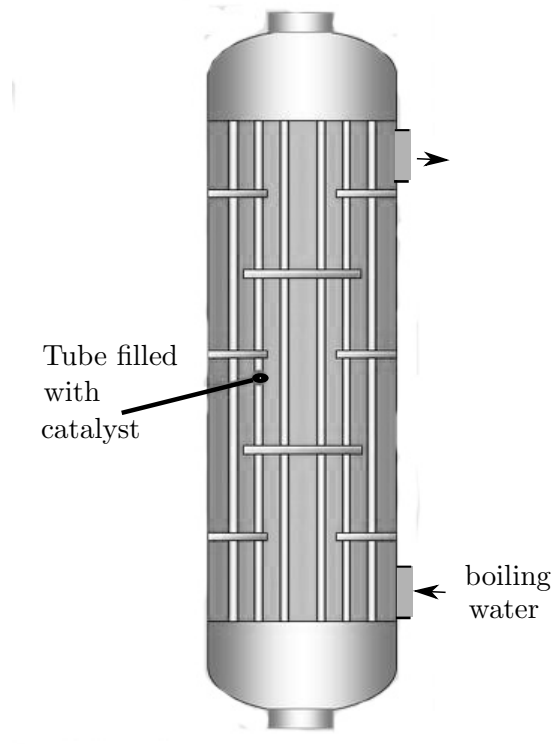


FIGURE 7.3: Boiling Water Reactor

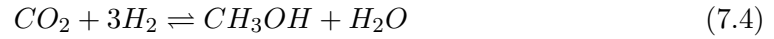
Pressure Drop:

$$\frac{dP}{dz} = - \left(1.75 + 150 \left(\frac{1 - \epsilon}{Re} \right) \right) \frac{u^2 \rho_g (1 - \epsilon)}{d_p \epsilon^3} \quad (7.3)$$

This set of equations has been implemented and solved in Athena Visual Studio. Particular attention must be paid to the calculation of the reaction rate r_j and the overall heat transfer coefficient U_{shell} .

Kinetic aspects

Even if methanol synthesis is a commercial process since 1923, still its kinetics is not fully understood. Many kinetic models have been suggested based on different assumptions of the methanol synthesis mechanism. This ambiguity could be due to the complex effect of several simultaneous reactions:



The first, who developed a model using $Cu/ZnO/Al_2O_3$ catalyst, was Leonov et al. 1973. In his work, Leonov assumed CO as the main reactant, neglecting the CO_2 influence. Klier et al. 1982, still considering CO as the main source of carbon for methanol production, introduced an empirical term to describe CO_2 hydrogenation. A similar approach has been used by Villa et al. 1985, who included the effect of the water gas shift reaction. Graaf et al. 1988, 1986 suggested a dual side mechanism with the hydrogenation of both CO and CO_2 . In 1995, Bussche and Froment 1996 considered the effect of water gas shift but assumed that methanol is mainly produced by CO_2 reaction. Based on these assumption, they obtained the following rate of reaction:

$$r_{MeOH} = \frac{K_{MeOH} P_{CO_2} P_{H_2} \left[1 - \frac{1}{K_{E1}} \left(\frac{P_{H_2O} P_{CH_3OH}}{P_{H_2}^3 P_{CO_2}} \right) \right]}{1 + K_1 \left(\frac{P_{H_2O}}{P_{H_2}} \right) + K_2 \sqrt{P_{H_2}} + K_3 P_{H_2O}} \quad (7.7)$$

$$r_{RWGS} = \frac{K_{RWGS} P_{CO_2} \left[1 - \frac{1}{K_{E2}} \left(\frac{P_{H_2O} P_{CO}}{P_{H_2} P_{CO_2}} \right) \right]}{1 + K_1 \left(\frac{P_{H_2O}}{P_{H_2}} \right) + K_2 \sqrt{P_{H_2}} + K_3 P_{H_2O}} \quad (7.8)$$

where P represent the partial pressure of the component expressed in bar and the reaction rate r_{MeOH} and r_{RWGS} are in $mol/kg_{cat}/s$. The values of the other parameters expressed through the Arrhenius equation

$$K = A \exp(B/RT) \quad (7.9)$$

are reported in table 7.2 while the equilibrium constant are determined from the following expressions:

$$\log_{10}K_{E1} = \frac{3066}{T} - 10,592 \quad (7.10)$$

$$\log_{10}\frac{1}{K_{E2}} = -\frac{2073}{T} + 2,029 \quad (7.11)$$

Bussche and Froment 1996 validated their model through experiments on a bench scale

TABLE 7.2: Parameter Values

Parameter	A	B
K1	3453.38	-
K2	0.499	17197
K3	$6.62 \cdot 10^{-11}$	124119
K_{MeOH}	1.07	36696
K_{RWGS}	$1.22 \cdot 10^{10}$	-94765

setup for an adiabatic fixed bed reactor. Their expressions have been used for modeling the reactor.

In their work, the effect of pressure was highlighted, as in figures 7.4 and 7.5, where their results are reproduced to verify the developed model.

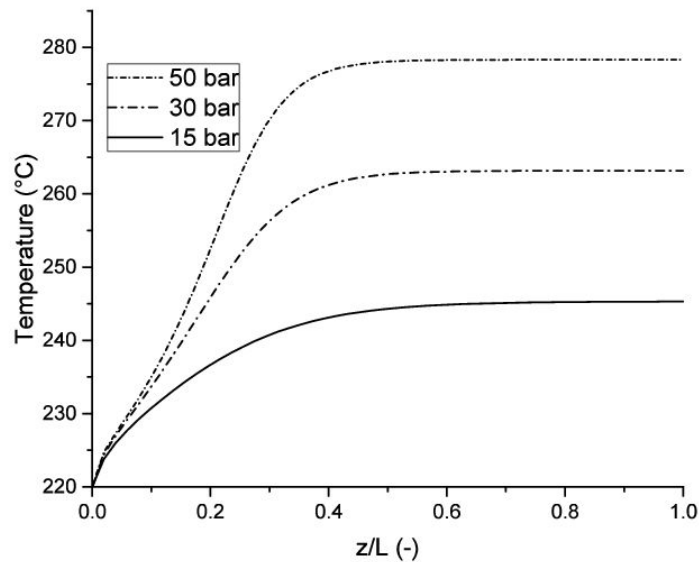


FIGURE 7.4: Temperature profile at different pressures

A higher conversion corresponds to the pressure increase, with consequently higher temperatures, due to the strongly exothermic reaction. Moreover, the effect of the inlet temperature has been analyzed by the authors showing higher conversion for temperatures in the range of 200-240°C. The reaction rate is in fact limited at lower

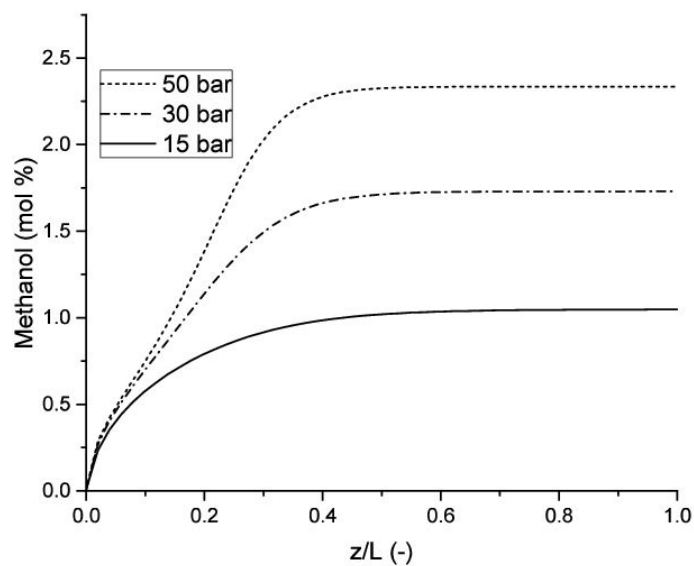


FIGURE 7.5: Methanol concentration at different pressures

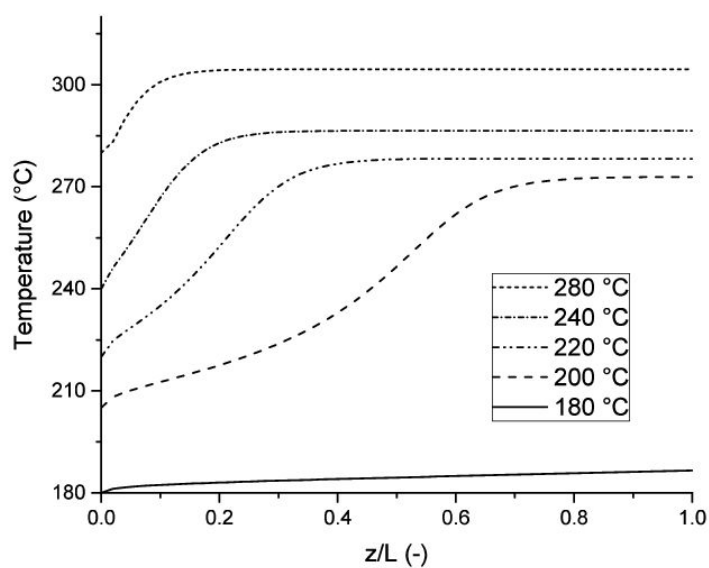


FIGURE 7.6: Temperature profiles in the adiabatic reactor for different inlet temperature

temperature by the kinetics and at higher temperatures by thermodynamic equilibrium. Since the operation in this range has a positive impact on the methanol synthesis, the use of boiling water reactor is even more attractive, allowing to work under almost isothermal conditions. For this reason, particularly important is to determine the heat transfer coefficient between the gas and the boiling water.

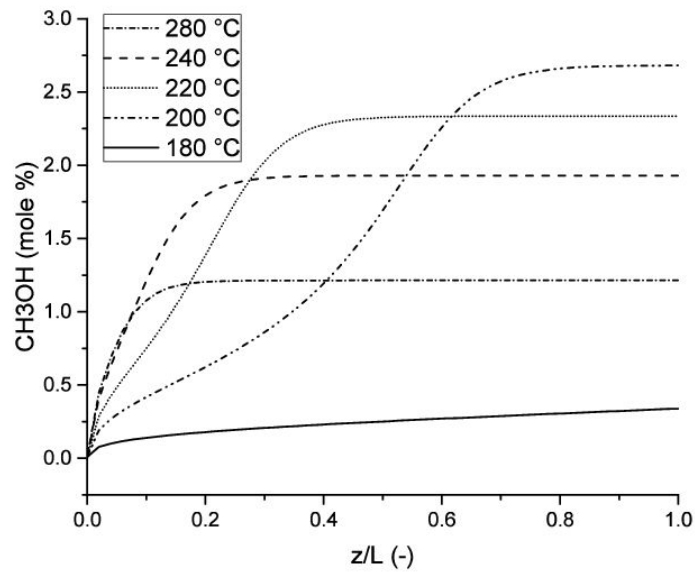


FIGURE 7.7: Methanol conversion profiles in the adiabatic reactor for different inlet temperature

Heat Transfer.

The overall heat transfer coefficient can be estimated through the following equation:

$$U_{shell} = \frac{1}{\frac{1}{h_i} + \frac{A_i \ln(r_o/r_i)}{2\pi L k} + \frac{A_i}{h_o A_o}} \quad (7.12)$$

Where the symbols used have the meaning described in figure 7.8 , k represents the tube thermal conductivity, h_i the internal heat transfer coefficient and h_o the external heat transfer coefficient.

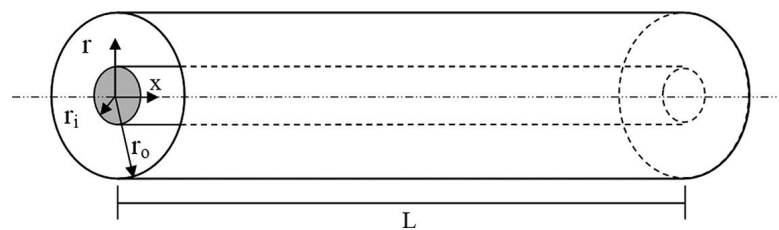


FIGURE 7.8: geometric reactor information to calculate the heat transfer coefficient

The value of the internal heat transfer coefficient has been determined through the Chilton–Colburn analogy:

$$\frac{h_i}{C_{pg}\rho\mu} \left(\frac{C_{pg}\mu}{k} \right)^{2/3} = \frac{0.458}{\epsilon} \left(\frac{\rho u d_p}{\mu} \right)^{-0.407} \quad (7.13)$$

For the external heat transfer coefficient (Knudsen et al., 1999), the Mostinski equation has been used:

$$h_0 = bP_c^{0.69} \left(\frac{q}{A} \right)^{0.7} \left[1.8 \left(\frac{P}{P_c} \right)^{0.17} + 4 \left(\frac{P}{P_c} \right)^{1.2} + 10 \left(\frac{P}{P_c} \right)^{10} \right] \quad (7.14)$$

where b is $3.75E - 5$, if the SI unit are used. The maximum heat flux can be estimated through the Cichelli-Bonilla correlation:

$$\frac{(q/A)_{max}}{P_c} = 0.368 \left(\frac{P}{P_c} \right)^{0.35} \left(1 - \frac{P}{P_c} \right)^{0.9} \quad (7.15)$$

7.1.2 Boiling water reactor model results

Based on the above described model, it is important to point out some relevant results that actually affect the whole methanol plant. In contrast to an adiabatic reactor, the inlet temperature of the feeding gas has a negligible effect, as figure 7.9 shows.

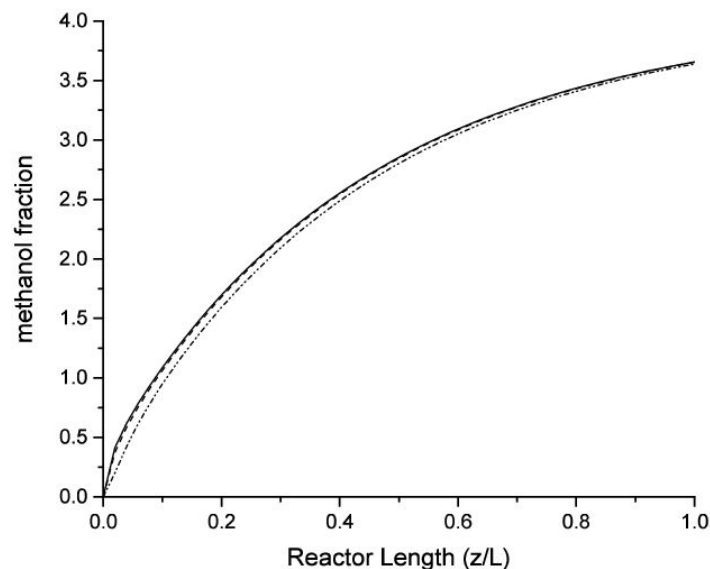


FIGURE 7.9: Effect of the inlet temperature variation (180-230-280°C) on methanol conversion.

The reactor temperature is mainly determined by the shell-side temperature thus, since boiling water is used as cooling agent, it will depend on the steam pressure (because of the strict connection between temperature and pressure). Too low shell temperatures determine lower methanol conversion. Similarly, because of thermodynamic equilibrium too high temperature leads to low methanol production, as highlighted in figure 7.10 and figure 7.11.

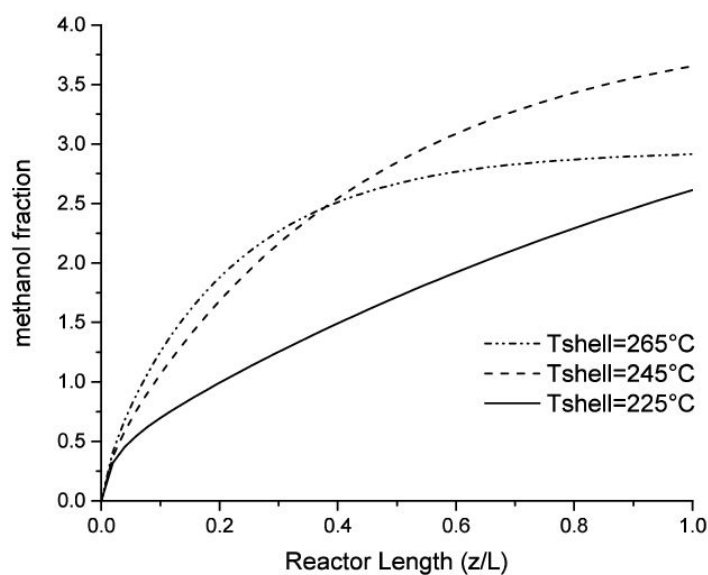


FIGURE 7.10: Effect of the shell temperature variation on methanol conversion

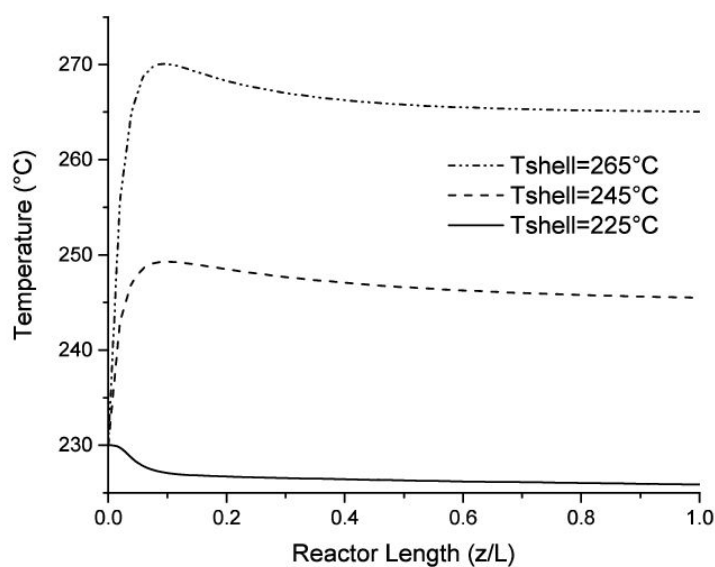


FIGURE 7.11: Effect of the shell temperature variation on the temperature profile

Moreover, the catalyst deactivation temperature has to be taken into account, usually 280-300°C.

It is also interesting to notice that a reduction of inlet flow rate, keeping constant all the other parameters, increases the temperature peak because of the higher conversion.

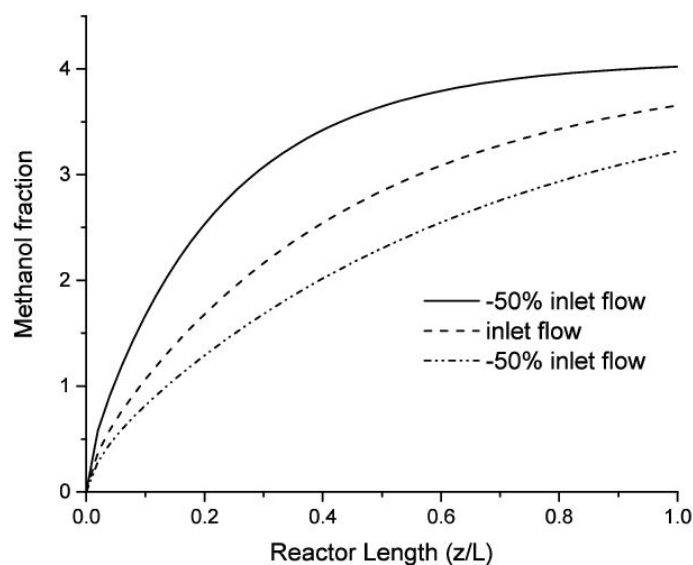


FIGURE 7.12: Effect of the inlet flow variation on methanol fraction

7.2 Process Design with cold gas desulphurization

In this section, methanol synthesis with cold gas desulphurization syngas is analyzed. In fact, the syngas exiting the water gas shift reactor has to be purified through a Rectisol Process. According to the model developed in UniSim and described in chapter 6, the syngas composition at the exit of the absorption column has been determined and reported in table 7.3.

TABLE 7.3: Clean Syngas after Rectisol Process

Syngas Composition	
Carbon monoxide (CO)	32.7
Carbon dioxide (CO ₂)	0.7
Hydrogen (H ₂)	66.1
Nitrogen (N ₂)	0.5
Water (H ₂ O)	0,0
Pressure (bar)	60
Temperature (°C)	-45
Molar flow (kmol/h)	13790

The clean syngas can finally be fed to the methanol plant, simulated in UniSim Design, based on the studies of De María et al. 2013, Luyben 2010.

In figure 7.13, the flowsheet of the whole methanol plant is reported. The syngas from the cleaning section is compressed to 110 bar. In order to reduce the energy required, two compressors with inter-cooling have been used. According to a common tendency, the compression ratio was assumed to be the same in each stage and equal to $\sqrt{P_0/P_3}$, where P_0 represent the syngas inlet pressure and P_3 is the final pressure at the exit of the second compressor, that is the operating reactor pressure, as shown in figure 7.13. In this case, since Rectisol has been used for the cleaning process, the syngas is already available at a pressure of 60 bar.

After mixing with the recycled gas, the syngas stream is preheated by the warmer gas exiting the methanol reactor which, as stated above, has been modeled in Athena. The model has been included in UniSim through the user defined operation unit. Writing the appropriate code, it is possible to control all the reactor parameters directly in UniSim. In this case, reactor length, tube diameter, number of tubes, shell temperature and catalyst properties, like density and size, have been considered. This allows to exploit all the potential of UniSim, performing accurate sensitivity analysis. The partially converted gas stream is sent to a separator, in order to recover the unreacted H_2 , CO_2 and CO which are recycled. A purge stream is also included to avoid inert gas accumulation. The liquid phase from the separator is sent to a flash tank to further remove light components, obtaining a purer methanol stream which reduces the energy required at the reboiler when it is introduced in the distillation column, designed to produce methanol with a purity of at least 99.5%.

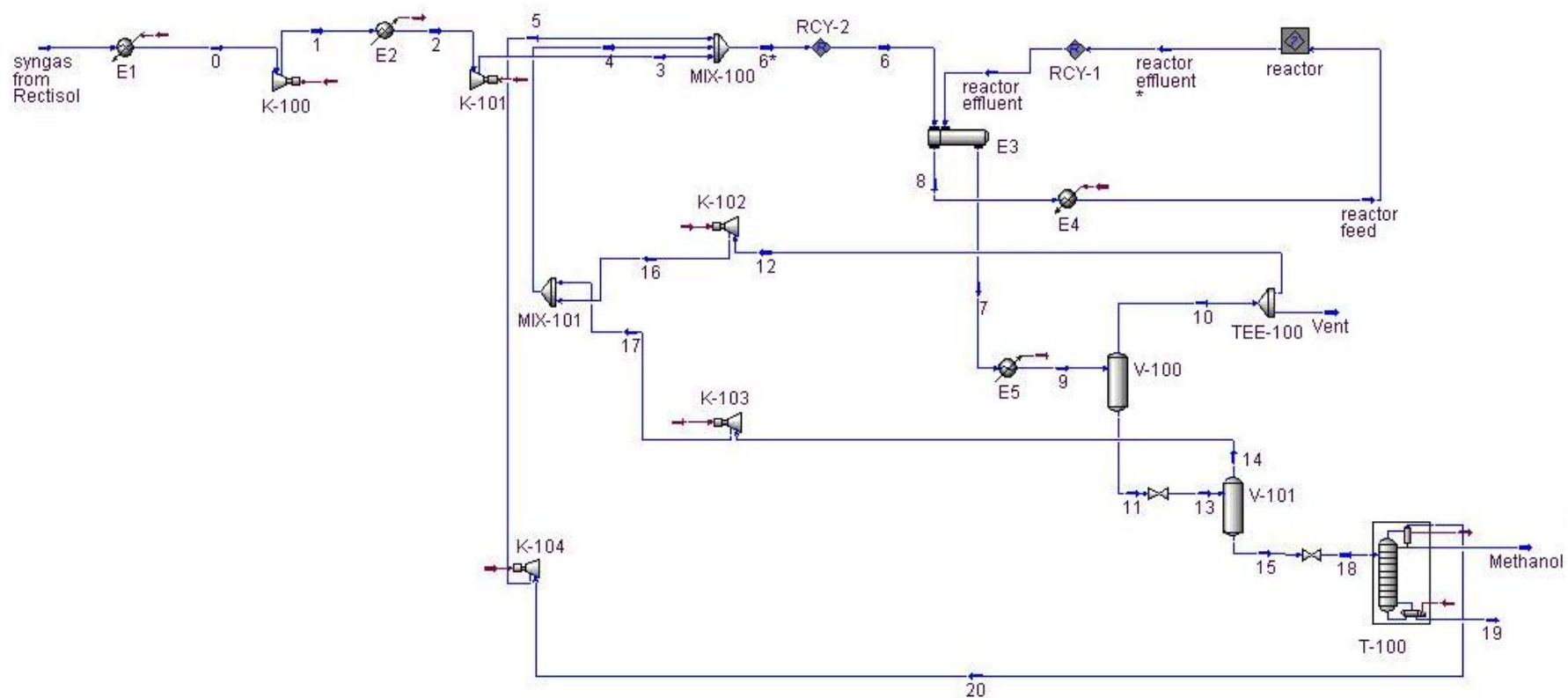


FIGURE 7.13: Flowsheet of the methanol production plant in UniSim Design

7.3 Optimization & analysis

System optimization is an important step to reduce the recirculated gas and the electric consumptions of the methanol plant, even more if the low methanol conversion rate is considered. The influence of reactor size, reactor length and operating pressure has been taken in to account, keeping constant the value of the other parameter set in order to obtain the highest methanol conversion, like the cooling temperature T_{shell} which, based on the analysis of the results for the BWR previously reported, is assumed to be 520K.

7.3.1 Effect of reactor size

Holding constant all the other variables and varying the number of tubes from 2000 to 7000, it was observed that increasing the reactor size the methanol production slightly increase while the recycle gas decreases until a minimum. The lower recycle can be

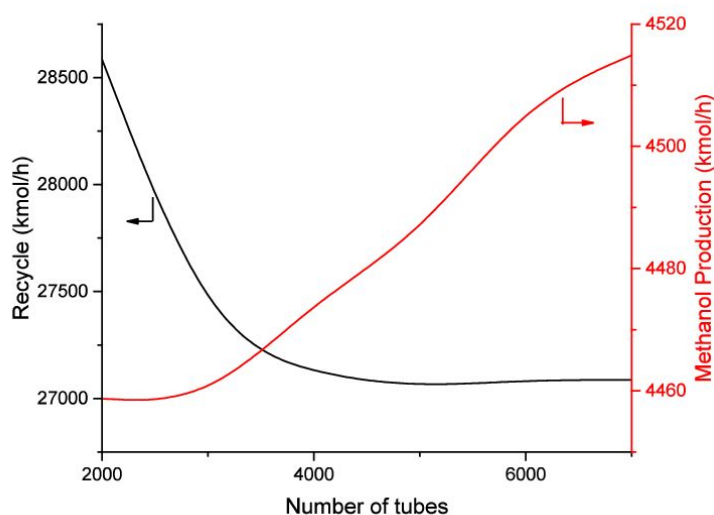


FIGURE 7.14: Effect of reactor size variation on recirculated gas and methanol production

explained considering the high methanol conversion in the synthesis reactor. Consequently, the power required to compress the recycled gas is lower. The analysis of figure 7.14 to figure 7.16 shows the existence of an appropriate value which represents a good compromise between the need to reduce the recycle and the energy required, and the installation costs due to the higher reactor size.

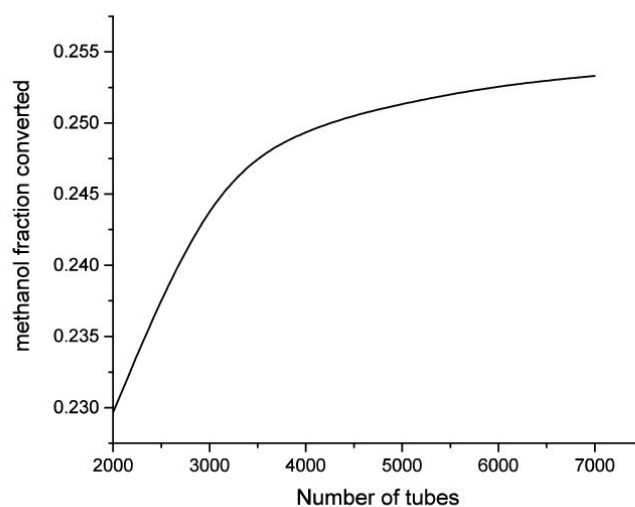


FIGURE 7.15: Effect of reactor size variation on the methanol fraction converted

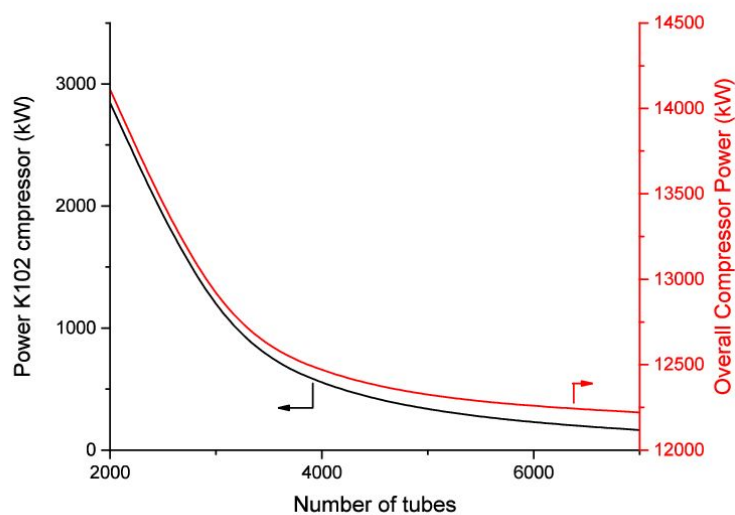


FIGURE 7.16: Effect of reactor size variation on compressor power

7.3.2 Effect of reactor length

As figure 7.17 shows, longer tubes reduce the recycle and slightly increase the methanol production. However, differently from the previous case, this does not correspond to a reduction of the recirculating compressor power, due to the higher ΔP needed to overcome the higher pressure drop inside each tube.

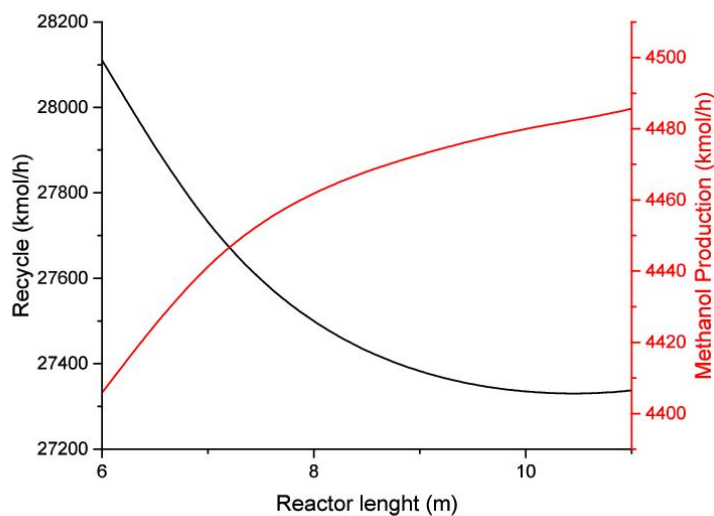


FIGURE 7.17: Effect of reactor length variation on recirculated gas and methanol production

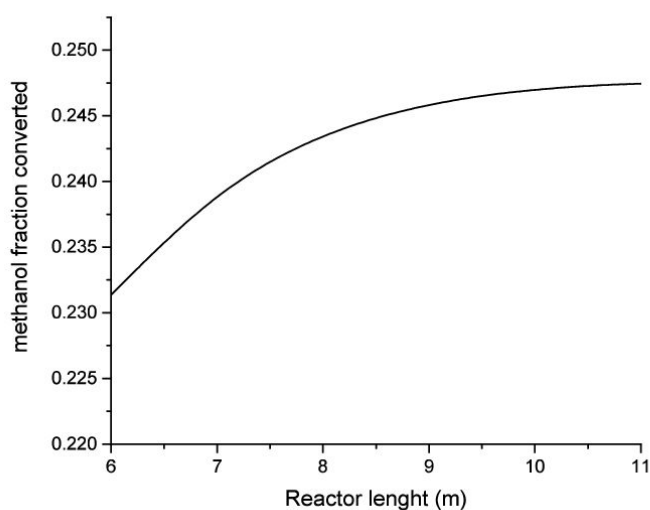


FIGURE 7.18: Effect of reactor size variation on the methanol fraction converted

7.3.3 Effect of the reactor pressure

Reactor operating pressure has a stronger influence on methanol conversion and on the overall plant production. Higher operating pressure leads to higher methanol conversion, more significant increase of methanol production and lower recycle.

However, even if the recirculation compressor consumption decreases, the overall power required significantly increases due to power required by compressors K100 and K101.

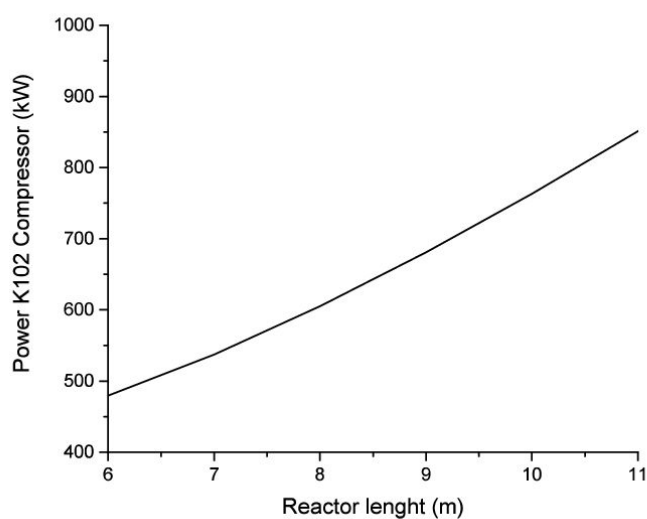


FIGURE 7.19: Effect of reactor length variation on compressor power

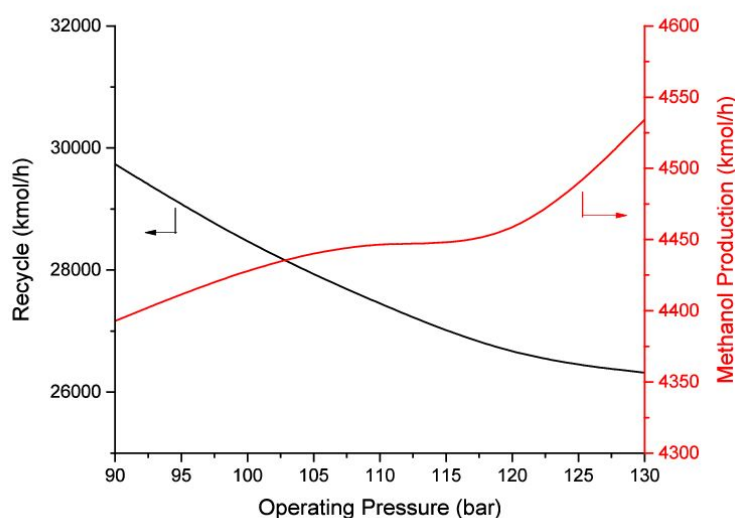


FIGURE 7.20: Effect of operating pressure variation on gas recycle and methanol production

Methanol synthesis plant shows design trade-offs between operating pressure and compressor consumptions as well as between number of tubes (i.e. reactor size) and the amount of gas recirculated. Investigating the effect of these parameter and the influence of other assumptions is then important to increase the plant performance. From this point of view, a key element is represented by the interaction between the home-made reactor model and the UniSim environment, as well as the possibility to change directly in UniSim the reactor variables, exploiting the optimization functions of UniSim Design.

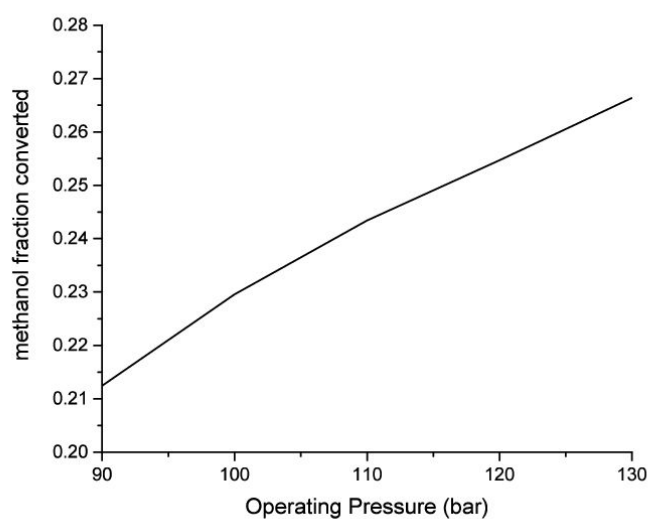


FIGURE 7.21: Effect of operating pressure variation on methanol conversion

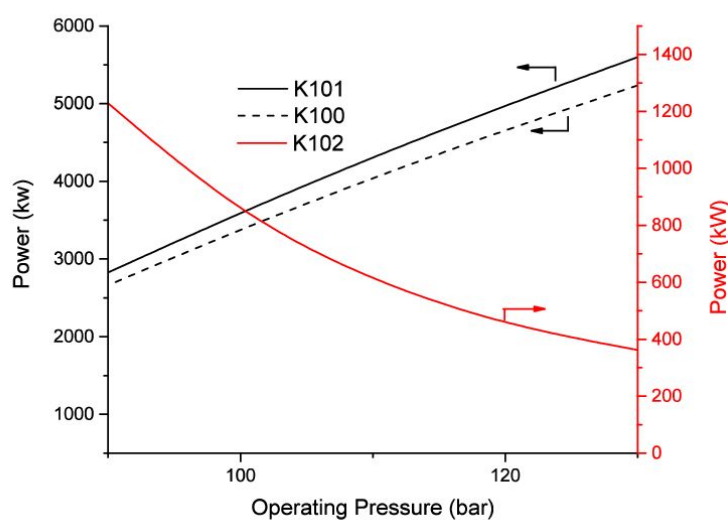


FIGURE 7.22: Effect of operating pressure variation on the power consumption of compressor K100, K101 and K102

7.4 Process design with hot gas desulphurization

For the hot gas desulphurization, the methanol plant configuration has not been changed, but the syngas composition is different. In table 7.4, the syngas composition at the exit of the hot gas desulphurization section is reported.

It is important to notice that, even if the optimal H_2/CO ratio is ensured by the water gas shift, the CO_2 which in the cold case is removed by Rectisol, is still in the gas stream increasing the overall inlet flow with consequently increasing of the reactor size.

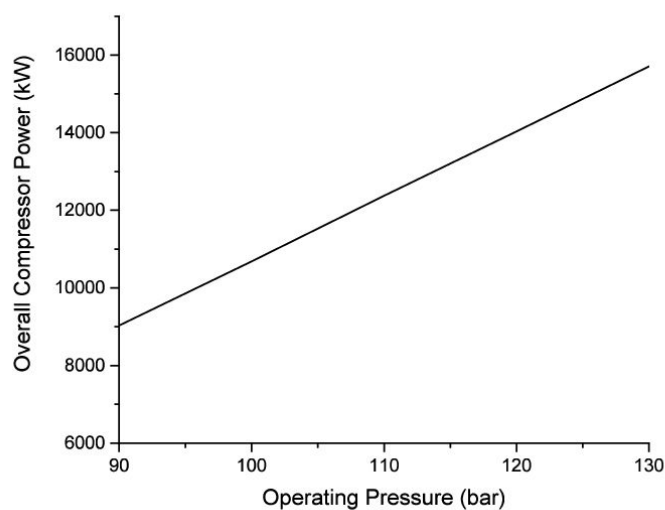


FIGURE 7.23: Effect of operating pressure variation on overall power consumption

TABLE 7.4: Clean Syngas after HGD

Syngas Composition	
Carbon monoxide (CO)	0.21
Carbon dioxide (CO ₂)	0.26
Hydrogen (H ₂)	0.42
Nitrogen (N ₂)	0.004
Water (H ₂ O)	0.106
Pressure (bar)	40
Temperature (°C)	150.0
Molar flow (kmol/h)	21590

Moreover it should be considered that the methanol conversion also decreases bringing the recycle to an unacceptable level (14 times higher than the inlet gas feed), increasing the reactor size and the overall compressors consumption and contemporary decrease of the methanol production.

The presence of water in high concentration could be responsible of a faster catalyst deactivation. On the other hand, if water is removed through condensation, the temperature of the inlet gas will be reduced in any case nullifying the advantage of a hot gas desulphurization.

7.5 Conclusions

In contrast to the excellent results obtained for hot gas desulphurization (HGD) applied to IGCC, the application of HGD to methanol synthesis does not show an equally positive result. The higher recirculation rate, with its negative impact on both reactor size and energy consumptions, determine a reduction of the overall plant performance.

The drawback is due to the presence of CO_2 which in the CGD is removed through the Rectisol process. This result shows how the development of hot gas desulphurization alone is not enough for systems like methanol synthesis where the gas composition play such a central role and specific relative concentration should be respected.

Chapter 8

Conclusions and outlooks

In this work, the chemical looping process for hot gas desulphurization has been analyzed and a one dimensional, steady state model has been developed with the software package Athena Visual Studio.

Afterward, this rate-based model was implemented in several process chain calculations to compare with state of the art cold gas cleaning. In particular, its applications to Integrated Gasification Combined Cycle, Methanation processes and methanol synthesis processes have been investigated.

The results obtained through modeling and simulation analysis showed that chemical looping represents a promising technology to increase the efficiency of IGCC power plants and contemporary ensure a high sulfur removal efficiency. An enhancement of the net electric efficiency of 1-2 point percent has been obtained, together with system simplification since the heat exchangers necessary for syngas cooling and reheating can be avoided by hot gas desulphurization. This is an extremely interesting result if considered that so high efficiency enhancement could not be obtained otherwise without a strong increase of the system complexity. A reduction of the power output could be noticed, mainly as a consequence of the reduction of the power generated by the steam turbine. In fact, compared to the cold gas desulphurization case, the high pressure steam produced in the syngas coolers is lower because of the higher temperature at which the syngas leaves the syngas coolers, 550°C rather than 300-350°C. A parametric analysis, performed for different desulphurization temperature in the range of 450-650°C has been performed. The results show that higher desulphurization temperatures lead to higher net electric efficiency but lower power output. The thermodynamic analysis performed in this study allowed to identify the optimal desulphurization temperature in the range of 500-600°C. Too low temperatures, below 500°C, reduce the desulphurization efficiency while temperature above 600°C would not allow for the condensation of trace metal responsible of fast corrosion phenomena.

In order to identify the optimal operating conditions, an economic analysis would be recommended. Moreover, it is worth noticing that the positive effects described will increase with the development of new sorbents, which allow to recover sulfur already during the regeneration phase, since in this case the sulfur recovery unit would not be necessary, with a reduction of the power required of 0.6 MW and subsequent further efficiency enhancement.

In the methanation process, a simplification of the system configuration can be obtained, too. Even if the gasification process is the same, the different gas clean up systems have a direct impact on plant design. Cold gas desulphurization by Rectisol allows to remove both H₂S and CO₂ at a temperature of -50°C; thus the syngas entering in the methanation reactor presents a stoichiometric composition. Due to the strongly exothermic reaction, recycle of the reacted gas is needed to keep the temperature below 700°C. In the hot gas desulphurization case instead, the chemical looping allows to selectively remove H₂S while the carbon dioxide in the gas stream shows a damping effect, which allows to avoid the recycle with a consequent reduction of both installation and operation costs of the recycling compressor. The electricity saved omitting the recycle cooler and the chiller in the Rectisol is equal to 25-30 kW per MW of produced SNG. Contemporary purer CO₂ can be separated downstream since the contaminants have been already removed upstream.

Moreover it should be noted that methanation reaches thermodynamic equilibrium in both cases, that is why there is no difference in amount of produced SNG and a high quality SNG is obtained, in fact the Wobbe index is in the range of 47.2-51.41 MJ/Nm³ as required in both of the analyzed cases.

In order to further exploit the advantages of hot gas desulphurization, a detailed pinch point analysis would allow to optimize the system reducing the energy demand; a cost analysis would allow for a comparison with respect to economic aspects.

Motivated by the positive results obtained for both IGCC power plants and methanation processes, the effects of using hot gas desulphurization in plants for methanol synthesis has been investigated. The chemical looping is also suitable for applications which require an extremely pure syngas stream, allowing to reach sulfur concentration below 1ppm, as the case of methanol synthesis to not poison the catalyst. However, methanol synthesis shows a low reaction rate even under stoichiometric conditions. This determines high recirculation rate, which further increases in the hot gas desulphurization case. In fact, the CO₂ in the stream negatively affects the reaction rate with subsequent increase of both reactor size and energy consumptions due to the recycling compressors. This problematic aspect could be reduced through high temperature CO₂ removal process.

The results presented show the great potential of the chemical looping desulphurization process but also the need of further studies for the development of

high temperature clean up technologies. The need to obtain the same or higher reliability compared to the corresponding cold gas systems, represents the key element for the commercial success of the hot gas clean up technologies. The chemical looping process, described in this study could be further improved, too. In particular, data in pilot/commercial scale would allow to increase the reliability of the model and consequently its predictions.

Appendix A

Flowsheet of the Methanation Process with CGD

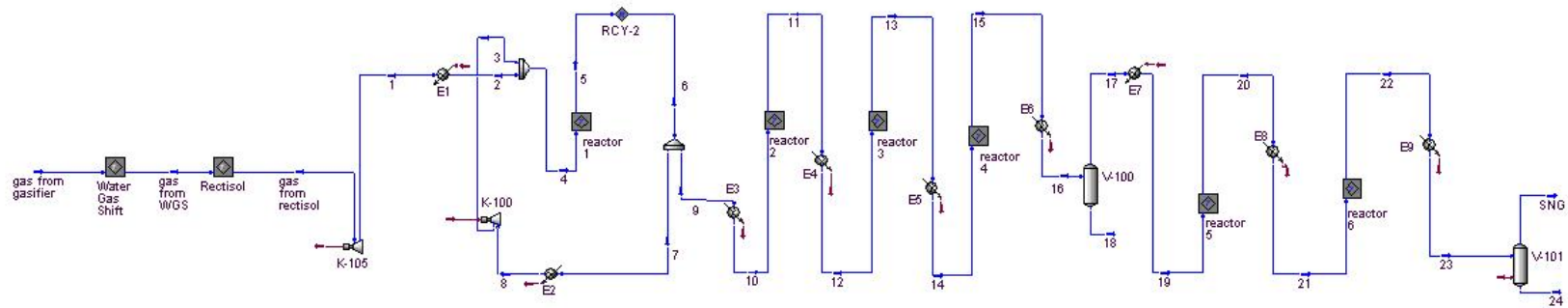


FIGURE A.1: Flowsheet of the methanation plant in UniSim Design

Calgary, Alberta
CANADA

Case Name: C:\Documents and Settings\...\SNG\CGD.usc

Unit Set: SI

Date/Time: Sunday Nov 22 2015, 11:03:13

Workbook: Case (Main)

Material Streams

Fluid Pkg:

All

Name	6	9	12	20	19
Vapour Fraction	1.0000	1.0000	1.0000	1.0000	1.0000
Temperature (C)	677.2	677.2	380.0	461.4	410.0
Pressure (kPa)	2963	2963	2961	2956	2957
Molar Flow (kgmole/h)	2.579e+004	7737	6861	3516	3631
Mass Flow (kg/h)	3.700e+005	1.110e+005	1.110e+005	5.586e+004	5.586e+004
Liquid Volume Flow (m3/h)	917.1	275.1	246.7	180.2	184.9
Heat Flow (kJ/h)	-2.380e+009	-7.140e+008	-9.059e+008	-2.127e+008	-2.126e+008
Name	10	7	8	4	13
Vapour Fraction	1.0000	1.0000	1.0000	1.0000	1.0000
Temperature (C)	220.0	677.2	200.0	200.5	419.2
Pressure (kPa)	2963	2963	2963	3000	2959
Molar Flow (kgmole/h)	7737	1.805e+004	1.805e+004	3.107e+004	6729
Mass Flow (kg/h)	1.110e+005	2.590e+005	2.590e+005	3.701e+005	1.110e+005
Liquid Volume Flow (m3/h)	275.1	642.0	642.0	1038	241.6
Heat Flow (kJ/h)	-8.679e+008	-1.666e+009	-2.039e+009	-2.334e+009	-9.059e+008

Calgary, Alberta
CANADA

Case Name: C:\Documents and Settings\...\SNG\CGD.usc

Unit Set: SI

Date/Time: Sunday Nov 22 2015, 11:03:13

Workbook: Case (Main) (continued)

Material Streams (continued)

Fluid Pkg:

All

Name	5	14	17	18	3
Vapour Fraction	1.0000	1.0000	1.0000	0.0000	1.0000
Temperature (C)	677.2	380.0	40.00	40.00	201.8
Pressure (kPa)	2963	2959	2957	2957	3000
Molar Flow (kgmole/h)	2.580e+004	6729	3631	3059	1.805e+004
Mass Flow (kg/h)	3.701e+005	1.110e+005	5.586e+004	5.513e+004	2.590e+005
Liquid Volume Flow (m3/h)	917.5	241.6	184.9	55.25	642.0
Heat Flow (kJ/h)	-2.381e+009	-9.182e+008	-2.736e+008	-8.720e+008	-2.038e+009
Name	11	24	SNG	21	gas from rectisol
Vapour Fraction	1.0000	0.0000	1.0000	1.0000	1.0000
Temperature (C)	486.5	15.00	15.00	400.0	-50.05
Pressure (kPa)	2961	2956	2956	2956	6000
Molar Flow (kgmole/h)	6861	143.5	3353	3516	1.301e+004
Mass Flow (kg/h)	1.110e+005	2585	5.327e+004	5.586e+004	1.111e+005
Liquid Volume Flow (m3/h)	246.7	2.590	176.9	180.2	395.8
Heat Flow (kJ/h)	-8.715e+008	-4.117e+007	-2.535e+008	-2.249e+008	-3.917e+008

Calgary, Alberta
CANADA

Case Name: C:\Documents and Settings\...\SNG\CGD.usc

Unit Set: SI

Date/Time: Sunday Nov 22 2015, 11:03:13

Workbook: Case (Main) (continued)

Material Streams (continued)

Fluid Pkg:

All

Name	gas from WGS	2	1	gas from gasifier	23
Vapour Fraction	1.0000	1.0000	1.0000	1.0000	0.9590
Temperature (C)	31.38	200.0	-81.93	1316	15.00
Pressure (kPa)	3000	3000	3000	3500	2956
Molar Flow (kgmole/h)	1.996e+004	1.301e+004	1.301e+004	1.897e+004	3496
Mass Flow (kg/h)	4.138e+005	1.111e+005	1.111e+005	3.960e+005	5.586e+004
Liquid Volume Flow (m3/h)	763.4	395.8	395.8	608.8	179.5
Heat Flow (kJ/h)	-2.997e+009	-2.961e+008	-4.030e+008	-1.688e+009	-2.947e+008
Name	22	15	16		
Vapour Fraction	1.0000	1.0000	0.5427		
Temperature (C)	409.9	391.5	40.00		
Pressure (kPa)	2956	2957	2957		
Molar Flow (kgmole/h)	3496	6691	6691		
Mass Flow (kg/h)	5.586e+004	1.110e+005	1.110e+005		
Liquid Volume Flow (m3/h)	179.5	240.1	240.1		
Heat Flow (kJ/h)	-2.249e+008	-9.182e+008	-1.146e+009		

Calgary, Alberta
CANADA

Case Name: C:\Documents and Settings\...\SNG\CGD.usc

Unit Set: SI

Date/Time: Sunday Nov 22 2015, 11:03:13

Workbook: Case (Main) (continued)

Compositions

Fluid Pkg:

All

Name	6	9	12	20	19
Comp Mole Frac (Methane)	0.339526	0.339526	0.446717	0.912575	0.867646
Comp Mole Frac (Methanol)	0.000000	0.000000	0.000000	0.000000	0.000000
Comp Mole Frac (Nitrogen)	0.001872	0.001872	0.002111	0.004119	0.003988
Comp Mole Frac (H2O)	0.289697	0.289697	0.423370	0.036795	0.002789
Comp Mole Frac (CO)	0.028413	0.028413	0.001045	0.001168	0.000102
Comp Mole Frac (CO2)	0.051060	0.051060	0.024734	0.008231	0.024901
Comp Mole Frac (H2S)	0.000000	0.000000	0.000000	0.000001	0.000001
Comp Mole Frac (DEAmine)	***	***	***	***	***
Comp Mole Frac (Hydrogen)	0.289433	0.289433	0.102022	0.037112	0.100573

Calgary, Alberta
CANADA

Case Name: C:\Documents and Settings\...\SNG\CGD.usc

Unit Set: SI

Date/Time: Sunday Nov 22 2015, 11:03:13

Workbook: Case (Main) (continued)

Compositions (continued)

Fluid Pkg:

All

Name	10	7	8	4	13
Comp Mole Frac (Methane)	0.339526	0.339526	0.339526	0.197310	0.465335
Comp Mole Frac (Methanol)	0.000000	0.000000	0.000000	0.000000	0.000000
Comp Mole Frac (Nitrogen)	0.001872	0.001872	0.001872	0.001507	0.002153
Comp Mole Frac (H2O)	0.289697	0.289697	0.289697	0.168353	0.450445
Comp Mole Frac (CO)	0.028413	0.028413	0.028413	0.120736	0.000149
Comp Mole Frac (CO2)	0.051060	0.051060	0.051060	0.029978	0.016304
Comp Mole Frac (H2S)	0.000000	0.000000	0.000000	0.000000	0.000000
Comp Mole Frac (DEAmine)	***	***	***	***	***
Comp Mole Frac (Hydrogen)	0.289433	0.289433	0.289433	0.482116	0.065614

Calgary, Alberta
CANADA

Case Name: C:\Documents and Settings\...\SNG\CGD.usc

Unit Set: SI

Date/Time: Sunday Nov 22 2015, 11:03:13

Workbook: Case (Main) (continued)

Compositions (continued)

Fluid Pkg:

All

Name	5	14	17	18	3
Comp Mole Frac (Methane)	0.339576	0.465335	0.867646	0.000000	0.339526
Comp Mole Frac (Methanol)	0.000000	0.000000	0.000000	0.000000	0.000000
Comp Mole Frac (Nitrogen)	0.001814	0.002153	0.003988	0.000001	0.001872
Comp Mole Frac (H2O)	0.289736	0.450445	0.002789	0.999768	0.289697
Comp Mole Frac (CO)	0.028384	0.000149	0.000102	0.000000	0.028413
Comp Mole Frac (CO2)	0.051069	0.016304	0.024901	0.000225	0.051060
Comp Mole Frac (H2S)	0.000000	0.000000	0.000001	0.000000	0.000000
Comp Mole Frac (DEAmine)	***	***	***	***	***
Comp Mole Frac (Hydrogen)	0.289421	0.065614	0.100573	0.000005	0.289433

Calgary, Alberta
CANADA

Case Name: C:\Documents and Settings\...\SNG\CGD.usc

Unit Set: SI

Date/Time: Sunday Nov 22 2015, 11:03:13

Workbook: Case (Main) (continued)

Compositions (continued)

Fluid Pkg: All

Name	11	24	SNG	21	gas from rectisol
Comp Mole Frac (Methane)	0.446717	0.000000	0.959879	0.912575	0.000000
Comp Mole Frac (Methanol)	0.000000	0.000000	0.000000	0.000000	0.000000
Comp Mole Frac (Nitrogen)	0.002111	0.000002	0.004319	0.004119	0.001000
Comp Mole Frac (H2O)	0.423370	0.999894	0.000646	0.036795	0.000000
Comp Mole Frac (CO)	0.001045	0.000000	0.000237	0.001168	0.248826
Comp Mole Frac (CO2)	0.024734	0.000103	0.006694	0.008231	0.000730
Comp Mole Frac (H2S)	0.000000	0.000000	0.000001	0.000001	0.000000
Comp Mole Frac (DEAmine)	***	***	***	***	***
Comp Mole Frac (Hydrogen)	0.102022	0.000001	0.028223	0.037112	0.749445

Calgary, Alberta
CANADA

Case Name: C:\Documents and Settings\...\SNG\CGD.usc

Unit Set: SI

Date/Time: Sunday Nov 22 2015, 11:03:13

Workbook: Case (Main) (continued)

Compositions (continued)

Fluid Pkg:

All

Name	gas from WGS	2	1	gas from gasifier	23
Comp Mole Frac (Methane)	0.000000	0.000000	0.000000	0.000000	0.920487
Comp Mole Frac (Methanol)	0.000000	0.000000	0.000000	0.000000	0.000000
Comp Mole Frac (Nitrogen)	0.000665	0.001000	0.001000	0.000700	0.004142
Comp Mole Frac (H2O)	0.000000	0.000000	0.000000	0.195504	0.041654
Comp Mole Frac (CO)	0.163018	0.248826	0.248826	0.419230	0.000227
Comp Mole Frac (CO2)	0.334634	0.000730	0.000730	0.104398	0.006424
Comp Mole Frac (H2S)	0.012633	0.000000	0.000000	0.013293	0.000001
Comp Mole Frac (DEAmine)	***	***	***	***	***
Comp Mole Frac (Hydrogen)	0.489050	0.749445	0.749445	0.266876	0.027065

Calgary, Alberta
CANADA

Case Name: C:\Documents and Settings\...\SNG\CGD.usc

Unit Set: SI

Date/Time: Sunday Nov 22 2015, 11:03:13

Workbook: Case (Main) (continued)

Compositions (continued)

Fluid Pkg:

All

Name	22	15	16		
Comp Mole Frac (Methane)	0.920487	0.470886	0.470886		
Comp Mole Frac (Methanol)	0.000000	0.000000	0.000000		
Comp Mole Frac (Nitrogen)	0.004142	0.002165	0.002165		
Comp Mole Frac (H2O)	0.041654	0.458691	0.458691		
Comp Mole Frac (CO)	0.000227	0.000055	0.000055		
Comp Mole Frac (CO2)	0.006424	0.013617	0.013617		
Comp Mole Frac (H2S)	0.000001	0.000000	0.000000		
Comp Mole Frac (DEAmine)	***	***	***		
Comp Mole Frac (Hydrogen)	0.027065	0.054585	0.054585		

Appendix B

Flowsheet of the Methanation Process with HGD

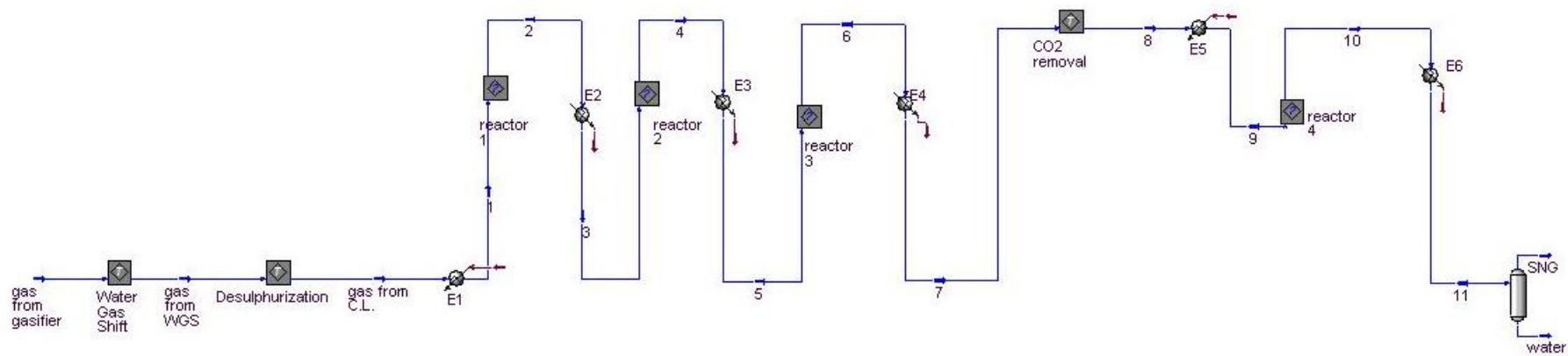


FIGURE B.1: Flowsheet of methanation process with hot gas desulphurization in UniSim Design

Calgary, Alberta
CANADA

Case Name: C:\Documents and Settings\...\SNG\HGD.usc

Unit Set: SI

Date/Time: Sunday Nov 22 2015, 11:18:08

Workbook: Case (Main)

Material Streams

Fluid Pkg:

All

Name	8	5	10	9	3
Vapour Fraction	1.0000	1.0000	1.0000	1.0000	1.0000
Temperature (C)	35.43	280.0	417.9	400.0	200.0
Pressure (kPa)	2870	2928	2869	2870	2951
Molar Flow (kgmole/h)	3440	1.778e+004	3400	3440	1.969e+004
Mass Flow (kg/h)	5.633e+004	4.809e+005	5.633e+004	5.633e+004	4.809e+005
Liquid Volume Flow (m3/h)	180.7	677.5	179.0	180.7	710.3
Heat Flow (kJ/h)	-2.796e+008	-4.477e+009	-2.216e+008	-2.216e+008	-4.311e+009
Name	6	2	7	4	1
Vapour Fraction	1.0000	1.0000	0.5741	1.0000	1.0000
Temperature (C)	321.6	680.0	25.00	477.1	200.0
Pressure (kPa)	2910	2951	2910	2928	2990
Molar Flow (kgmole/h)	1.747e+004	1.969e+004	1.747e+004	1.778e+004	2.391e+004
Mass Flow (kg/h)	4.809e+005	4.809e+005	4.809e+005	4.809e+005	4.809e+005
Liquid Volume Flow (m3/h)	668.1	710.3	668.1	677.5	828.3
Heat Flow (kJ/h)	-4.476e+009	-3.909e+009	-5.009e+009	-4.318e+009	-3.874e+009

Calgary, Alberta
CANADA

Case Name: C:\Documents and Settings\...\SNG\HGD.usc

Unit Set: SI

Date/Time: Sunday Nov 22 2015, 11:18:08

Workbook: Case (Main) (continued)

Material Streams (continued)

Fluid Pkg: All

Name	gas from C.L.	11	water	SNG	gas from gasifier
Vapour Fraction	1.0000	0.9857	0.0000	1.0000	1.0000
Temperature (C)	503.8	15.00	15.00	15.00	900.0
Pressure (kPa)	2990	2869	2869	2869	3500
Molar Flow (kgmole/h)	2.391e+004	3400	48.49	3352	1.897e+004
Mass Flow (kg/h)	4.809e+005	5.633e+004	874.0	5.546e+004	3.960e+005
Liquid Volume Flow (m3/h)	828.3	179.0	0.8759	178.2	608.8
Heat Flow (kJ/h)	-3.609e+009	-2.876e+008	-1.392e+007	-2.737e+008	-1.993e+009
Name	gas from WGS				
Vapour Fraction	1.0000				
Temperature (C)	503.7				
Pressure (kPa)	3000				
Molar Flow (kgmole/h)	2.416e+004				
Mass Flow (kg/h)	4.895e+005				
Liquid Volume Flow (m3/h)	839.2				
Heat Flow (kJ/h)	-3.610e+009				

Calgary, Alberta
CANADA

Case Name: C:\Documents and Settings\...\SNG\HGD.usc

Unit Set: SI

Date/Time: Sunday Nov 22 2015, 11:18:08

Workbook: Case (Main) (continued)

Compositions

Fluid Pkg:

All

Name	8	5	10	9	3
Comp Mole Frac (Methane)	0.929818	0.172586	0.946385	0.929818	0.107312
Comp Mole Frac (Methanol)	0.000000	0.000000	0.000000	0.000000	0.000000
Comp Mole Frac (Nitrogen)	0.003843	0.000747	0.003888	0.003843	0.000674
Comp Mole Frac (H2O)	0.002250	0.403919	0.014913	0.002250	0.342320
Comp Mole Frac (CO)	0.000563	0.005590	0.001621	0.000563	0.079698
Comp Mole Frac (CO2)	0.027786	0.380745	0.021264	0.027786	0.317668
Comp Mole Frac (H2S)	0.000000	0.000000	0.000000	0.000000	0.000000
Comp Mole Frac (DEAmine)	***	***	***	***	***
Comp Mole Frac (Hydrogen)	0.035740	0.036415	0.011930	0.035740	0.152329

Calgary, Alberta
CANADA

Case Name: C:\Documents and Settings\...\SNG\HGD.usc

Unit Set: SI

Date/Time: Sunday Nov 22 2015, 11:18:08

Workbook: Case (Main) (continued)

Compositions (continued)

Fluid Pkg:

All

Name	6	2	7	4	1
Comp Mole Frac (Methane)	0.184542	0.107312	0.184542	0.172586	0.000000
Comp Mole Frac (Methanol)	0.000000	0.000000	0.000000	0.000000	0.000000
Comp Mole Frac (Nitrogen)	0.000760	0.000674	0.000760	0.000747	0.000555
Comp Mole Frac (H2O)	0.423298	0.342320	0.423298	0.403919	0.175624
Comp Mole Frac (CO)	0.000112	0.079698	0.000112	0.005590	0.136107
Comp Mole Frac (CO2)	0.384202	0.317668	0.384202	0.380745	0.279394
Comp Mole Frac (H2S)	0.000000	0.000000	0.000000	0.000000	0.000000
Comp Mole Frac (DEAmine)	***	***	***	***	***
Comp Mole Frac (Hydrogen)	0.007087	0.152329	0.007087	0.036415	0.408320

Calgary, Alberta
CANADA

Case Name: C:\Documents and Settings\...\SNG\HGD.usc

Unit Set: SI

Date/Time: Sunday Nov 22 2015, 11:18:08

Workbook: Case (Main) (continued)

Compositions (continued)

Fluid Pkg: All

Name	gas from C.L.	11	water	SNG	gas from gasifier
Comp Mole Frac (Methane)	0.000000	0.946385	0.000000	0.960076	0.000000
Comp Mole Frac (Methanol)	0.000000	0.000000	0.000000	0.000000	0.000000
Comp Mole Frac (Nitrogen)	0.000555	0.003888	0.000002	0.003944	0.000700
Comp Mole Frac (H2O)	0.175624	0.014913	0.999674	0.000666	0.195504
Comp Mole Frac (CO)	0.136107	0.001621	0.000000	0.001644	0.419230
Comp Mole Frac (CO2)	0.279394	0.021264	0.000324	0.021567	0.104398
Comp Mole Frac (H2S)	0.000000	0.000000	0.000000	0.000000	0.013293
Comp Mole Frac (DEAmine)	***	***	***	***	***
Comp Mole Frac (Hydrogen)	0.408320	0.011930	0.000000	0.012103	0.266876

Calgary, Alberta
CANADA

Case Name: C:\Documents and Settings\...\SNG\HGD.usc

Unit Set: SI

Date/Time: Sunday Nov 22 2015, 11:18:08

Workbook: Case (Main) (continued)

Compositions (continued)

Fluid Pkg:

All

Name	gas from WGS				
Comp Mole Frac (Methane)	0.000000				
Comp Mole Frac (Methanol)	0.000000				
Comp Mole Frac (Nitrogen)	0.000549				
Comp Mole Frac (H2O)	0.173791				
Comp Mole Frac (CO)	0.134687				
Comp Mole Frac (CO2)	0.276477				
Comp Mole Frac (H2S)	0.010438				
Comp Mole Frac (DEAmine)	***				
Comp Mole Frac (Hydrogen)	0.404058				

Appendix C

Flowsheet of the Methanol Synthesis Process with CGD

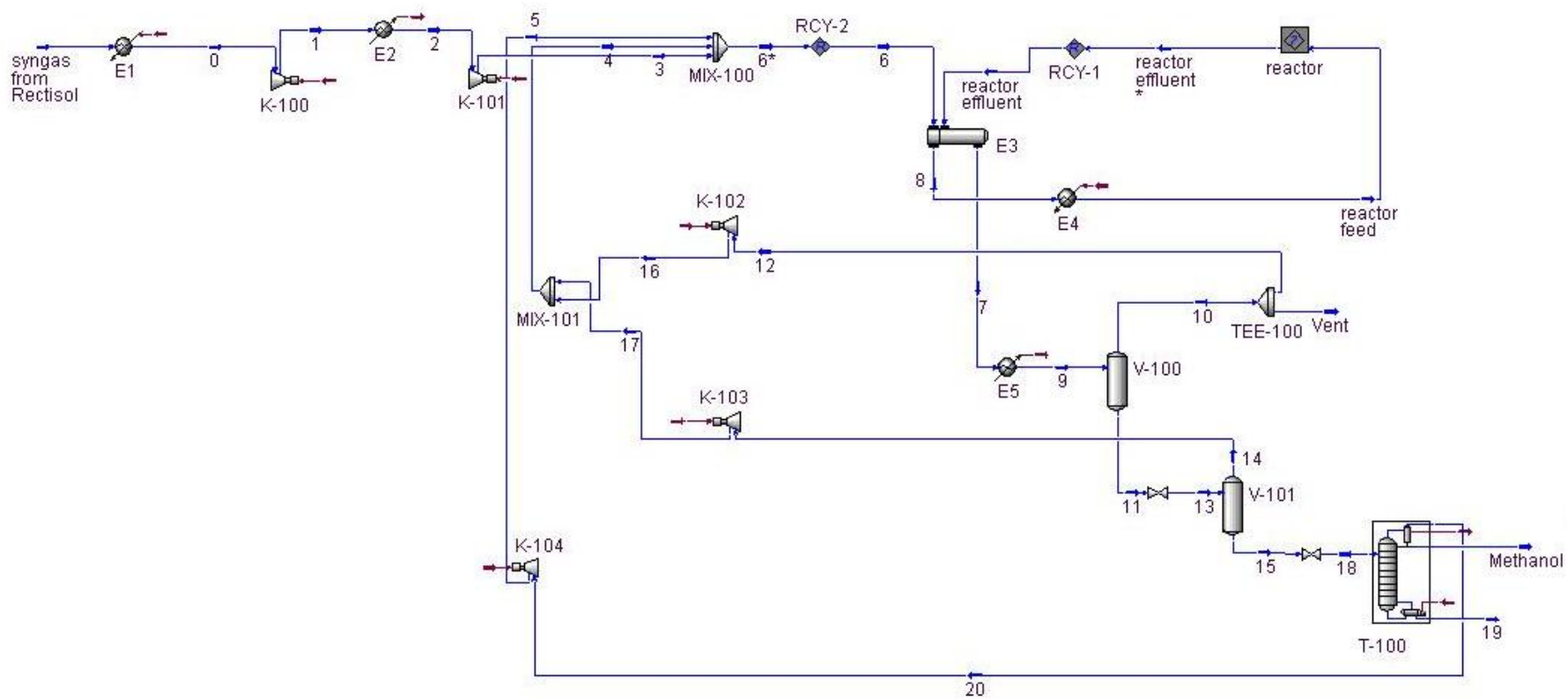


FIGURE C.1: Flowsheet of the methanol production plant in UniSim Design

Calgary, Alberta
CANADA

Case Name: C:\Documents and Settings\...\Methano\CGD.usc

Unit Set: SI

Date/Time: Sunday Nov 22 2015, 10:39:43

Workbook: Case (Main)

Material Streams

Fluid Pkg:

All

Name	1	2	3	6	7
Vapour Fraction	1.0000	1.0000	1.0000	1.0000	0.9308
Temperature (C)	58.04	38.00	76.16	71.23	156.9
Pressure (kPa)	8124	8124	1.100e+004	1.100e+004	1.075e+004
Molar Flow (kgmole/h)	1.379e+004	1.379e+004	1.379e+004	2.591e+004	1.696e+004
Mass Flow (kg/h)	1.508e+005	1.508e+005	1.508e+005	3.862e+005	3.862e+005
Liquid Volume Flow (m3/h)	428.5	428.5	428.5	848.9	613.1
Heat Flow (kJ/h)	-5.248e+008	-5.330e+008	-5.175e+008	-1.367e+009	-1.776e+009
Name	reactor effluent	8	reactor feed	12	Vent
Vapour Fraction	1.0000	1.0000	1.0000	1.0000	1.0000
Temperature (C)	246.8	186.5	150.0	37.95	37.95
Pressure (kPa)	1.075e+004	1.100e+004	1.100e+004	1.075e+004	1.075e+004
Molar Flow (kgmole/h)	1.696e+004	2.591e+004	2.591e+004	1.171e+004	263.5
Mass Flow (kg/h)	3.862e+005	3.862e+005	3.862e+005	2.199e+005	4946
Liquid Volume Flow (m3/h)	613.1	848.9	848.9	401.2	9.026
Heat Flow (kJ/h)	-1.682e+009	-1.273e+009	-1.303e+009	-7.471e+008	-1.681e+007

Calgary, Alberta
CANADA

Case Name: C:\Documents and Settings\...\Methanol\CGD.usc

Unit Set: SI

Date/Time: Sunday Nov 22 2015, 10:39:43

Workbook: Case (Main) (continued)

Material Streams (continued)

Fluid Pkg: All

Name	6*	4	9	10	11
Vapour Fraction	1.0000	1.0000	0.7061	1.0000	0.0000
Temperature (C)	71.31	64.23	37.95	37.95	37.95
Pressure (kPa)	1.100e+004	1.100e+004	1.075e+004	1.075e+004	1.075e+004
Molar Flow (kgmole/h)	2.597e+004	1.213e+004	1.696e+004	1.198e+004	4986
Mass Flow (kg/h)	3.876e+005	2.347e+005	3.862e+005	2.248e+005	1.614e+005
Liquid Volume Flow (m3/h)	851.2	420.2	613.1	410.3	202.9
Heat Flow (kJ/h)	-1.377e+009	-8.453e+008	-1.981e+009	-7.639e+008	-1.217e+009
Name	13	14	15	16	17
Vapour Fraction	0.0827	1.0000	0.0000	1.0000	1.0000
Temperature (C)	34.18	34.18	34.18	40.60	539.4
Pressure (kPa)	200.0	200.0	200.0	1.100e+004	1.100e+004
Molar Flow (kgmole/h)	4986	412.2	4573	1.171e+004	412.2
Mass Flow (kg/h)	1.614e+005	1.482e+004	1.466e+005	2.199e+005	1.482e+004
Liquid Volume Flow (m3/h)	202.9	18.93	183.9	401.2	18.93
Heat Flow (kJ/h)	-1.217e+009	-1.080e+008	-1.110e+009	-7.462e+008	-9.913e+007

Calgary, Alberta
CANADA

Case Name: C:\Documents and Settings\...\Methanol\CGD.usc

Unit Set: SI

Date/Time: Sunday Nov 22 2015, 10:39:43

Workbook: Case (Main) (continued)

Material Streams (continued)

Fluid Pkg:

All

Name	18	Methanol	20	19	5
Vapour Fraction	0.0015	0.0000	1.0000	0.0000	1.0000
Temperature (C)	34.02	49.85	49.85	109.3	519.4
Pressure (kPa)	140.0	99.99	100.0	140.0	1.100e+004
Molar Flow (kgmole/h)	4573	4490	54.66	29.09	54.66
Mass Flow (kg/h)	1.466e+005	1.440e+005	2065	524.2	2065
Liquid Volume Flow (m3/h)	183.9	180.9	2.544	0.5252	2.544
Heat Flow (kJ/h)	-1.110e+009	-1.076e+009	-1.593e+007	-8.135e+006	-1.462e+007
Name	reactor effluent *	syngas from Rectisol	0		
Vapour Fraction	1.0000	1.0000	1.0000		
Temperature (C)	246.8	-45.00	21.85		
Pressure (kPa)	1.075e+004	6000	6000		
Molar Flow (kgmole/h)	1.696e+004	1.379e+004	1.379e+004		
Mass Flow (kg/h)	3.862e+005	1.508e+005	1.508e+005		
Liquid Volume Flow (m3/h)	613.1	428.5	428.5		
Heat Flow (kJ/h)	-1.682e+009	-5.671e+008	-5.393e+008		

Calgary, Alberta CANADA	Case Name:	C:\Documents and Settings\...\Methanol\CGD.usc
	Unit Set:	SI
	Date/Time:	Sunday Nov 22 2015, 10:39:43

Workbook: Case (Main) (continued)

Compositions					Fluid Pkg:	All
Name	1	2	3	6	7	
Comp Mole Frac (CO2)	0.007000	0.007000	0.007000	0.059059	0.088234	
Comp Mole Frac (Nitrogen)	0.005000	0.005000	0.005000	0.127305	0.194462	
Comp Mole Frac (H2S)	0.000000	0.000000	0.000000	0.000000	0.000000	
Comp Mole Frac (H2O)	0.000000	0.000000	0.000000	0.000005	0.001989	
Comp Mole Frac (Hydrogen)	0.661000	0.661000	0.661000	0.541399	0.297492	
Comp Mole Frac (CO)	0.327000	0.327000	0.327000	0.266486	0.145281	
Comp Mole Frac (Methanol)	0.000000	0.000000	0.000000	0.005746	0.272543	
Comp Mole Frac (Methane)	0.000000	0.000000	0.000000	0.000000	0.000000	
Name	reactor effluent	8	reactor feed	12	Vent	
Comp Mole Frac (CO2)	0.088234	0.059059	0.059059	0.101251	0.101251	
Comp Mole Frac (Nitrogen)	0.194462	0.127305	0.127305	0.269809	0.269809	
Comp Mole Frac (H2S)	0.000000	0.000000	0.000000	0.000000	0.000000	
Comp Mole Frac (H2O)	0.001989	0.000005	0.000005	0.000007	0.000007	
Comp Mole Frac (Hydrogen)	0.297492	0.541399	0.541399	0.418706	0.418706	
Comp Mole Frac (CO)	0.145281	0.266486	0.266486	0.203865	0.203865	
Comp Mole Frac (Methanol)	0.272543	0.005746	0.005746	0.006361	0.006361	
Comp Mole Frac (Methane)	0.000000	0.000000	0.000000	0.000000	0.000000	

Calgary, Alberta CANADA	Case Name: C:\Documents and Settings\...\Methanol\CGD.usc
	Unit Set: SI
	Date/Time: Sunday Nov 22 2015, 10:39:43

Workbook: Case (Main) (continued)

Compositions (continued)

Fluid Pkg: All

Name	6*	4	9	10	11
Comp Mole Frac (CO2)	0.059786	0.117878	0.088234	0.101251	0.056964
Comp Mole Frac (Nitrogen)	0.126938	0.266114	0.194462	0.269809	0.013465
Comp Mole Frac (H2S)	0.000000	0.000000	0.000000	0.000000	0.000000
Comp Mole Frac (H2O)	0.000005	0.000011	0.001989	0.000007	0.006748
Comp Mole Frac (Hydrogen)	0.541040	0.407061	0.297492	0.418706	0.006315
Comp Mole Frac (CO)	0.266454	0.198798	0.145281	0.203865	0.004552
Comp Mole Frac (Methanol)	0.005776	0.010139	0.272543	0.006361	0.911955
Comp Mole Frac (Methane)	0.000000	0.000000	0.000000	0.000000	0.000000
Name	13	14	15	16	17
Comp Mole Frac (CO2)	0.056964	0.590315	0.008892	0.101251	0.590315
Comp Mole Frac (Nitrogen)	0.013465	0.161103	0.000158	0.269809	0.161103
Comp Mole Frac (H2S)	0.000000	0.000000	0.000000	0.000000	0.000000
Comp Mole Frac (H2O)	0.006748	0.000118	0.007346	0.000007	0.000118
Comp Mole Frac (Hydrogen)	0.006315	0.076172	0.000019	0.418706	0.076172
Comp Mole Frac (CO)	0.004552	0.054810	0.000023	0.203865	0.054810
Comp Mole Frac (Methanol)	0.911955	0.117482	0.983562	0.006361	0.117482
Comp Mole Frac (Methane)	0.000000	0.000000	0.000000	0.000000	0.000000

Calgary, Alberta CANADA	Case Name:	C:\Documents and Settings\...\Methanol\CGD.usc
	Unit Set:	SI
	Date/Time:	Sunday Nov 22 2015, 10:39:43

Workbook: Case (Main) (continued)

Compositions (continued)

Fluid Pkg: All

Name	18	Methanol	20	19	5
Comp Mole Frac (CO2)	0.008892	0.003106	0.488875	0.000000	0.488875
Comp Mole Frac (Nitrogen)	0.000158	0.000007	0.012694	0.000000	0.012694
Comp Mole Frac (H2S)	0.000000	0.000000	0.000001	0.000000	0.000001
Comp Mole Frac (H2O)	0.007346	0.001003	0.000078	0.999900	0.000078
Comp Mole Frac (Hydrogen)	0.000019	0.000000	0.001578	0.000000	0.001578
Comp Mole Frac (CO)	0.000023	0.000000	0.001860	0.000000	0.001860
Comp Mole Frac (Methanol)	0.983562	0.995884	0.494914	0.000100	0.494914
Comp Mole Frac (Methane)	0.000000	0.000000	0.000000	0.000000	0.000000
Name	reactor effluent *	syngas from Rectisol	0		
Comp Mole Frac (CO2)	0.088234	0.007000	0.007000		
Comp Mole Frac (Nitrogen)	0.194462	0.005000	0.005000		
Comp Mole Frac (H2S)	0.000000	0.000000	0.000000		
Comp Mole Frac (H2O)	0.001989	0.000000	0.000000		
Comp Mole Frac (Hydrogen)	0.297492	0.661000	0.661000		
Comp Mole Frac (CO)	0.145281	0.327000	0.327000		
Comp Mole Frac (Methanol)	0.272543	0.000000	0.000000		
Comp Mole Frac (Methane)	0.000000	0.000000	0.000000		

Appendix D

Flowsheet of the Methanol Synthesis Process with HGD

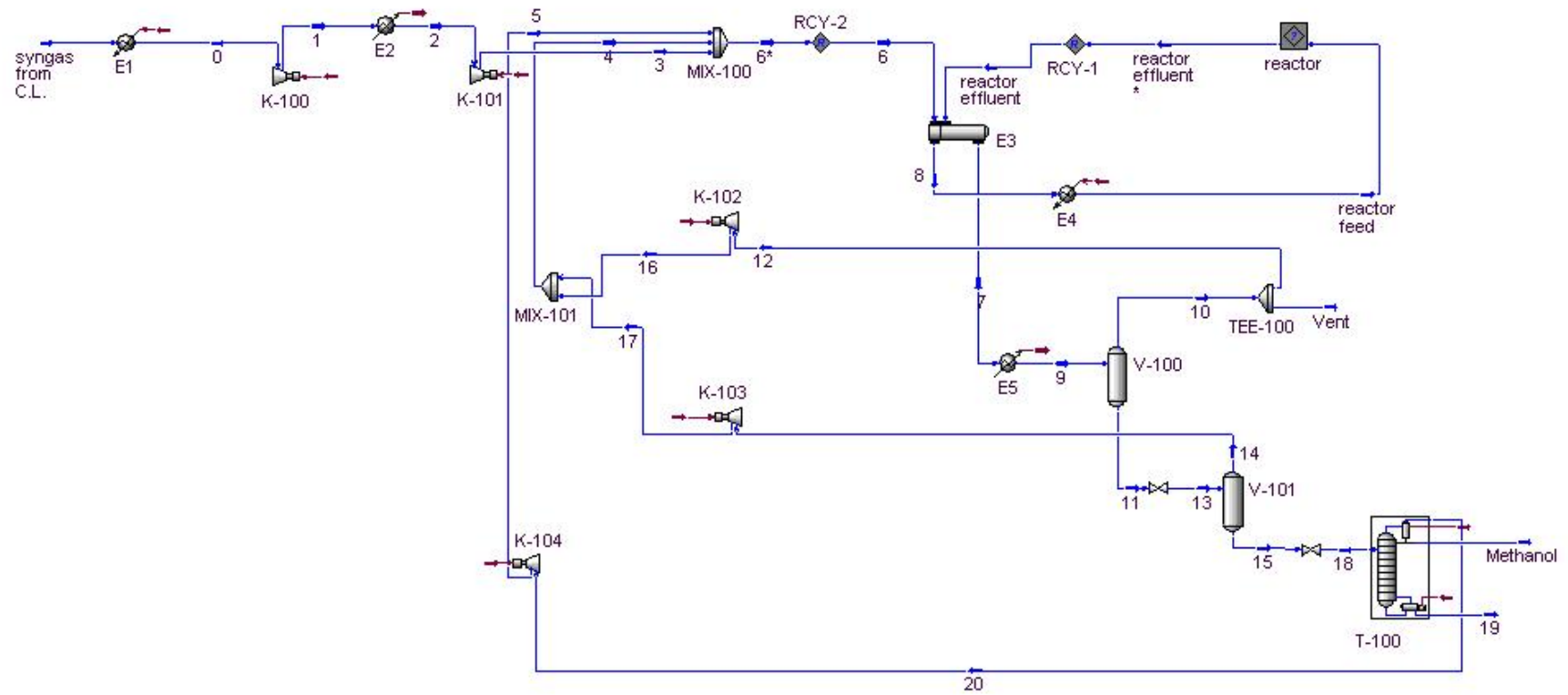


FIGURE D.1: Flowsheet of the methanol production plant with HGD in UniSim Design

Calgary, Alberta
CANADA

Case Name: C:\Documents and Settings\...\Methano\HGD.usc

Unit Set: SI

Date/Time: Sunday Nov 22 2015, 10:45:04

Workbook: Case (Main)

Material Streams

Fluid Pkg:

All

Name	1	2	3	6	7
Vapour Fraction	1.0000	1.0000	1.0000	0.9946	1.0000
Temperature (C)	218.6	160.0	241.9	63.36	229.3
Pressure (kPa)	6465	6465	1.100e+004	1.100e+004	9545
Molar Flow (kgmole/h)	2.159e+004	2.159e+004	2.159e+004	2.813e+005	2.733e+005
Mass Flow (kg/h)	4.360e+005	4.360e+005	4.360e+005	1.008e+007	1.008e+007
Liquid Volume Flow (m3/h)	764.2	764.2	764.2	1.330e+004	1.308e+004
Heat Flow (kJ/h)	-3.136e+009	-3.181e+009	-3.122e+009	-8.495e+010	-8.300e+010
Name	reactor effluent	8	reactor feed	12	Vent
Vapour Fraction	1.0000	0.9985	1.0000	1.0000	1.0000
Temperature (C)	246.6	74.99	150.0	37.95	37.95
Pressure (kPa)	9545	1.100e+004	1.100e+004	9545	9545
Molar Flow (kgmole/h)	2.733e+005	2.813e+005	2.813e+005	2.590e+005	5825
Mass Flow (kg/h)	1.008e+007	1.008e+007	1.008e+007	9.607e+006	2.161e+005
Liquid Volume Flow (m3/h)	1.308e+004	1.330e+004	1.330e+004	1.249e+004	281.1
Heat Flow (kJ/h)	-8.278e+010	-8.473e+010	-8.365e+010	-8.158e+010	-1.835e+009

Calgary, Alberta
CANADA

Case Name: C:\Documents and Settings\...\Methano\HGD.usc

Unit Set: SI

Date/Time: Sunday Nov 22 2015, 10:45:04

Workbook: Case (Main) (continued)

Material Streams (continued)

Fluid Pkg: All

Name	6*	4	9	10	11
Vapour Fraction	0.9946	1.0000	0.9689	1.0000	0.0000
Temperature (C)	63.46	53.02	37.95	37.95	37.95
Pressure (kPa)	1.100e+004	1.100e+004	9545	9545	9545
Molar Flow (kgmole/h)	2.825e+005	2.609e+005	2.733e+005	2.648e+005	8487
Mass Flow (kg/h)	1.013e+007	9.689e+006	1.008e+007	9.823e+006	2.580e+005
Liquid Volume Flow (m3/h)	1.336e+004	1.259e+004	1.308e+004	1.278e+004	309.1
Heat Flow (kJ/h)	-8.533e+010	-8.218e+010	-8.587e+010	-8.342e+010	-2.458e+009
Name	13	14	15	16	17
Vapour Fraction	0.2234	1.0000	0.0000	1.0000	1.0000
Temperature (C)	17.35	17.35	17.35	50.46	472.9
Pressure (kPa)	200.0	200.0	200.0	1.100e+004	1.100e+004
Molar Flow (kgmole/h)	8487	1896	6591	2.590e+005	1896
Mass Flow (kg/h)	2.580e+005	8.203e+004	1.760e+005	9.607e+006	8.203e+004
Liquid Volume Flow (m3/h)	309.1	99.74	209.3	1.249e+004	99.74
Heat Flow (kJ/h)	-2.458e+009	-7.280e+008	-1.730e+009	-8.149e+010	-6.906e+008

Calgary, Alberta
CANADA

Case Name: C:\Documents and Settings\...\Methanol\HGD.usc

Unit Set: SI

Date/Time: Sunday Nov 22 2015, 10:45:04

Workbook: Case (Main) (continued)

Material Streams (continued)

Fluid Pkg: All

Name	18	Methanol	20	19	5
Vapour Fraction	0.0026	0.0000	1.0000	0.0000	1.0000
Temperature (C)	17.10	49.85	49.85	109.3	517.3
Pressure (kPa)	140.0	99.99	100.0	140.0	1.100e+004
Molar Flow (kgmole/h)	6591	3956	83.09	2551	83.09
Mass Flow (kg/h)	1.760e+005	1.269e+005	3164	4.597e+004	3164
Liquid Volume Flow (m3/h)	209.3	159.4	3.894	46.06	3.894
Heat Flow (kJ/h)	-1.730e+009	-9.480e+008	-2.472e+007	-7.134e+008	-2.273e+007
Name	reactor effluent *	syngas from C.L.	0		
Vapour Fraction	1.0000	1.0000	1.0000		
Temperature (C)	246.6	150.0	140.0		
Pressure (kPa)	9545	3800	3800		
Molar Flow (kgmole/h)	2.733e+005	2.159e+004	2.159e+004		
Mass Flow (kg/h)	1.008e+007	4.360e+005	4.360e+005		
Liquid Volume Flow (m3/h)	1.308e+004	764.2	764.2		
Heat Flow (kJ/h)	-8.278e+010	-3.184e+009	-3.192e+009		

Calgary, Alberta CANADA	Case Name:	C:\Documents and Settings\...\Methanol\HGD.usc
	Unit Set:	SI
	Date/Time:	Sunday Nov 22 2015, 10:45:04

Workbook: Case (Main) (continued)

Compositions					Fluid Pkg:	All
Name	1	2	3	6	7	
Comp Mole Frac (CO2)	0.260000	0.260000	0.260000	0.725254	0.745453	
Comp Mole Frac (Nitrogen)	0.004000	0.004000	0.004000	0.013925	0.014332	
Comp Mole Frac (H2S)	0.000000	0.000000	0.000000	0.000000	0.000000	
Comp Mole Frac (H2O)	0.106000	0.106000	0.106000	0.009130	0.010393	
Comp Mole Frac (Hydrogen)	0.420000	0.420000	0.420000	0.142567	0.116513	
Comp Mole Frac (CO)	0.210000	0.210000	0.210000	0.102300	0.091674	
Comp Mole Frac (Methanol)	0.000000	0.000000	0.000000	0.006824	0.021636	
Comp Mole Frac (Methane)	0.000000	0.000000	0.000000	0.000000	0.000000	
Name	reactor effluent	8	reactor feed	12	Vent	
Comp Mole Frac (CO2)	0.745453	0.725254	0.725254	0.762287	0.762287	
Comp Mole Frac (Nitrogen)	0.014332	0.013925	0.013925	0.014776	0.014776	
Comp Mole Frac (H2S)	0.000000	0.000000	0.000000	0.000000	0.000000	
Comp Mole Frac (H2O)	0.010393	0.009130	0.009130	0.001056	0.001056	
Comp Mole Frac (Hydrogen)	0.116513	0.142567	0.142567	0.120207	0.120207	
Comp Mole Frac (CO)	0.091674	0.102300	0.102300	0.094571	0.094571	
Comp Mole Frac (Methanol)	0.021636	0.006824	0.006824	0.007103	0.007103	
Comp Mole Frac (Methane)	0.000000	0.000000	0.000000	0.000000	0.000000	

Calgary, Alberta
CANADA

Case Name: C:\Documents and Settings\...\Methanol\HGD.usc

Unit Set: SI

Date/Time: Sunday Nov 22 2015, 10:45:04

Workbook: Case (Main) (continued)

Compositions (continued)

Fluid Pkg:

All

Name	6*	4	9	10	11
Comp Mole Frac (CO2)	0.725135	0.763703	0.745453	0.762287	0.220275
Comp Mole Frac (Nitrogen)	0.013863	0.014684	0.014332	0.014776	0.000462
Comp Mole Frac (H2S)	0.000000	0.000000	0.000000	0.000000	0.000000
Comp Mole Frac (H2O)	0.009087	0.001068	0.010393	0.001056	0.301659
Comp Mole Frac (Hydrogen)	0.142312	0.119374	0.116513	0.120207	0.001272
Comp Mole Frac (CO)	0.102768	0.093926	0.091674	0.094571	0.001302
Comp Mole Frac (Methanol)	0.006835	0.007245	0.021636	0.007103	0.475030
Comp Mole Frac (Methane)	0.000000	0.000000	0.000000	0.000000	0.000000
Name	13	14	15	16	17
Comp Mole Frac (CO2)	0.220275	0.957020	0.008291	0.762287	0.957020
Comp Mole Frac (Nitrogen)	0.000462	0.002065	0.000001	0.014776	0.002065
Comp Mole Frac (H2S)	0.000000	0.000000	0.000000	0.000000	0.000000
Comp Mole Frac (H2O)	0.301659	0.002664	0.387688	0.001056	0.002664
Comp Mole Frac (Hydrogen)	0.001272	0.005693	0.000000	0.120207	0.005693
Comp Mole Frac (CO)	0.001302	0.005823	0.000001	0.094571	0.005823
Comp Mole Frac (Methanol)	0.475030	0.026734	0.604018	0.007103	0.026734
Comp Mole Frac (Methane)	0.000000	0.000000	0.000000	0.000000	0.000000

Calgary, Alberta CANADA	Case Name:	C:\Documents and Settings\...\Methano\HGD.usc
	Unit Set:	SI
	Date/Time:	Sunday Nov 22 2015, 10:45:04

Workbook: Case (Main) (continued)

Compositions (continued)

Fluid Pkg: All

Name	18	Methanol	20	19	5
Comp Mole Frac (CO2)	0.008291	0.003208	0.504916	0.000000	0.504916
Comp Mole Frac (Nitrogen)	0.000001	0.000000	0.000058	0.000000	0.000058
Comp Mole Frac (H2S)	0.000000	0.000000	0.000000	0.000000	0.000000
Comp Mole Frac (H2O)	0.387688	0.001003	0.000078	0.999900	0.000078
Comp Mole Frac (Hydrogen)	0.000000	0.000000	0.000028	0.000000	0.000028
Comp Mole Frac (CO)	0.000001	0.000000	0.000047	0.000000	0.000047
Comp Mole Frac (Methanol)	0.604018	0.995789	0.494873	0.000100	0.494873
Comp Mole Frac (Methane)	0.000000	0.000000	0.000000	0.000000	0.000000
Name	reactor effluent *	syngas from C.L.	0		
Comp Mole Frac (CO2)	0.745453	0.260000	0.260000		
Comp Mole Frac (Nitrogen)	0.014332	0.004000	0.004000		
Comp Mole Frac (H2S)	0.000000	0.000000	0.000000		
Comp Mole Frac (H2O)	0.010393	0.106000	0.106000		
Comp Mole Frac (Hydrogen)	0.116513	0.420000	0.420000		
Comp Mole Frac (CO)	0.091674	0.210000	0.210000		
Comp Mole Frac (Methanol)	0.021636	0.000000	0.000000		
Comp Mole Frac (Methane)	0.000000	0.000000	0.000000		

Bibliography

- J. Abbasian, A. Rehmat, D. Leppin, and D. D. Banerjee. Desulfurization of fuels with calcium-based sorbents. *Fuel Processing Technology*, 25(1):1–15, Apr. 1990a. ISSN 03783820.
- J. Abbasian, A. Rehmat, D. Leppin, and D. Bannerjee. H₂S removal from fuel gas during coal gasification. *Argonne National Laboratory*, 1990b.
- J. Adanez, A. Abad, F. Garcia-Labiano, P. Gayan, and L. F. de Diego. Progress in Chemical-Looping Combustion and Reforming technologies. *Progress in Energy and Combustion Science*, 38(2):215–282, Apr. 2012. ISSN 03601285.
- R. Álvarez Rodríguez and C. Clemente-Jul. Hot gas desulphurisation with dolomite sorbent in coal gasification. *Fuel*, 87(17-18):3513–3521, Dec. 2008. ISSN 00162361.
- A. T. Atimtay and D. P. Harrison. *Desulfurization of Hot Coal Gas*. NATO ASI series: Ecological sciences. Springer Berlin Heidelberg, 1998.
- P. Biedermann, T. Grube, and B. H. Hrsg. *Methanol as an Energy Carrier*. 2006.
- R. H. Borgwardt and N. F. Roache. Reaction of H₂S and Sulfur with Limestone Particles. *Industrial & Engineering Chemistry Process Design and Development*, 23(4):742–748, 1984.
- K. Bussche and G. F. Froment. A Steady-State Kinetic Model for Methanol Synthesis and the Water Gas Shift Reaction on a Commercial Cu/ZnO/Al₂O₃Catalyst. *Journal of Catalysis*, 161(1):1–10, 1996. ISSN 0021-9517.
- J. J. Carberry. *Chemical and Catalytic Reaction Engineering*. Dover Books on Chemistry. Dover Publications, 1976.
- G. Cau and D. Cocco. Processi di gassificazione.
- H. Chang and M. Louge. Fluid dynamic similarity of circulating fluidized-beds. *Powder Technology*, 70(3):259–270, 1992. ISSN 0032-5910.

- H. Chestnut. *Systems engineering tools*. Wiley series on systems engineering and analysis. Wiley, 1965.
- R. De María, I. Díaz, M. Rodríguez, and A. Sáiz. Industrial Methanol from Syngas: Kinetic Study and Process Simulation. *International Journal of Chemical Reactor Engineering*, 11(1):469–477, Jan. 2013. ISSN 2194-5748.
- DoE. Technology Readness Assessment Guide. Technical report, 2011.
- B. Dou, C. Wang, H. Chen, Y. Song, B. Xie, Y. Xu, and C. Tan. Research progress of hot gas filtration, desulphurization and HCl removal in coal-derived fuel gas: A review. *Chemical Engineering Research and Design*, 90(11):1901–1917, Nov. 2012. ISSN 02638762.
- W. F. Elseviers and H. Verelst. Transition metal oxides for hot gas desulphurisation. *Fuel*, 78(5):601–612, Apr. 1999. ISSN 0016-2361.
- D. Fairbanks and C. Wilke. Diffusion coefficients in multicomponent gas mixtures. *Industrial & Engineering Chemistry*, (March):471–475, 1950.
- L. S. Fan. *Chemical Looping Systems for Fossil Energy Conversions*. Wiley, 2011. ISBN 9781118063132.
- L. A. Fenouil and S. Lynn. Study of Calcium-Based Sorbents for High-Temperature H₂S Removal. 2. Kinetics of H₂S Sorption by Calcined Limestone. *Industrial & Engineering Chemistry Research*, 34(7):2334–2342, July 1995a. ISSN 0888-5885.
- L. A. Fenouil and S. Lynn. Study of Calcium-Based Sorbents for High-Temperature H₂S Removal. 1. Kinetics of H₂S Sorption by Uncalcined Limestone. *Industrial & Engineering Chemistry Research*, 34(7):2324–2333, July 1995b. ISSN 0888-5885.
- L. A. Fenouil and S. Lynn. Design of Entrained-Flow and Moving-, Packed-, and Fluidized-Bed Sorption Systems: Grain-Model Kinetics for Hot Coal-Gas Desulfurization with Limestone. *Industrial & Engineering Chemistry Research*, 35(4):1024–1043, Jan. 1996. ISSN 0888-5885.
- C. Frau. Analisi comparativa di diversi sorbenti nel processo di desolforazione a caldo. Technical report, ENEA, 2009.
- E. N. Fuller, P. D. Schettler, and J. C. Giddings. A new method for prediction of binary gas - phase diffusion coefficients. *Industrial & Engineering Chemistry*, 58(5):18–27, 1966.
- M. Gatti, E. Martelli, F. Marechal, and S. Consonni. Review, modeling, Heat Integration, and improved schemes of Rectisol®-based processes for CO₂ capture. *Applied Thermal Engineering*, 70(2):1123–1140, Sept. 2014. ISSN 13594311.

- V. Girard, A. Baudot, D. Chiche, D. Bazer-Bachi, C. Bounie, and C. Geantet. Rational selection of single oxide sorbents for syngas desulfurization regenerable at reduced temperature: Thermochemical calculations and experimental study. *Fuel*, 128:220–230, July 2014. ISSN 00162361.
- A. Giuffrida, M. Romano, and G. Lozza. Thermodynamic assessment of IGCC power plants with hot fuel gas desulfurization. *Applied Energy*, 87(11):3374–3383, Nov. 2010. ISSN 0306-2619.
- A. Giuffrida, M. C. Romano, and G. Lozza. Efficiency enhancement in IGCC power plants with air-blown gasification and hot gas clean-up. *Energy*, 53:221–229, May 2013. ISSN 03605442.
- L. R. Glicksman, M. R. Hyre, and P. A. Farrell. Dynamic similarity in fluidization. *International Journal of Multiphase Flow*, 20:331–386, 1994. ISSN 0301-9322.
- G. Graaf, E. Stamhuis, and A. Beenackers. Kinetics of low-pressure methanol synthesis. *Chemical Engineering Science*, 43(12):3185–3195, 1988. ISSN 00092509.
- G. H. Graaf, P. J. J. M. Sijtsma, E. J. Stamhuis, and G. E. H. Joostes. Chemical equilibria in methanol synthesis. *Chemical Engineering Science*, 41(11):2883–2890, 1986.
- D. J. Gunn. Transfer of heat or mass to particles in fixed and fluidised beds. *International Journal of Heat and Mass Transfer*, 21:467–476, 1978.
- A. Haider and O. Levenspiel. Drag coefficient and terminal velocity of spherical and nonspherical particles. *Powder Technology*, 58(1):63–70, May 1989. ISSN 00325910.
- A. Heesink, W. Prins, and W. van Swaaij. A grain size distribution model for non-catalytic gas-solid reactions. *The Chemical Engineering Journal and the Biochemical Engineering Journal*, 53(1):25–37, Nov. 1993. ISSN 09230467.
- G. Hochgesand. Rectisol and Purisol. *Industrial & Engineering Chemistry*, 62(7):37–43, July 1970. ISSN 0019-7866.
- Honeywell. *UniSim [®] Design Reference Guide*. 2010.
- G. A. Hughmark. Mass and heat transfer from rigid spheres. *AIChE Journal*, 13(6):1219–1221, Nov. 1967. ISSN 0001-1541.
- P. C. Ian R Fantom and P. W. Sage. Hot Gas Cleaning - An Overview. In *Desulfurization of Hot Coal Gas*, pages 103–115. 1998.
- J. H. Jensen, J. M. Poulsen, and N. Andersen. From coal to clean energy. *nitrogen+syngas*, 310(April), 2011.

- H. K. Jun, T. J. Lee, S. O. Ryu, and J. C. Kim. A study of Zn-Ti-based H₂S removal sorbents promoted with cobalt oxides. *Industrial & Engineering Chemistry Research*, 40(16):3547–3556, 2001. ISSN 0888-5885.
- K. Klier, V. Chatikavanij, R. G. Herman, and G. W. Simmons. Catalytic synthesis of methanol from COH₂. *Journal of Catalysis*, 74(2):343–360, 1982. ISSN 0021-9517.
- T. Knowlton, S. Karri, and A. Issangya. Scale-up of fluidized-bed hydrodynamics. *Powder Technology*, 150(2):72–77, Feb. 2005. ISSN 00325910.
- T. M. Knowlton. Fluidized bed reactor design and scale-up. In *Fluidized bed technologies for near-zero emission combustion and gasification*, number 1962, chapter 10, pages 481–523. Elsevier, 2013.
- J. G. Knudsen, H. C. Hottel, A. F. Sarofim, P. C. Wankat, and K. S. Knaebel. Heat and Mass Transfer. 1999.
- J. Konttinen. Hot gas desulfurization with zinc titanate sorbents in a fluidized bed. 1. Determination of sorbent particle conversion rate model parameters. *Industrial & Engineering Chemistry Research*, 36:2332–2339, 1997.
- J. T. Konttinen, C. A. P. Zevenhoven, and M. M. Hupa. Hot Gas Desulfurization with Zinc Titanate Sorbents in a Fluidized Bed. 2. Reactor Model. *Industrial & Engineering Chemistry Research*, 36(6):2340–2345, June 1997. ISSN 0888-5885.
- J. Kopyscinski, T. J. Schildhauer, and S. M. Biollaz. Methanation in a fluidized bed reactor with high initial CO partial pressure: Part II— Modeling and sensitivity study. *Chemical Engineering Science*, 66(8):1612–1621, Apr. 2011. ISSN 00092509.
- V. E. Leonov, Atroshch.Vi, and M. M. Karavaev. Mechanism of methanol synthesis in presence of carbon-dioxide. *Zhurnal Prikladnoi Khimii*, 46(4):894–897, 1973. ISSN 0044-4618.
- O. Levenspiel. *Chemical reaction engineering*. Wiley, 1999.
- W. Lewis and E. Gilliland. Production of pure carbon dioxide., 1954.
- G. Lozza. *Turbine a gas e cicli combinati*. 2006.
- G. Lozza, A. Giuffrida, and M. Romano. Sviluppo di modellistica di impianti di generazione elettrica integrati con processi di gassificazione di carbone che utilizzano tecnologie di desolforazione a caldo del syngas prodotto. Technical report, ENEA, 2009.
- W. L. Luyben. Design and Control of a Methanol Reactor/Column Process. *Industrial & Engineering Chemistry Research*, 49(13):6150–6163, July 2010. ISSN 0888-5885.

- F. Manenti, S. Cieri, and M. Restelli. Considerations on the steady-state modeling of methanol synthesis fixed-bed reactor. *Chemical Engineering Science*, 66(2):152–162, 2011. ISSN 0009-2509.
- A. Maria. Introduction to Modeling and Simulation. In *Proceedings of the 29th Conference on Winter Simulation, WSC '97*, pages 7–13. IEEE Computer Society, 1997. ISBN 0-7803-4278-X.
- K. M. McGrath, G. K. S. Prakash, and G. A. Olah. Direct methanol fuel cells. *Journal of Industrial and Engineering Chemistry*, 10(7):1063–1080, 2004. ISSN 1226-086X.
- X. Meng, W. De Jong, and A. Verkooijen. Thermodynamic analysis and kinetics model of H₂S sorption using different sorbents. *Environmental Progress & Sustainable Energy*, 28(3):360–371, Oct. 2009. ISSN 19447442.
- X. Meng, W. de Jong, R. Pal, and A. H. M. Verkooijen. In bed and downstream hot gas desulphurization during solid fuel gasification: A review. *Fuel Processing Technology*, 91(8):964–981, Aug. 2010. ISSN 0378-3820.
- P. Mirek. A simplified methodology for scaling hydrodynamic data from Lagisza 460 MWe supercritical CFB boiler. *Chemical and Process Engineering*, 32(4):245–253, Jan. 2011. ISSN 0208-6425.
- E. Monazam and L. Shadle. Analysis of the acceleration region in a circulating fluidized bed riser operating above fast fluidization velocities. *Industrial & Engineering Chemistry Research*, 47:8423–8429, 2008.
- E. R. Monazam and L. J. Shadle. Fuel gas clean-up in a transport reactor: Model development and analysis. In *Proceedings of the 18th International Conference on Fluidized Bed Combustion*, pages 409–416. ASME, Amer Soc Mechanical Engineers, 2005. ISBN 0-7918-4698-9.
- E. R. Monazam, L. J. Shadle, and D. A. Berry. Model validation of S-sorption with ZnO in a transport reactor. In *Circulating Fluidized bed Technology VIII*, 2005.
- E. R. Monazam, L. J. Shadle, and D. a. Berry. Modeling and analysis of S-sorption with ZnO in a transport reactor. *Chemical Engineering Science*, 63(10):2614–2623, May 2008. ISSN 00092509.
- G. A. Olah. Beyond Oil and Gas: The Methanol Economy. *Angewandte Chemie International Edition*, 44(18):2636–2639, 2005. ISSN 1521-3773.
- D. Pallarès and F. Johnsson. Macroscopic modelling of fluid dynamics in large-scale circulating fluidized beds. *Progress in Energy and Combustion Science*, 32(5-6):539–569, Sept. 2006. ISSN 03601285.

- N. R. Parlikkad, S. Chambrey, P. Fongarland, N. Fatah, A. Khodakov, S. Capela, and O. Guerrini. Modeling of fixed bed methanation reactor for syngas production: Operating window and performance characteristics. *Fuel*, 107:254–260, May 2013. ISSN 00162361.
- P. Ranade and D. Harrison. The variable property grain model applied to the zinc oxide-hydrogen sulfide reaction. *Chemical Engineering Science*, 36:1079–1089, 1981.
- S. Ray, F. Pino, V. Mihajlovic, and T. V. Leeuwen. Design and Analysis of a Simulated Methanol Production Plant. In *Proceedings of the 2015 International Conference on Industrial Engineering and Operations Management*, number 1996, pages 1–7, 2015. ISBN 9781479960651.
- L. Romano, F. Ruggeri, and R. Marx. SNG production from Coal: a possible solution to Energy Demand. In A. Morini, GL and Bianchi, M and Saccani, C and Cocchi, editor, *ATI 2013 – 68th conference of the italian thermal machines engineering association*, volume 45 of *Energy Procedia*, pages 1330–1336, 2014.
- T. J. Schildhauer, J. Settino, and S. L. Teske. Modelling study of fixed bed reactors with dumped catalyst particles and structured catalyst supports for CO₂ methanation in Power-to-Gas applications. *submitted to International Journal of Hydrogen Energy*.
- R. B. Slimane and J. Abbasian. Copper-based sorbents for coal gas desulfurization at moderate temperatures. *Industrial & Engineering Chemistry Research*, 39(5):1338–1344, 2000a. ISSN 0888-5885.
- R. B. Slimane and J. Abbasian. Regenerable mixed metal oxide sorbents for coal gas desulfurization at moderate temperatures. *Advances in Environmental Research*, 4(2):147–162, May 2000b. ISSN 1093-0191.
- W. E. Stewart and M. Caracotsios. *Computer-Aided Modeling of Reactive Systems*. Wiley, 2008.
- J. Szekely and J. Evans. A structural model for gas—solid reactions with a moving boundary. *Chemical Engineering Science*, 25(6):1091–1107, Jan. 1970. ISSN 00092509.
- J. Szekely and J. Evans. A structural model for gas-solid reactions with a moving boundary-II. *Chemical Engineering Science*, 26(11):1901–1913, Nov. 1971. ISSN 00092509.
- J. Szekely and M. Propster. A structural model for gas solid reactions with a moving boundary—VI. *Chemical Engineering Science*, 30(9):1049–1055, Sept. 1975. ISSN 00092509.

- J. Szekely, J. Evans, and H. Sohn. *Gas-Solid Reactions*. Academic Press: New York, 1976.
- S. L. Teske. *Integrating Rate Based Models into a Multi-Objective Process Design & Optimisation Framework using Surrogate Model*. PhD thesis, 2014.
- R. Turton, D. a. Berry, T. H. Gardner, and A. Miltz. Evaluation of Zinc Oxide Sorbents in a Pilot-Scale Transport Reactor: Sulfidation Kinetics and Reactor Modeling. *Industrial & Engineering Chemistry Research*, 43(5):1235–1243, Mar. 2004. ISSN 0888-5885.
- M. V. Twigg. *Catalyst handbook*. Wolfe, 1989.
- L. V. van der Ham. Improving the exergy efficiency of a cryogenic air separation unit as part of an integrated gasification combined cycle. *Energy Conversion and Management*, 61:31–42, 2012. ISSN 0196-8904.
- Van der Meer E.H., T. R.B., and D. J.F. Dimensionless groups for practicable similarity of circulating fluidised beds. *Chemical Engineering Science*, 54:5369–5376, 1999.
- P. Villa, P. Forzatti, G. Buzzi-Ferraris, G. Garone, and I. Pasquon. Synthesis of alcohols from carbon oxides and hydrogen. 1. Kinetics of the low-pressure methanol synthesis. *Industrial & Engineering Chemistry Process Design and Development*, 24(1):12–19, 1985.
- P. R. Westmoreland and D. P. Harrison. Evaluation of Candidate Solids for High Temperature Desulfurization of Low-Btu Gases. *Environmental Science & Technology*, 10(7):659–661, 1976.
- A. D. Wiheeb, I. K. Shamsudin, M. A. Ahmad, M. N. Murat, J. Ki, and M. R. Othman. Present technologies for hydrogen sulfide removal from gaseous mixtures, 2013.
- J. Xu and G. F. Froment. Methane steam reforming, methanation and water-gas shift: I. Intrinsic kinetics. *AIChE Journal*, 35(1):88–96, 1989. ISSN 1547-5905.
- S. Yagi and D. Kunii. Studies on combustion of carbon particles in flames and fluidized beds. *Symposium (International) on Combustion*, 5(1):231–244, 1955. ISSN 0082-0784.
- W. C. Yang. *Handbook of Fluidization and Fluid-Particle Systems*. Chemical Industries. Taylor & Francis, 2003. ISBN 9780203912744.
- C. a. P. Zevenhoven, K. P. Yrjas, and M. M. Hupa. Hydrogen Sulfide Capture by Limestone and Dolomite at Elevated Pressure. 2. Sorbent Particle Conversion Modeling. *Industrial & Engineering Chemistry Research*, 35(3):943–949, Jan. 1996. ISSN 0888-5885.

- C. A. P. Zevenhoven, K. P. Yrjas, and M. M. Hupa. Product Layer Development during Sulfation and Sulfidation of Uncalcined Limestone Particles at Elevated Pressures. *Industrial & Engineering Chemistry Research*, 37(7):2639–2646, July 1998. ISSN 0888-5885.

Activities

Education

Teoria e sviluppo dei processi chimici held by Prof. F. Di Maio and A. Di Renzo at University of Calabria

Athena Visual Studio Workshop held by Dr. M. Caracotsios at Paul Scherrer Institut

Conference

70th Conference of the ATI Engineering Association

Model of a chemical looping process for hot gas desulfurization in power plants. J. Settino

Awarded with "Premio Caputo"

Publications

Modelling study of fixed bed reactors with dumped catalyst particles and structured catalyst supports for CO₂ methanation in Power-to-Gas applications T. J. Schildhauer, J. Settino, S. L. Teske. International Journal of Hydrogen Energy (2015)

Model of a chemical looping process for hot gas desulfurization in power plants. J. Settino. Energy Procedia 2015

Mobility

24th August 2013 - 31st August 2014 Paul Scherrer Institut, Switzerland (CH)

21st March 2015 - 29th March 2015 Paul Scherrer Institut, Switzerland (CH)

11th August 2015 - 30th August 2015 Paul Scherrer Institut, Switzerland (CH)